Empirical analysis of risk spillovers in financial markets under crisis events

张，文婷

(Degree)
博士（経済学）
(Date of Degree)
2024-03-25
(Date of Publication)
2025-03-01
(Resource Type)
doctoral thesis
(Report Number)
甲第8827号
(URL)
https://hdl.handle.net/20.500.14094/0100490052

博　士　論　文

令和 5 年 12 月

神戸大学大学院経済学研究科

経済学専攻

指導教員　羽森茂之

張　文婷

博　士　論　文

Empirical analysis of risk spillovers in financial markets under crisis events

（危機下の金融市場におけるリスク波及の実証分析）

令和 5 年 12 月

神戸大学大学院経済学研究科

経済学専攻

指導教員　羽森茂之

張　文婷

Contents

Chapter 1. Introduction

[1]An important trigger for the outbreak of the financial crisis is the accumulation of financial vulnerabilities. The vulnerability of financial markets mainly comes from the volatility of asset price returns and the connectedness of volatility. A characteristic of financial market volatility is that it is not directly observable. However, volatility clustering in the context of asset returns is common. Moreover, such clustering is usually contagious. For example, during a crisis, the volatility of financial markets usually increases and spreads throughout the market (Diebold and Yilmaz, 2012). Reinhart and Rogoff (2008) argue that there are significant patterns and similarities in the occurrence of financial crises. Therefore, to capture this regularity and similarity, more and more researchers are measuring and monitoring return and volatility spillovers between financial markets. Umar et al. (2021) explore the dynamic return and volatility connectedness of some significant industrial and precious metals with crude oil shocks using the Diebold and Yilmaz (2012, 2014) method. Their conclusion demonstrates that oil risk shocks are the most important driver of industrial and precious metals return and volatility (over demand shocks and supply shocks), which implies that the policy actions taken by market regulators to control the impact of crude oil price shocks on each situation will be of a different nature. Not only the return and volatility spillover effects between oil and metal markets but also between cryptocurrency and commodity markets (Hassan et al., 2022; Mo et al., 2022), stock and foreign exchange markets (Rai & Garg, 2022; Malik, 2021), green finance markets (Zhang et al., 2022; Lorente et al., 2023) and other different financial markets have been widely studied.

The outbreak of the COVID-19 epidemic in 2020 has brought an unprecedented human and health crisis. The necessary measures to contain the virus have triggered an economic downturn. At this juncture, there is significant uncertainty about the severity and duration of the crisis. In March 2020, the oil and stock markets already reflected this severe crisis. The worldwide blockade due to the COVID-19 pandemic has almost dried the oil demand. On April 20, 2020, oil prices fell into negative territory for the first time in history at minus $37.63 per barrel, a drop of 320% (Heinlein et al., 2021). The U.S. stock market also saw four meltdowns in just eight consecutive trading days, an unprecedented occurrence. The meltdowns occurred when U.S. stocks were hitting record highs, triggered by the rapid spread of the COVID-19 outbreak and the global crude oil prices plunge. The heavy impact of COVID-19 on the oil and equity markets has affected investor sentiment. The high level of uncertainty and extreme volatility in the oil and stock markets has left investors depressed and anxious. It may have even prompted some investors to fundamentally change their views on the oil and stock markets in search of safer assets (Mili et al., 2023). Therefore, in this background, studying the impact of investor sentiment on returns and volatility spillovers in oil and

[1] Chapter 1 is based on the published paper: Zhang, W., & Hamori, S. (2021). The connectedness between the sentiment index and stock return volatility under COVID-19: a time-varying parameter vector autoregression approach. *The Singapore Economic Review*, 1-32. https://doi.org/10.1142/s0217590822500023

equity markets during the COVID-19 outbreak will allow investors to adjust their investment strategies and exposures in times of extreme distress to respond effectively to the crisis. Understanding the direction and intensity of sentiment spillovers in the connectedness system will help investors allocate capital across markets in response to changes in sentiment, thereby allowing them to maximize the benefits of a well-diversified portfolio.

The global economy is gradually recovering from the post-COVID-19 epidemic. However, the outbreak of the Russia-Ukraine war in February 2022 has dimmed the prospects for post-epidemic economic recovery in the emerging and developing economies of Europe and Central Asia. The Russia-Ukraine war has significantly impacted the world's political, economic, and social development, especially in the global energy market, energy security, and energy settlements. As the war continues, the energy crisis will further ferment, the global energy pattern and financial system will face a new adjustment, and the world economic recovery will suffer a drag. In the face of increased energy risks from war, more and more countries are paying more attention to stable energy supplies, gradually reducing their dependence on traditional fossil fuels, seeking alternative energy sources, and increasing their energy independence (Bricout et al., 2022). In addition, the economic risks of climate change have been rising in recent years. Achieving sustainable energy development globally, accelerating the green and low-carbon energy transition, and promoting cleaner alternatives to energy production have become common goals for all countries (Al Mamun et al., 2022). In these contexts, green finance is increasingly gaining attention. Green finance is considered one of the most effective and popular ways to meet the needs of environmentalism and capitalism (Atsu & Adams, 2021; Banga, 2019). Reboredo et al. (2020) and Naeem et al. (2021) manifest that investing in green finance significantly protects other investments from volatile and discouraging events, accelerating cross-market financialization. Based on these prior papers, the analysis of return and volatility connectedness among green financial assets proposes a new dimension that helps investors and policymakers allocate their portfolios rationally, develop applicable policies, and implement them to obtain returns.

Most prior literature currently focuses on the first and second-order moments (return and volatility) when studying the spillover effects among financial markets. The return distribution of some risky assets does not obey a normal distribution, and there is a fat tail phenomenon (Chunhachinda et al., 1997). At this time, it becomes essential to study the spillover effects of not only the lower-order moments but also the higher-order moments (skewness and kurtosis). Skewness reflects the asymmetry of asset returns and risky collapses, and kurtosis reflects tail fatness. Therefore, skewness spillover reflects the propagation of return asymmetries in the market, and kurtosis spillover reflects the propagation of extreme events in the market (Zhang, Jin, et al., 2022; Nekhili & Bouri, 2023). The volatility effects of financial spillovers are usually asymmetric. “Bad” spillovers (spillovers that may reduce asset prices) are more volatile than “good” spillovers (spillovers that may raise asset prices) because financial markets are more sensitive to negative shocks (Cui et al., 2022). However, the existing literature on the asymmetric analysis of spillover effects in financial markets mainly focuses on traditional financial markets such as commodity markets (Bouri et al., 2021; Finta & Aboura, 2020). The higher-order moment spillover effects of green financial markets are currently untapped areas.

Based on the above background, this dissertation applies a newly developed econometric model to assess the impact of global economic, political, and other crisis events, such as COVID-19 and the Russia-Ukrainian war, on low-order and high-order moments spillovers in traditional and green financial markets. This helps investors and policymakers to effectively capture the upside and downside risks in financial markets for effective risk aversion and early warning system establishment. The outline and main findings of this dissertation are summarized as follows:

In chapter 2, we analyze the connectedness between the sentiment index and the return and volatility of the crude oil, stock and gold markets by employing the time-varying parameter vector autoregression model during the coronavirus disease (COVID-19) epidemic. Our sentiment index is constructed via text mining technology. We also employ a network to visualize and better understand the structure of the connectedness. The results confirm that the sentiment index is the net pairwise directional connectedness receiver, while the infectious disease equity market volatility tracker is the transmitter. Furthermore, the impact of the COVID-19 pandemic on the total connectedness of volatility is unprecedented.

In chapter 3, we investigate the dynamic connectedness between the ESG stock index, the renewable energy stock index, the green bond stock index, the sustainability stock index, and the carbon emission futures by employing a novel method: the DCC-GARCH-based dynamic connectedness approach. Given the strong volatility spillover among these indexes, we adopt the DCC-GARCH t-copula model to calculate these indexes' hedging ratios and portfolio weights. Our findings show that the carbon emission futures are the volatility transmitter, and the green bond is the volatility receiver. The total dynamic connectedness is affected by international political, economic, and other events. Furthermore, for stock market volatility investors, taking the long position in carbon emission futures and the short position in renewable energy stock can achieve the highest hedging effect.

In chapter 4, we assess the impact of the COVID-19 pandemic and the Russia-Ukraine war on the connectedness of lower-order moments (returns and volatility) and higher-order moments (skewness and kurtosis) in the markets of green bonds, clean energy, wind, solar, and sustainability indexes. To compare the spillover effects of these moments, we use the Diebold and Yilmaz and Barunik and Krehlik methods. Our findings show that the total spillover effect of lower-order moments is higher than that of higher-order moments in the time domain. In the frequency domain, the total return and skewness spillover are primarily concentrated in the short term, whereas the total volatility spillover is mainly concentrated in the long term. Furthermore, we observe that the spillover effect of the Russia-Ukraine war on the green finance market is mild, while the COVID-19 pandemic has a significant and unprecedented influence on the spillover of both lower- and higher-order moments in this market. Additionally, we note that before the COVID-19 outbreak, the total kurtosis spillover was irregular, but it became concentrated in the long term after the outbreak. Moreover, the continuation of

COVID-19 has had an unprecedented and long-lasting impact on the kurtosis and skewness of the green bond market.

References

Al Mamun, M., Boubaker, S., & Nguyen, D. K. (2022). Green finance and decarbonization: Evidence from around the world. *Finance Research Letters*, *46*, 102807. https://doi.org/10.1016/j.frl.2022.102807

Atsu, F., & Adams, S. (2021). Energy consumption, finance, and climate change: Does policy uncertainty matter? *Economic Analysis and Policy*, *70*, 490–501. https://doi.org/10.1016/j.eap.2021.03.013

Banga, J. (2019). The green bond market: a potential source of climate finance for developing countries. *Journal of Sustainable Finance & Investment*, *9*(1), 17–32. https://doi.org/10.1080/20430795.2018.1498617

Bouri, E., Lei, X., Jalkh, N., Xu, Y., & Zhang, H. (2021). Spillovers in higher moments and jumps across US stock and strategic commodity markets. *Resources Policy*, *72*, 102060. https://doi.org/10.1016/j.resourpol.2021.102060

Bricout, A., Slade, R., Staffell, I., & Halttunen, K. (2022). From the geopolitics of oil and gas to the geopolitics of the energy transition: Is there a role for European supermajors? *Energy Research & Social Science*, *88*, 102634. https://doi.org/10.1016/j.erss.2022.102634

Chunhachinda, P., Dandapani, K., Hamid, S., & Prakash, A. J. (1997). Portfolio selection and skewness: Evidence from international stock markets. *Journal of*

Banking & Finance, *21*(2), 143–167. https://doi.org/10.1016/s0378-4266(96)00032-5

Cui, J., Maghyereh, A., Goh, M., & Zou, H. (2022). Risk spillovers and time-varying links between international oil and China's commodity futures markets: Fresh evidence from the higher-order moments. *Energy*, *238*, 121751. https://doi.org/10.1016/j.energy.2021.121751

Diebold, F. X., & Yilmaz, K. (2012). Better to give than to receive: Predictive directional measurement of volatility spillovers. *International Journal of Forecasting*, *28*(1), 57–66. https://doi.org/10.1016/j.ijforecast.2011.02.006

Diebold, F. X., & Yılmaz, K. (2014). On the network topology of variance decompositions: Measuring the connectedness of financial firms. *Journal of Econometrics*, *182*(1), 119–134. https://doi.org/10.1016/j.jeconom.2014.04.012

Finta, M. A., & Aboura, S. (2020). Risk premium spillovers among stock markets: Evidence from higher-order moments. *Journal of Financial Markets*, *49*, 100533. https://doi.org/10.1016/j.finmar.2020.100533

Gkillas, K., Bouri, E., Gupta, R., & Roubaud, D. (2020). Spillovers in Higher-Order Moments of Crude Oil, Gold, and Bitcoin. *The Quarterly Review of Economics and Finance*, *84*. https://doi.org/10.1016/j.qref.2020.08.004

Hassan, M. K., Hasan, Md. B., Halim, Z. A., Maroney, N., & Rashid, Md. M. (2022). Exploring the dynamic spillover of cryptocurrency environmental attention across the commodities, green bonds, and environment-related stocks. *The*

North American Journal of Economics and Finance, *61*, 101700. https://doi.org/10.1016/j.najef.2022.101700

Heinlein, R., Legrenzi, G. D., & Mahadeo, S. M. R. (2021). Crude oil and stock markets in the COVID-19 crisis: Evidence from oil exporters and importers. *The Quarterly Review of Economics and Finance*, *82*, 223–229. https://doi.org/10.1016/j.qref.2021.09.007

Lorente, D. B., Mohammed, K. S., Cifuentes-Faura, J., & Shahzad, U. (2023). Dynamic connectedness among climate change index, green financial assets and renewable energy markets: Novel evidence from sustainable development perspective. *Renewable Energy*, *204*, 94–105. https://doi.org/10.1016/j.renene.2022.12.085

Malik, F. (2021). Volatility spillover between exchange rate and stock returns under volatility shifts. *The Quarterly Review of Economics and Finance*, *80*, 605–613. https://doi.org/10.1016/j.qref.2021.04.011

Mili, M., Al Amoodi, A. Y., & Bawazir, H. (2023). The asymmetric effect of COVID-19 on investor sentiment: evidence from NARDL model. *Review of Behavioral Finance*. https://doi.org/10.1108/rbf-02-2022-0068

Mo, B., Meng, J., & Zheng, L. (2022). Time and frequency dynamics of connectedness between cryptocurrencies and commodity markets. *Resources Policy*, *77*, 102731. https://doi.org/10.1016/j.resourpol.2022.102731

Naeem, M. A., Adekoya, O. B., & Oliyide, J. A. (2021). Asymmetric spillovers between green bonds and commodities. *Journal of Cleaner Production*, *314*, 128100. https://doi.org/10.1016/j.jclepro.2021.128100

Nekhili, R., & Bouri, E. (2023). Higher-order moments and co-moments' contribution to spillover analysis and portfolio risk management. *Energy Economics*, *119*, 106596. https://doi.org/10.1016/j.eneco.2023.106596

Rai, K., & Garg, B. (2022). Dynamic correlations and volatility spillovers between stock price and exchange rate in BRIICS economies: evidence from the COVID-19 outbreak period. *Applied Economics Letters*, *29*(8), 738–745. https://doi.org/10.1080/13504851.2021.1884835

Reboredo, J. C., Ugolini, A., & Aiube, F. A. L. (2020). Network connectedness of green bonds and asset classes. *Energy Economics*, *86*, 104629. https://doi.org/10.1016/j.eneco.2019.104629

Reinhart, C. M., & Rogoff, K. S. (2008). Is the 2007 US Sub-Prime Financial Crisis So Different? An International Historical Comparison. *American Economic Review*, *98*(2), 339–344. https://doi.org/10.1257/aer.98.2.339

Umar, Z., Jareño, F., & Escribano, A. (2021). Oil price shocks and the return and volatility spillover between industrial and precious metals. *Energy Economics*, *99*, 105291. https://doi.org/10.1016/j.eneco.2021.105291

Zhang, H., Jin, C., Bouri, E., Gao, W., & Xu, Y. (2022). Realized higher-order moments spillovers between commodity and stock markets: Evidence from

China. *Journal of Commodity Markets*, 100275.
https://doi.org/10.1016/j.jcomm.2022.100275

Zhang, J., Chen, Z., & Altuntaş, M. (2022). Tracing volatility in natural resources, green finance and investment in energy resources: Fresh evidence from China. *Resources Policy*, *79*, 102946.
https://doi.org/10.1016/j.resourpol.2022.102946

Chapter 2. The connectedness between the sentiment index and stock return volatility under COVID-19: a time-varying parameter vector autoregression approach

2.1. Introduction

[2]News has always been an important source of information for establishing market investment concepts. In recent years, the innovation of information technology has significantly increased the scope and speed of news dissemination. However, with the rapid increase in the volume of news and its sources, it has become increasingly impossible for investors or even a group of investors to find relevant news from a large amount of available news. Furthermore, an increasing number of countries, especially emerging markets, have opened their financial markets to the outside world. This allows foreign news to directly affect local market conditions. Nevertheless, for a long time, investigating the impact of news on investor behavior, as well as stock returns and volatility remains an arduous task. Moreover, it is important to make reasonable choices through news orientation and invest in a timely manner to obtain the maximum profit from the investment plan. Therefore, how do we deal with this news to guide our investment? How do we systematically identify good news (or bad news)? Fortunately, in the past decade, natural language processing has made text mining and the analysis of large amounts of text information to extract key features, such as themes or tone, significant. Therefore, in our study, we select the dataset of "a million news headlines" constructed by Kulkarni (2018), which contains data of news headlines published over 18 years and sourced from a reputable Australian news source (ABC, Australian Broadcasting Corporation) for text mining. This news headline dataset comprises the entire content of articles published on the ABC news website within a given date range. There are 200 articles worldwide every day. Therefore, this dataset is very representative of global data, and it can be assured that every significant event worldwide will be captured therein.

Moreover, owing to the coronavirus disease (COVID-19) pandemic, daily life and economic activities have been severely disrupted. After the outbreak, the impact of the disease has exceeded the range of mortality and morbidity worldwide. Transportation between countries is restricted, which further decelerates the development of the global economy. Most importantly, certain panicky situations between consumers and companies have distorted the usual consumption patterns and caused market anomalies (McKibbin and Fernando, 2020). Furthermore, some policies adopted by the government, such as the banning of public gatherings, restriction on international travel, and so on, as well as the collapse of the healthcare system in some countries will affect people's emotions, and even market sentiments. According to Donadelli et al. (2017), the spread of infectious diseases also brings fear to the market, thereby prompting investors to invest in safe assets to deal with the uncertainty. Meanwhile, global financial markets have also responded to changes, and global stock indexes have

[2] Chapter 2 is based on the published paper: Zhang, W., & Hamori, S. (2021). THE CONNECTEDNESS BETWEEN THE SENTIMENT INDEX AND STOCK RETURN VOLATILITY UNDER COVID-19: A TIME-VARYING PARAMETER VECTOR AUTOREGRESSION APPROACH. *The Singapore Economic Review*, 1–32. https://doi.org/10.1142/s0217590822500023

plummeted. In March 2020, circuit breakers were triggered four times within ten days, and prices surged by 20% in three days in the US stock market. This phenomenon is very rare in history, and its appearance can be traced back to 1997. Owing to the global blockade of the 2020 COVID-19 epidemic, the demand for crude oil has almost diminished. Consequently, investors continue to sell the May West Texas Intermediate (WTI) crude oil futures contract which will expire on Tuesday. The large-scale sell-off caused US oil prices to fall into the "negative" range, exceeding US$ 40 at the lowest point, indicating a decline of 320%. However, while the COVID-19 epidemic has severely affected the stock and oil markets, the price of gold has continued to rise. Because of concerns about the impact of the COVID-19 pandemic on the global economy, investors have invested money in precious metals, thus the price of gold has climbed to a record high.

With these factors in mind, the objectives of our study are as follows: first, by using the text mining method to analyze the sentiment of the dataset of a million news headlines, we successfully construct the sentiment index (SI). Thereafter, we employ the time-varying parameter vector autoregression (TVP-VAR) model to investigate the connectedness between the sentiment index (SI) and stock market under the impact of the COVID-19 pandemic. With the continuity of the pandemic worldwide, people are still panicky about COVID-19, and news media continue to focus on situation. Through the dissemination of information by the news media, the panic about the COVID-19 pandemic will not only spread among the global populace but also affect the stock market. Therefore, investigating the connectedness between the SI and the return and volatility of the stock market under the impact of the COVID-19 pandemic is important for investment orientation. Second, based on pairwise directional connectedness, we can observe the individual connectedness between the SI and other variables. Furthermore, based on the results of the pairwise directional connectedness, we can apply the connectedness network, which can visualize and facilitate our understanding of the connectedness structure. Third, analyzing the total connectedness over time allows us to comprehend the impact of specific extreme events on connectedness.

Our study is the first to employ the text mining method to construct the SI and subsequently evaluate the connectedness between the SI, as well as the crude oil, stock, and gold markets under the impact of the COVID-19 pandemic. Similarly, Sun et al. (2021) explore whether investor sentiment driven by COVID-19- and economic-related announcements is priced in medical stock portfolios in China, Hong Kong, South Korea, Japan, and the US. Furthermore, Gondaliya et al. (2021) investigate the sentiment analysis and prediction of the Indian stock market under the impact of the COVID-19 pandemic and establish that sentiment has a major impact on the trend of the Indian stock market, and the pandemic will only increase its momentum. However, they use a preconstructed SI, whereas, in our study, we employ the text mining method to construct the SI, which allows us to freely choose the data source of the SI to better realize the variable combination. Moreover, we use the more excellent TVP-VAR model, which is applied to the stock, crude oil, and gold markets.

The main findings of our study are as follows: first, the empirical results of averaged connectedness dynamics show that there is a strong connectedness between the SI and Infectious Disease Equity Market Volatility Tracker (IDEMVT) both in return and volatility series. The SI contributes the most spillover effect to the return of the Standard and Poor's (S&P) 500 among the S&P 500 Index, WTI futures, and Gold futures, and contributes the most spillover effect on the volatility of the WTI among the three stock volatility series. Second, the net directional connectedness values of SI and IDEMVT are negative and positive, respectively, indicating that SI is the net pairwise directional connectedness (NPDC) receiver and IDEMVT is the NPDC transmitter in both the return and volatility series. Third, the network analysis further demonstrates that SI acts mainly as a spillover receiver, whereas IDEMVT acts as a spillover transmitter, either in return series or volatility series. Finally, the result of the total connectedness using the TVP-VAR model indicates that, compared with the impact of the 2008 financial crisis, the 2010 European debt crisis, and the 2013 sharp drop in gold prices, the impact of the 2020 COVID-19 epidemic on the financial market is unprecedented. The impact of the 2020 COVID-19 pandemic on stock markets acutely surpasses the impact of the 2008 global financial crisis and the 2010 European debt crisis on stock markets.

The remainder of this paper is organized as follows: the related research is introduced in Section 2.2, while the algorithm for the TVP-VAR and Diebold–Yilmaz (2014) models is explained in Section 2.3. In Section 2.4, the employed variables and their descriptive statistics are presented, while the empirical results of the averaged connectedness dynamics and total connectedness over time are presented in Section 2.5. Finally, the conclusions are given in Section 2.6.

2.2. Literature review

In recent years, with the accumulation of financial big data and the increase in the availability of internet text data, an increasing number of studies have tried to extract emotional information from multiple links, such as media reports, company news, and social networks, for asset price fluctuation forecasts and behavioral assets. Therefore, text mining technology is widely employed in various fields. For example, Antweiler et al. (2004) employ text mining to establish that the text sentiment contained in online media information can predict future stock fluctuations. Crone et al. (2014) apply text mining to construct sentiment indicators to predict exchange rates and conclude that sentiment indicators can explain the market trend of exchange rate returns. Furthermore, Feldman et al. (2010) and Price et al. (2012) extract the sentiment information contained in a company's disclosed text and report that this information is closely related to the company's future stock value and profitability. Jiang et al. (2019) construct a manager's SI through text mining and discover that it can reversely predict the overall return of the stock market in the future. Several studies have analyzed the connectedness between SI and the stock market. Johnman et al. (2018) use Guardian Media Group's business news to investigate the statistical and economic impact of the Financial Times Stock Exchange (FTSE) 100 Index on the positive and negative sentiments of daily excess return and volatility and report that business news sentiment does not affect the excess returns of the FTSE 100 Index, but it does affect volatility. Wang et al. (2006)

investigate the relationship between sentiment and return/volatility and find that most of their sentiment measures are caused by return and volatility rather than vice versa.

The TVP-VAR model with random volatility proposed by Primiceri (2005) has been widely employed because it allows us to capture the potentially time-varying nature of the economic infrastructure (Nakajima, 2011) flexibly and powerfully. Jebabli et al. (2014) employed the TVP-VAR model to estimate the shock transmission between food, energy, and financial markets and find that the stock market became a net transmitter of volatility shocks, while crude oil became a net receiver after the 2008 global financial crisis. Wen et al. (2019) use the TVP-VAR model to investigate the combined impact of speculative activities in the US dollar, gold, stock, and crude oil futures market on crude oil prices and determine the time-varying effects of these financial factors on oil prices, which is reflected in the change in the impact of financial factors on crude oil prices over time, and the 2008 financial crisis has strengthened the relationship between financial markets and crude oil prices. Some researchers compare the results of the TVP-VAR model with those of the rolling window model developed by Diebold and Yilmaz (2009, 2012, 2014). For example, Liu et al. (2020) report that although the rolling window method is simple, it has some disadvantages. First, the results of the rolling window method are directly affected by the manually specified window size in advance. The results always differ for various window sizes. Additionally, it is difficult to choose the optimal window size. Second, the rolling window method cannot obtain the result in the first window, which leads to the loss of observations, especially when the window size is large. Finally, the rolling window method is extremely sensitive. When the window contains or rejects outliers for the first time, the results may jump according to Gabauer et al. (2018), Dahir et al. (2019), Geraci et al. (2018), and Antonakakis et al. (2018).

The COVID-19 epidemic has significantly impacted the global economy. On the one hand, the spread of the epidemic has accelerated globally, uncertainty has risen sharply, and investor confidence has been frustrated, which has triggered turmoil in financial and capital markets. On the other hand, to control the spread of the epidemic, countries strictly restrict the movement of people and transportation, thereby stagnating the economy, which puts pressure on the economic operation from both the consumer and production sides (Baker, Bloom, Davis, and Terry, 2020; Barro, Ursua, and Weng, 2020). Furthermore, as the panic caused by the spread of the COVID-19 epidemic has not been effectively alleviated initially, the US stock market has fluctuated sharply and experienced four circuit breakers in March 2020. Along with the circuit breakers in the US stock market, the world's major stock markets have also begun to show a declining trend, which is undoubtedly a disaster for investors. Similar to Onali et al. (2020), Gil-Alana et al. (2020), and Al-Awadhi et al. (2020), many researchers have begun to investigate the impact of the COVID-19 epidemic on stock market return volatilities.

2.3. Empirical Techniques

2.3.1. An algorithm for the TVP-VAR model

To accurately evaluate the spillover effects of SI and IDEMVT on three other stock indexes, we employ the dynamic connectedness methodology (Diebold and Yilmaz, 2009, 2012, 2014) on the estimation results of the TVP-VAR with time-varying covariances (Koop and Korobilis, 2014). Employing the TVP-VAR model based on the dynamic connectedness methodology has several advantages: (1) Compared with the VAR model with a rolling window, the overall fluctuations of the TVP-VAR model are relatively stable, as found by Korobilis and Yilmaz (2018); (2) The rolling window can be chosen more arbitrarily because it does not need to stick to the window size. (Chatziantoniou and Gabauer, 2021).

Following Chatziantoniou and Gabauer (2021), we summarize the TVP-VAR model. The TVP-VAR model with a p lag can be defined as follows:

$$\boldsymbol{x}_t = \sum_{i=1}^{p} \boldsymbol{\Phi}_{it}\boldsymbol{x}_{t-i} + \boldsymbol{\varepsilon}_t,\ \ \boldsymbol{\varepsilon}_t|\boldsymbol{\Omega}_{t-1} \sim N(\boldsymbol{0}, \boldsymbol{\Sigma}_t) \tag{2.1}$$

$$vec(\boldsymbol{\Phi}_{it}) = vec(\boldsymbol{\Phi}_{it-1}) + \boldsymbol{\eta}_t,\ \ \boldsymbol{\eta}_t|\boldsymbol{\Omega}_{t-1} \sim N(\boldsymbol{0}, \boldsymbol{\Xi}_t) \tag{2.2}$$

where $\boldsymbol{\Omega}_{t-1}$ indicates that all available information until $t-1$. The variable $\boldsymbol{x}_t$ is an $m\times1$ dimensional vector, $\boldsymbol{\varepsilon}_t$ is an $m\times1$ dimensional vector of independent and identically distributed disturbance, $\boldsymbol{\Sigma}_t$ is an $m\times m$ dimensional matrix, $\boldsymbol{\eta}_t$ is an $m^2\times1$ dimensional vector, and $\boldsymbol{\Xi}_t$ is an $m^2\times m^2$ dimensional matrix. We select five lags for the return series and six lags for the volatility series of the variables using the Hannan–Quinn information criterion (HQC).

Next, we employ Primiceri (2005) prior to the initialization of the Kalman filter. Therefore, we define $\boldsymbol{\Phi}_{OLS}$, $\boldsymbol{\Sigma}^{\Phi}_{OLS}$, and $\boldsymbol{\Sigma}_{OLS}$, which are equal to the VAR evaluation results of the first 250 days by Korobilis and Yilmaz (2018), as follows:

$$vec(\boldsymbol{\Phi}_0) \sim N(vec(\boldsymbol{\Phi}_{OLS}), \boldsymbol{\Sigma}^{\Phi}_{OLS}) \tag{2.3}$$

$$\boldsymbol{\Sigma}_0 = \boldsymbol{\Sigma}_{OLS} \tag{2.4}$$

Because of the numerical stability, we consider employing the decay factors in the Kalman filter methodology. The choice of decay factors is similar to the choice of priors in general, and it is based on the amount of time variation predicted in the parameters. In our study, we also employ two decay factors: $k_1 = 0.99$ and $k_2 = 0.99$. Thus, the multivariate Kalman filter is defined as follows:

$$vec(\boldsymbol{\Phi}_t)|\boldsymbol{x}_{1:t-1} \sim N(vec(\boldsymbol{\Phi}_{t|t-1}), \boldsymbol{\Sigma}^{\Phi}_{t|t-1}) \tag{2.5}$$

$$\boldsymbol{\Phi}_{t|t-1} = \boldsymbol{\Phi}_{t-1|t-1} \tag{2.6}$$

$$\boldsymbol{\varepsilon}_t = \boldsymbol{x}_t - \boldsymbol{\Phi}_{t|t-1}\boldsymbol{x}_{t-1} \tag{2.7}$$

$$\boldsymbol{\Sigma}_t = k_2\boldsymbol{\Sigma}_{t-1|t-1} + (1-k_2)\boldsymbol{\varepsilon}'_t\boldsymbol{\varepsilon}_t \tag{2.8}$$

$$\boldsymbol{\Xi}_t = (1-k_1^{-1})\,\boldsymbol{\Sigma}^{\Phi}_{t-1|t-1} \tag{2.9}$$

$$\boldsymbol{\Sigma}^{\Phi}_{t|t-1} = \boldsymbol{\Sigma}^{\Phi}_{t-1|t-1} - \boldsymbol{\Xi}_t \tag{2.10}$$

$$\boldsymbol{\Sigma}_{t|t-1} = \boldsymbol{x}_{t-1}\boldsymbol{\Sigma}^{\Phi}_{t|t-1}\boldsymbol{x}'_{t-1} + \boldsymbol{\Sigma}_t \tag{2.11}$$

We update $\boldsymbol{\Phi}_t$, $\boldsymbol{\Sigma}^{\Phi}_t$, and $\boldsymbol{\Sigma}_t$ given the information at time t as follows:

$$vec(\boldsymbol{\Phi}_t)|\boldsymbol{x}_{1:t} \sim N(vec(\boldsymbol{\Phi}_{t|t}), \boldsymbol{\Sigma}^{\Phi}_{t|t}) \tag{2.12}$$

$$\boldsymbol{KG}_t = \boldsymbol{\Sigma}^{\Phi}_{t|t-1}\boldsymbol{x}'_{t-1}\boldsymbol{\Sigma}^{-1}_{t|t-1} \tag{2.13}$$

$$\boldsymbol{\Phi}_{t|t} = \boldsymbol{\Phi}_{t|t-1} + \boldsymbol{KG}_t(\boldsymbol{x}_t - \boldsymbol{\Phi}_{t|t-1}\boldsymbol{x}_{t-1}) \tag{2.14}$$

$$\boldsymbol{\Sigma}^{\Phi}_{t|t} = (\boldsymbol{I} - \boldsymbol{KG}_t)\boldsymbol{\Sigma}^{\Phi}_{t|t-1} \tag{2.15}$$

$$\boldsymbol{\varepsilon}_{t|t} = \boldsymbol{x}_t - \boldsymbol{\Phi}_{t|t}\boldsymbol{x}_{t-1} \tag{2.16}$$

$$\boldsymbol{\Sigma}_{t|t} = k_2\boldsymbol{\Sigma}_{t-1|t-1} + (1-k_2)\boldsymbol{\varepsilon}'_{t|t}\boldsymbol{\varepsilon}_{t|t} \tag{2.17}$$

where $\boldsymbol{KG}_t$ is the Kalman gain, which accounts for the extent to which the parameter $\boldsymbol{\Phi}_t$ should be changed in a given state. Moreover, if the parameter $\boldsymbol{\Sigma}^{\Phi}_{t|t-1}$ is uncertain, for example, if the parameter $\boldsymbol{\Sigma}^{\Phi}_{t|t-1}$ is small, then the parameter $\boldsymbol{\Phi}_t$ should be similar to its prior state. However, if the parameter $\boldsymbol{\Sigma}^{\Phi}_{t|t-1}$ is large, then the parameter $\boldsymbol{\Phi}_t$ should be adjusted to its prior state. Next, regarding the error variance $\boldsymbol{\Sigma}_t$, if it is small, then the evaluation results are very accurate, and the parameter $\boldsymbol{\Phi}_t$ should be similar to its prior value. However, if the error variance $\boldsymbol{\Sigma}_t$ is large, then the evaluation results are inaccurate, and the parameter $\boldsymbol{\Phi}_t$ should be adjusted to its prior value.

Although we have evaluated the TVP, the generalized impulse response and the generalized forecast error variance decomposition (GFEVD) (Koop et al. 1996; Pesaran and Shin, 1998) where the dynamic connectedness spillover tables are built on (Diebold and Yilmaz, 2009, 2012, 2014) still depend on the moving average (MA) representation of the VAR model. Hence, we should transform the TVP-VAR model into a TVP-VMA model using the following equation:

$$\boldsymbol{x}_t = \sum_{i=1}^{p}\boldsymbol{\Phi}_{it}\boldsymbol{x}_{t-i} + \boldsymbol{\varepsilon}_t = \sum_{j=1}^{\infty}\boldsymbol{\Lambda}_{jt}\boldsymbol{\varepsilon}_{t-j} + \boldsymbol{\varepsilon}_t \tag{2.18}$$

2.3.2. Dynamic connectedness method: Diebold and Yilmaz (2014)

After explaining the principles of the TVP-VAR model, we provide a detailed description of the Diebold and Yilmaz connectedness index method, which is developed by Diebold and Yilmaz (2009, 2012, 2014). Compared with other methods, the Pearson correlation coefficient is used to measure the degree of correlation (linear correlation) between two variables, and its value is between -1 and 1[3], while connectedness can be used to analyze the spillover effect between two variables. Conditional correlation is generally used to study the relationship between two variables, while connectedness is used to study the relationship between multiple variables. Granger causality is a statistical concept of causality that is based on prediction, but connectedness is based

[3] We put the correlation matrix of return and volatility series in appendix respectively.

on assessing the share of changes in forecast errors in different locations (companies, markets, countries, etc.) due to shocks occurring elsewhere. Connectedness is closely related to the familiar econometric concept of variance decomposition, where the prediction error variance of a variable is decomposed into parts attributed to various variables in the system. Diebold and Yilmaz (2014) claimed that connectedness is at the core of modern risk measurement and management. The idea of connectedness is critical in market risk (return connectivity and portfolio concentration), credit risk (default connectivity), counterparty and deadlock risk (bilateral and multilateral contract connectivity), especially systemic risks (system-wide connectivity). This is also very important for understanding the underlying basic macroeconomic risks, especially business cycle risks (the correlation of actual activities within and between countries). So, for example, the high connectedness between two stocks means that there is a strong spillover effect between them. Therefore, when investors invest in one stock, they should also consider whether to invest in the other stock.

This methodology is built based on combining GFEVD with the VAR(p) model. Hence, the contribution of variable j to variable i's H-step-ahead GFEVD can be expressed as follows:

$$\boldsymbol{\Psi}_{ij}^{g}(H) = \frac{\boldsymbol{\sigma}_{jj}^{-1}\sum_{h=0}^{H-1}(\boldsymbol{e}_i'\boldsymbol{\Lambda}_h\boldsymbol{\Sigma}\boldsymbol{e}_j)^2}{\sum_{h=0}^{H}(\boldsymbol{e}_i'\boldsymbol{\Lambda}_h\boldsymbol{\Sigma}\boldsymbol{\Lambda}_h'\boldsymbol{e}_i)} \tag{2.19}$$

where $\boldsymbol{\Sigma}$ is the variance matrix of the error vector $\boldsymbol{\varepsilon}$, $\boldsymbol{\sigma}_{ii}$ represents the standard deviation of the error term for the *jth* equation, and $\boldsymbol{e}_i$ is the selection vector with one as the *ith* element and zero otherwise. Moreover, the sum of each row's elements in the variance decomposition table is not consequentially equal to 1: $\Sigma_{j=1}^{N}\boldsymbol{\Psi}_{ij}^{g}(H) \neq 1$. To compute the connectedness index by employing the information obtained from the variance decomposition matrix, Diebold and Yilmaz (2012) standardize each entry of the variance decomposition table by the sum of the rows as follows:

$$\widetilde{\boldsymbol{\Psi}}_{ij}^{g}(H) = \frac{\boldsymbol{\Psi}_{ij}^{g}(H)}{\sum_{j=1}^{N}\boldsymbol{\Psi}_{ij}^{g}(H)} \tag{2.20}$$

$\widetilde{\boldsymbol{\Psi}}_{ij}^{g}(H)$ represents the pairwise connectedness from variable j to variable i at horizon H. Furthermore, $\Sigma_{j=1}^{N}\widetilde{\boldsymbol{\Psi}}_{ij}^{g}(H) = 1$ and $\Sigma_{i,j=1}^{N}\widetilde{\boldsymbol{\Psi}}_{ij}^{g}(H) = N$. After obtaining the pairwise spillover, we aggregate the total connectedness. In traditional terms, the total connectedness index is defined as follows:

$$C(H) = \frac{\sum_{\substack{i,j=1\\ i\neq j}}^{N}\widetilde{\boldsymbol{\Psi}}_{ij}^{g}(H)}{\Sigma_{i,j=1}^{N}\widetilde{\boldsymbol{\Psi}}_{ij}^{g}(H)} = \frac{\sum_{\substack{i,j=1\\ i\neq j}}^{N}\widetilde{\boldsymbol{\Psi}}_{ij}^{g}(H)}{N} \tag{2.21}$$

However, in our study, we refer to Chatziantoniou and Gabauer (2021), who explain that their variance shares are always larger or equal to all cross-variance shares because of the construction based on the results of Monte Carlo simulations. This finding indicates that the traditional total connectedness index ranges between $[0, \frac{N-1}{N}]$. Therefore, Chatziantoniou and Gabauer (2021) adjust the total connectedness index slightly to obtain the average amount of network co-movement in percent as follows:

$$C(H) = \frac{\sum_{\substack{i,j=1 \\ i \neq j}}^{N} \widetilde{\boldsymbol{\Psi}}_{ij}^{g}(H)}{N-1} \tag{2.22}$$

Additionally, the directional connectedness series is defined as follows:

Total directional connectedness (FROM):

$$C_{i\leftarrow\cdot}(H) = \frac{\sum_{\substack{j=1 \\ j \neq i}}^{N} \widetilde{\boldsymbol{\Psi}}_{ij}^{g}(H)}{\sum_{i=1}^{N} \widetilde{\boldsymbol{\Psi}}_{ij}^{g}(H)} \tag{2.23}$$

The total directional connectedness (FROM) measures the total directional connectedness received by variable *i* from all other variables.

Total directional connectedness (TO):

$$C_{\cdot\leftarrow i}(H) = \frac{\sum_{\substack{j=1 \\ j \neq i}}^{N} \widetilde{\boldsymbol{\Psi}}_{ji}^{g}(H)}{\sum_{j=1}^{N} \widetilde{\boldsymbol{\Psi}}_{ji}^{g}(H)} \tag{2.24}$$

The total directional connectedness (TO) measures the total directional connectedness transmitted by variable *i* to all other variables.

Net total directional connectedness:

$$C_i(H) = C_{\cdot\leftarrow i}(H) - C_{i\leftarrow\cdot}(H) \tag{2.25}$$

The net total directional connectedness of variable *i* is the difference between total directional connectedness (TO) and total directional connectedness (FROM). If the net total directional connectedness $C_i(H) > 0$ $(C_i(H) < 0)$, then variable *i* can be seen as an NPDC transmitter (receiver) because it transmits (receives) a greater spillover effect to (from) other variables.

Net pairwise directional connectedness:

$$NPDC_{ij}(H) = \widetilde{\boldsymbol{\Psi}}_{ji}^{g}(H) - \widetilde{\boldsymbol{\Psi}}_{ij}^{g}(H) \tag{2.26}$$

The net pairwise directional is the difference between pairwise (TO) connectedness and pairwise (FROM) connectedness, exhibiting bilateral transmission connectedness between variable *i* and variable *j*.

2.4. Data

This study employs the daily data of a million news headlines SI, IDEMVT, Crude Oil WTI futures (WTI), S&P 500 (SP500), and COMEX Gold futures (GC). Our data, which include the 2008 global crisis, the 2010 European sovereign debt crisis, and the 2020 COVID-19 pandemic, span from January 4, 2006 to December 30, 2020. To eliminate the influence of the exchange rate on the analysis results, we unify the currency units of all variables to US dollars. More details of the variables used in this study can be found in Table 2.1.

Table 2.1. Variables in this study.

Variable	Data	Source
SI	A Million News Headlines Sentiment Index	kaggle.com
IDEMVT	Infectious Disease Equity Market Volatility Tracker	Economic Policy Uncertainty
WTI	Crude Oil WTI Futures (USD/Barrel)	Investing.com
SP500	S&P 500 Index	Investing.com
GC	COMEX Gold futures	Bloomberg

We obtain a million news headlines from kaggle.com[4], as developed by Kulkarni (2018), which contains data on news headlines published over 18 years and sourced from a reputable Australian news source, i.e., ABC[5]. This news headline dataset contains the historical summary records of important global events from the beginning of 2003 and is still in a state of continuous updating. As we aim to compare the impact of the 2008 financial crisis and the 2020 COVID-19 pandemic on the variables used in our study, we select the sample period from January 4, 2006 to December 30, 2020, not only in the news headline dataset but also in all other variables. Moreover, this dataset includes the entire content of articles published on the ABC website within a given time frame. With a daily volume of 200 articles and a strong emphasis on foreign news, it can be reasonably ascertained that any significant event has been covered.

After we derive the news headline data, we employ the text mining methodology to approach the emotional content of text programmatically by applying the R studio. Herein, we adopt the method of analyzing the sentiment of the text to treat the text as a combination of its individual words and the sentiment content of the entire text as the sum of the sentiment content of individual words. In text mining, there are a variety of methods and dictionaries for evaluating opinions or sentiments, such as Hu & Liu Opinion Lexicon (Hu and Liu, 2014), National Research Council Canada (NRC) Word-Sentiment Association Lexicon (Mohammad and Turney, 2013), and so on. In our study, we employ the tidy package in R studio developed by Silge and Robinson (2016), which provides access to several sentiment lexicons:

- Finn Årup Nielsen (AFINN) Sentiment Lexicon developed by Nielsen (2011)
- NRC Word-Sentiment Association Lexicon developed by Mohammad and Turney (2013)

Both lexicons are based on monograms, i.e., single words. The two dictionaries contain numerous English words and assign scores for positive/negative emotions to the words; they may also assign scores for emotions, such as joy, anger, and sadness. The AFINN dictionary from Nielsen (2011) assigns a score from -5 to 5 for words, where negative and positive scores indicate negative and positive emotions, respectively. The NRC dictionary by Mohammad and Turney (2013) categorizes words in a binary fashion ("1"/ "0") as angry, expecting, disgusting, fear, happiness, sadness, surprise, and trust. Kulkarni (2018) summarized the notable events around the world from the beginning of 2003 to the end of 2020. This includes the entire corpus of articles published on the ABC website within a given time frame. There are 200 articles every day, and the

[4] Available at: https://www.kaggle.com/therohk/million-headlines

[5] Australian Broadcasting Corporation's official site: https://www.abc.net.au/

attention to international news is very high. Kulkarni (2018) deleted all the punctuation minus signs of all news headlines collected, and arranged them in time series into a table. Since Kulkarni (2018) has removed the punctuation when constructing a million news headlines data set, so we don't need to delete the punctuation in the news headlines. In addition, the AFINN dictionary and NRC dictionary have separately evaluated various types of words by score evaluation and "1"/ "0" classification, so here we don't need to standardize verbs and nouns.

After these two dictionaries score each news item each day separately, we take the average of the scores for all news items on that day, and the average value is the SI for that day. Therefore, after the test mining process, a million news headlines, 200 news items per day, and a total of 1,017,058 rows of original data are processed into the daily SI from January 4, 2006 to December 30, 2020. However, when analyzing the spillover impact of return and volatility, we find that the SI obtained through AFINN and NRC dictionaries has almost the same spillover effect on the return and volatility of other variables. Therefore, we finally consider the SI obtained by the AFINN dictionary to fit the TVP-VAR model and include the spillover table of the NRC dictionary case in the appendix.

Additionally, regarding the IDEMVT developed by Baker et al. (2020), we derive this dataset from the Economic Policy Uncertainty index. Assessing the economy of the COVID-19 pandemic is crucial for policymakers, but it is challenging because of the rapid development of the crisis. Therefore, Baker et al. (2020) have identified three indicators: stock market volatility, newspaper-based economic uncertainty, and subjective uncertainty in business expectations surveys which provide real-time forward-looking uncertainty measures. They employed these indicators to construct the IDEMVT to record and quantify the tremendous increase in economic uncertainty. More precisely, The IDEMVT is processed using the following steps:

- E: {economic, economy, financial}
- M: {"stock market," equity, equities, "Standard and Poor's"}
- V: {volatility, volatile, uncertain, uncertainty, risk, risky}
- ID: {epidemic, pandemic, virus, flu, disease, coronavirus, mers, sars, ebola, H5N1, H1N1}.

First, the terms are specified in four sets, as shown above. Second, approximately 3000 daily newspaper articles in the US, where E, M, V, and ID contain at least one term, are counted. Third, the original EMV-ID count is scaled by the count of all articles on the same day. Finally, the resulting series is rescaled multiplicatively to reflect their approach to scale a categorical EMV series. Next, regarding the other three variables, for the crude oil market, we employ the daily data of WTI futures, whose price is often used as a reference price reflecting the current world oil market. For the stock market, we select the S&P 500 Index in the US. The S&P 500 Index is the best representation of the American stock market because it measures the stock performance of 500 large companies listed on the American Stock Exchange. For the gold market, we use the daily GC data, which are the world's most widely traded gold futures contract. The contract offers superior liquidity, trading an equivalent of approximately 27 million ounces daily[6].

A plot of the raw data series is shown in Figure 2.1, where SI is the SI data, IDEMVT is the volatility data, and WTI, S&P 500, and GC are the price data. It is evident that the SI data are distributed around 0. Besides, we can observe that the SI moves significantly in the beginning of 2015 and the end of 2015. We checked the raw data series of SI and found the outlier on January 7, 2015 and December 31, 2015 because of the Charlie Hebdo shooting event[7] on January 7, 2015 and New Year's Eve sexual assaults in Germany[8] on December 31, 2015. Around mid-2008 and 2020, there are some fluctuations in the uptrend or downtrend in IDEMVT, WTI, S&P 500, and GC.

In our study, we employ the logarithmic method for WTI, S&P 500, and GC to calculate the return series, except for SI and IDEMVT. Figure 2.2 shows a plot of the return series. After we derive the return series of dataset, we use autoregressive moving average (ARMA)-GARCH model to calculate the volatilities of the WTI, S&P 500, and GC which are visualized in Figure 2.3. We choose the lag of GARCH model based on the Akaike information criterion (AIC) and employ the GARCH (1, 1) model.[9] As shown in Figure 2.3, compared with S&P 500 and GC, the volatility of WTI exhibits a relatively stable trend and fluctuates fiercely around 2020. Additionally, the volatility of WTI and S&P 500 show a relatively similar fluctuation trend. Specifically, there is an evident sudden upward fluctuation around 2009, late-2011, and 2020.

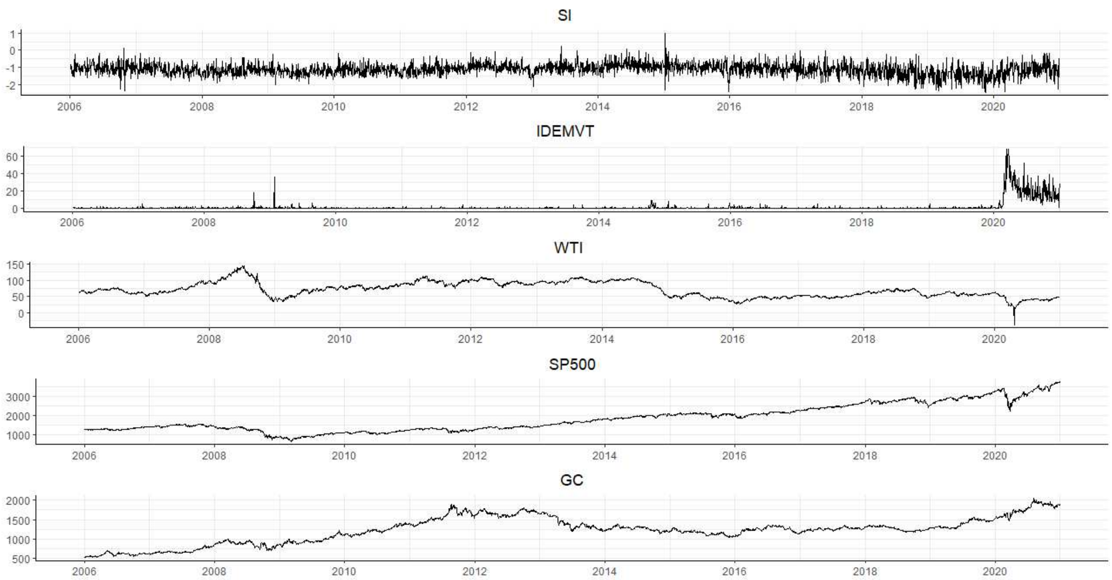

Figure 2.1. Time variations of raw data series.

Notes: SI refers to A Million News Headlines Sentiment Index; IDEMVT refers to the Infectious Disease Equity Market Volatility Tracker, WTI refers to crude oil WTI futures, SP500 refers to the S&P 500 Index, GC refers to COMEX Gold futures, SI is sentiment index data, IDEMVT is volatility data, WTI, SP500, and GC are price data.

---

6 See the homepage for details: https://www.cmegroup.com/trading/why-futures/welcome-to-comex-gold-futures.html

7 Charlie Hebdo shooting event: https://en.wikipedia.org/wiki/Charlie_Hebdo_shooting

8 New Year's Eve sexual assaults in Germany: https://en.wikipedia.org/wiki/2015%E2%80%9316_New_Year%27s_Eve_sexual_assaults_in_Germany

9 Appendix reports the empirical results of ARMA-GARCH model.

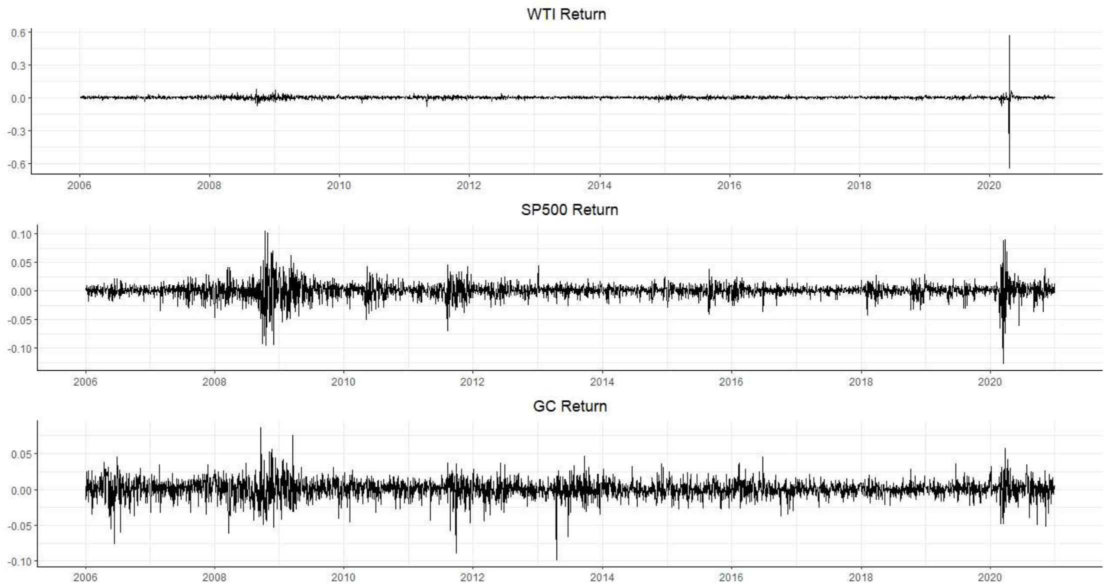

Figure 2.2. Time variations of return series.

Notes: WTI Return refers to the return of crude oil WTI futures; SP500 Return refers to the return of the S&P 500 Index; GC Return refers to the return of COMEX Gold futures; SI is the sentiment index, and IDEMVT is the volatility tracker, so we do not need to calculate their returns.

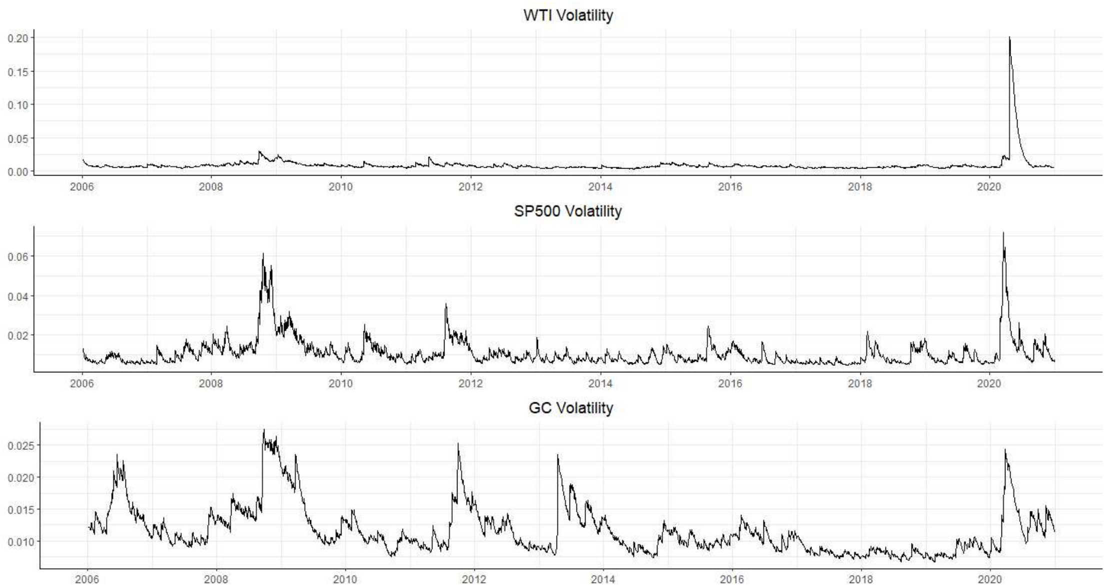

Figure 2.3. Time variations of volatility series by ARMA-GARCH model.

Notes: WTI volatility refers to the volatility of crude oil WTI futures; SP500 volatility refers to the volatility of the S&P 500 Index; GC volatility refers to the volatility of the COMEX Gold futures; SI is the sentiment index, and IDEMVT is volatility tracker, so we do not need to calculate their volatility.

Table 2.2 shows the descriptive statistics of the return series of WTI, S&P 500, and GC, including the raw SI and IDEMVT data series. Regarding the mean of the return series, among the S&P 500 Index, WTI futures, and Gold futures, only the return of WTI has a negative mean value, and SI has the smallest mean value. Furthermore, we can observe that there is a wide gap between the maximum and minimum IDEMVT values. According to the standard deviation, IDEMVT is the most volatile among the five variables, and WTI is the most volatile among the S&P 500 Index, WTI futures, and Gold futures. Additionally, for the skewness values, except for IDEMVT, the skewness values of the four other variables indicate that they are left-skewed. The positive value of the kurtosis value of these five variables indicates the leptokurtic, i.e., the five variables will see more peaked and fat tails.

Table 2.3 shows the volatility series of the WTI, S&P 500, and GC. Except for SI, the skewness values of the four other variables indicate that they are right-skewed. The kurtosis is the same as the return situation wherein these five variables are leptokurtic. Moreover, to ensure the stationarity of the return and volatility series, we use the augmented Dickey–Fuller (ADF) test exploited by Said et al. (1984). The results of the ADF tests show that the null hypothesis of each variable with a unit is rejected at a 5% significance level in both return and volatility, i.e., each variable does not have a unit root.

Table 2.2. Descriptive statistics of the return series.

Descriptive Statistics for Return					
	SI	IDEMVT	WTI	SP500	GC
Mean	−1.1036	1.6980	−0.0000	0.0003	0.0004
Median	−1.1042	0.0000	0.0003	0.0008	0.0004
Maximum	1.0000	68.3700	0.5675	0.1042	0.0863
Minimum	−2.4186	0.0000	−0.6399	−0.1277	−0.0982
Std. Deviation	0.3380	6.0163	0.0174	0.0132	0.0122
Skewness	−0.0006	5.5683	−4.3411	−0.6540	−0.3926
Kurtosis	1.2533	36.4571	841.0321	12.7788	5.8272
ADF	−6.4012***	−8.4981***	−55.8921***	−44.0957***	−42.3421***

Note. ADF: Augmented Dickey and Fuller Unit Root Test (1979); *** denotes rejection of the null hypothesis at 1% significance levels. SI is the sentiment index; IDEMVT is the volatility tracker.

Table 2.3. Descriptive statistics of the volatility series.

Descriptive Statistics for Volatility					
	SI	IDEMVT	WTI	SP500	GC
Mean	−1.1036	1.6980	0.0090	0.0110	0.0116
Median	−1.1042	0.0000	0.0071	0.0088	0.0106
Maximum	1.0000	68.3700	0.2018	0.0715	0.0275
Minimum	−2.4186	0.0000	0.0034	0.0048	0.0067
Std. Deviation	0.3380	6.0163	0.0116	0.0072	0.0038
Skewness	−0.0006	5.5683	10.6605	3.4938	1.5547
Kurtosis	1.2532	36.4571	134.1853	16.4971	2.4549
ADF	−6.4012***	−8.4981***	−7.0686***	−3.1159***	−4.7597***

Note. ADF: Augmented Dickey and Fuller Unit Root Test (1979); *** denotes rejection of the null hypothesis at the 1% significance level. SI is the sentiment index and IDEMVT is the volatility tracker.

2.5. Empirical results

2.5.1. Overview of averaged connectedness dynamics

We employ the TVP-VAR model to investigate the averaged connectedness between the SI, IDEMVT, WTI, S&P 500, and GC. Before the estimation process, we must choose the optimal lag length p for the VAR model. According to the Hannan–Quinn information criterion (HQC), we select lag lengths of 5 and 6 for the return and volatility series, respectively. Following Bekiros (2014), we choose the HQC to select the lags for the TVP-VAR model. We also employed the BIC to select the lags of return and volatility series. However, compared with the BIC, we think the lags selected by HQC can better capture the fluctuation of return and volatility. We also put the averaged dynamic connectedness table of return and volatility series whose lags selected by BIC in the appendix. Next, for the ahead forecasting horizon, we choose Horizon as H=10, according to Chatziantoniou and Gabauer (2021).

Tables 2.4 and 2.5 indicate the averaged dynamic connectedness of return and volatility using the TVP-VAR model. The values in the ith row and jth column indicate the spillover effect from market j to market i, and vice versa. “TO” represents the spillover effect from one market to other all markets, equal to the sum of the values in column j without the trace value, and “FROM” refers to the spillover effect received from all other markets, equal to the sum of the value in row i without the trace value. Moreover, the value of “NET directional connectedness” is the difference between "TO" and "FROM." “NPDC transmitter” represents the number of variables in which variable i transmits more spillover effects to rather than receiving spillover effect from. Finally, “TCI” is the total connectedness index which is the sum of “TO” or “FROM” and divided by N-1, consistent with the explanation given in Section 2.2. Furthermore, the SI in Tables 2.4 and 2.5 is constructed based on the AFINN lexicon by employing the text mining method. To confirm whether the differences between dictionaries will affect the construction of the SI, we also fit the TVP-VAR model for the NRC-based SI and find that the averaged dynamic connectedness results are virtually the same as the situation of the AFINN-based SI. Therefore, we consider the AFINN-based SI for our study and include the averaged dynamic connectedness results of the NRC dictionary-based SI index in the appendix.

From Tables 2.4 and 2.5, it is evident that the total connectedness of returns is 21.4%, which is smaller than the total connectedness of volatility (24.5%). Next, from Table 2.4, we can see that SI contributes the most spillover effect to IDEMVT (2.7%). Among the S&P 500 Index, WTI futures, and Gold futures, SI contributes the most spillover effect to the return of S&P 500 (2.1%), followed by GC (2%) and WTI (1.8%). Additionally, IDEMVT also contributes the most spillover effect to SI (8.3%). Among the S&P 500 Index, WTI futures, and Gold futures, IDEMVT contributes the most spillover effect to the return of GC (6.8%), followed by S&P 500 (5.4%) and WTI (4.3%). This implies that there is a strong connectedness between SI and IDEMVT. Furthermore, WTI receives the most return spillover effect from S&P 500 (9.5%), S&P 500 receives the most return spillover effect from WTI (9.5%), and GC receives the most return spillover effect from WTI (7%). From the results of NET directional connectedness, we can observe that the NET directional connectedness of SI is negative (6.7%), but IDEMVT is positive (17%). This result explains that SI receives more spillover effect than transmitting, but IDEMVT transmits more spillover effect than receiving. Therefore, the value of the SI's NPDC transmitter is zero, which means that SI is the NPDC receiver rather than the transmitter, while the value of IDEMVT's NPDC transmitter is 4, which indicates that IDEMVT is an absolute spillover effect transmitter.

From the averaged dynamic connectedness of the volatility series in Table 2.5, we can see that SI contributes the most spillover effect to IDEMVT (2.4%) and the volatility of WTI (2.4%). However, SI contributes the least spillover effect to the return of WTI (1.8%). Therefore, this conclusion indicates that compared with the return of WTI, the volatility of WTI has a stronger connectedness with SI. The IDEMVT contributes the most volatility spillover effect to the SI (7.2%). Among the S&P 500 Index, WTI futures, and Gold futures, IDEMVT contributes the most volatility spillover to S&P 500 (6.7%), followed by WTI (5.6%) and GC (3.8%). Moreover, WTI receives the most volatility spillover effect from S&P 500 (9.1%); S&P 500 receives the most volatility spillover effect from WTI (8.5%), and GC receives the most volatility spillover effect from S&P 500 (10.7%). Furthermore, the NET directional connectedness values of SI and IDEMVT are relatively negative and positive, which also indicates that SI is the NPDC receiver and IDEMVT is the NPDC transmitter in the volatility series.

Table 2.4. Averaged dynamic connectedness table of return series.

	SI	IDEMVT	WTI_Return	SP500_Return	GC_Return	FROM
SI	84.7	8.3	2.2	2.7	2	15.3
IDEMVT	2.7	92.1	1.6	2.1	1.5	7.9
WTI_Return	1.8	4.3	77.9	9.5	6.5	22.1
SP500_Return	2.1	5.4	9.5	79.4	3.5	20.6
GC_Return	2	6.8	7	3.9	80.3	19.7
TO	8.6	24.9	20.4	18.2	13.5	85.6
NET directional connectedness	−6.7	17	−1.7	−2.4	−6.2	TCI
NPDC transmitter	0	4	2	3	1	21.4

Notes: Estimation results are based on a TVP-VAR (0.99, 0.99) model with a lag length of order 5 (HQC) and a 10-step ahead forecast. SI is the sentiment index, IDEMVT is the volatility tracker, WTI_Return refers to the return of crude oil WTI futures; SP500_Return refers to the return of the S&P 500 Index; GC_Return refers to the return of COMEX Gold futures; NPDC transmitter refers to the net pairwise directional connectedness transmitter. "TO" represents the spillover effect from one market to other all markets, equal to the sum of the values in column *j* without the trace value, and "FROM" means the spillover effect received from all other markets, equal to the sum of the value in row *i* without the trace value. "TCL" is the total connectedness index which is the sum of "TO" or "FROM" and divided by the number of variables−1.

Table 2.5. Averaged dynamic connectedness table of volatility series.

	SI	IDEMVT	WTI_Vol	SP500_Vol	GC_Vol	FROM
SI	84.3	7.2	2.5	3.4	2.6	15.7
IDEMVT	2.4	88.4	3.5	3.7	2.1	11.6
WTI_Vol	2.4	5.6	76.9	9.1	6	23.1
SP500_Vol	1.6	6.7	8.5	76	7.2	24
GC_Vol	2.2	3.8	7	10.7	76.4	23.6
TO	8.5	23.4	21.4	26.9	17.9	98.1
NET directional connectedness	−7.2	11.8	−1.6	2.8	−5.7	TCI
NPDC transmitter	0	4	2	3	1	24.5

Notes: Estimation results are based on a TVP-VAR (0.99, 0.99) model with a lag length of order 6 (HQC) and a 10-step ahead forecast. SI is the sentiment index, IDEMVT is the volatility tracker, WTI_Vol refers to the volatility of crude oil WTI futures, SP500_Vol refers to the volatility of the S&P 500 Index, GC_Vol refers to the volatility of COMEX Gold futures, and NPDC transmitter refers to the net pairwise directional connectedness transmitter. "TO" represents the spillover effect from one market to other all markets, equal to the sum of the values in column *j* without the trace value, and "FROM" means the spillover effect received from all other markets, equal to the sum of the value in row *i* without the trace value. "TCL" is the total connectedness index which is the sum of "TO" or "FROM" and divided by the number of variables−1.

Following Diebold and Yilmaz (2016), we focus on the dynamic pairwise spillovers between the five variables in our study by drawing connectedness networks, which can help us to better understand the structure of connectedness by employing the size of nodes, the direction of the arrow, etc., to convey information about the estimated network characteristics.[10] Node size indicates the value of "TO"; the larger the value of "TO", the larger the size of the node. Edge arrow directions indicate the pairwise directional connectedness "to" and "from"; edge arrow size indicates the value of pairwise directional connectedness "to" and "from."

Following Diebold and Yilmaz (2016), we show the network based on the averaged pairwise directional return and volatility in Figure 2.4 and Figure 2.5. Figure 2.4 exhibits the network based on the averaged pairwise directional return. In Figure 2.4, we can observe that the node size of IDEMVT is largest which indicates that the return spillover effect from IDEMVT to other variables is greatest and IDEMVT is a return spillover transmitter. On the contrary, the node size of SI is smallest which indicates that the return spillover effect from SI to other variables is smallest, therefore, SI acts mainly as a return spillover receiver. Furthermore, through observing the size of edge arrow, we can see that the SI receives the most return spillover from the IDEMVT. Moreover, there is a largest edge arrow between the WTI and S&P 500 which indicates a strong connectedness between the WTI and S&P 500. Our result is consistent with the previous literature, Zhang and Hamori (2021), Liu and Hamori (2021), Shaikh (2020). Liu and Hamori (2021) employed TVP-VAR model to investigate the connectedness of return and volatility series between clean energy stock, technology stock, crude oil, natural gas, and investor sentiment index. They also found that SI was a pairwise connectedness receiver rather than transmitter in return system. Shaikh (2020) analyzed the relationship of 12 major equity markets during the COVID-19 pandemic, and found that the number of new cases and deaths recorded every day due to COVID-19 has disrupted global investor sentiment and the market has also experienced unprecedented negative returns. These results indicate IDEMVT is a spillover transmitter and affects other variables significantly. Shaikh (2020) explained that investment decisions are influenced by "investor sentiment", which can affect the pricing of various assets classes.

Figure 2.5 exhibits the network based on the averaged pairwise directional volatility. The empirical results for volatility system are similar to those for return system. Figure 2.5 shows that the node size of SI is the smallest among all variables which indicates that the volatility spillover effect from SI to other variables is the smallest and SI also is a spillover receiver in volatility system. Besides, the SI receives the most volatility spillover effect from the IDEMVT. Unlike the case of return system, however, the node size of S&P 500 rather than IDEMVT is the largest among all variables which indicates that S&P 500 is a spillover transmitter in volatility system. Furthermore, the size of edge arrow between one stock index and other two commodity future indexes are relatively thick, indicating a strong connectedness among the stock market, the crude oil market, and the gold market. These findings suggest that the spillover effect of S&P 500 on other variables in the volatility system is greater than those in the return system, which indicates that investors should pay attention to the risk of S&P 500 in their investment portfolio. Zhang and Hamori (2021) also analyzed the spillover effect of return and volatility system between the crude oil market and stock markets under COVID-19 pandemic and found that S&P 500 has the largest

[10] We employ the software: Gephi (https://gephi.org/) to draw the network graphs.

spillover effect on other variables. Their results are consistent with ours.

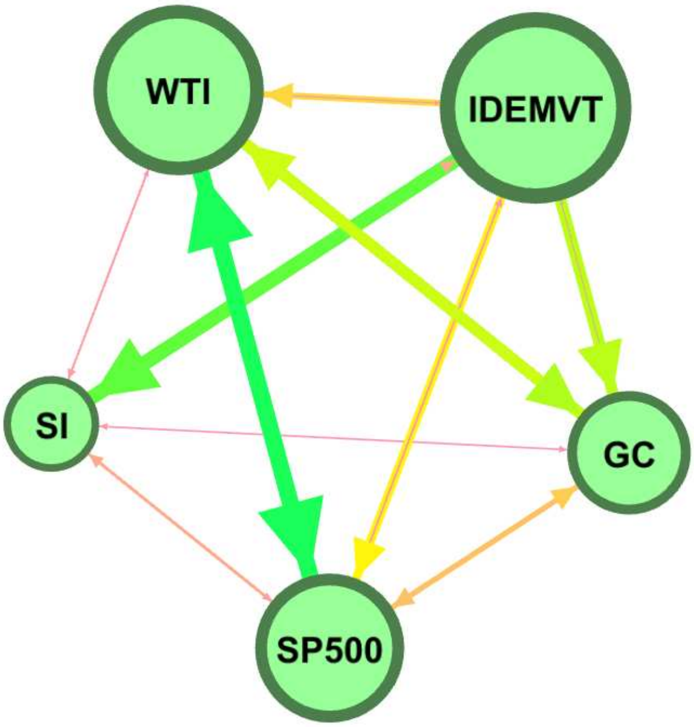

Figure 2.4. Network based on averaged pairwise directional return connectedness over the full sample.

Notes: SI is the sentiment index, IDEMVT is volatility tracker, WTI refers to the return of crude oil WTI futures, SP500 refers to the return of the S&P 500 Index, and GC refers to the return of COMEX Gold futures.

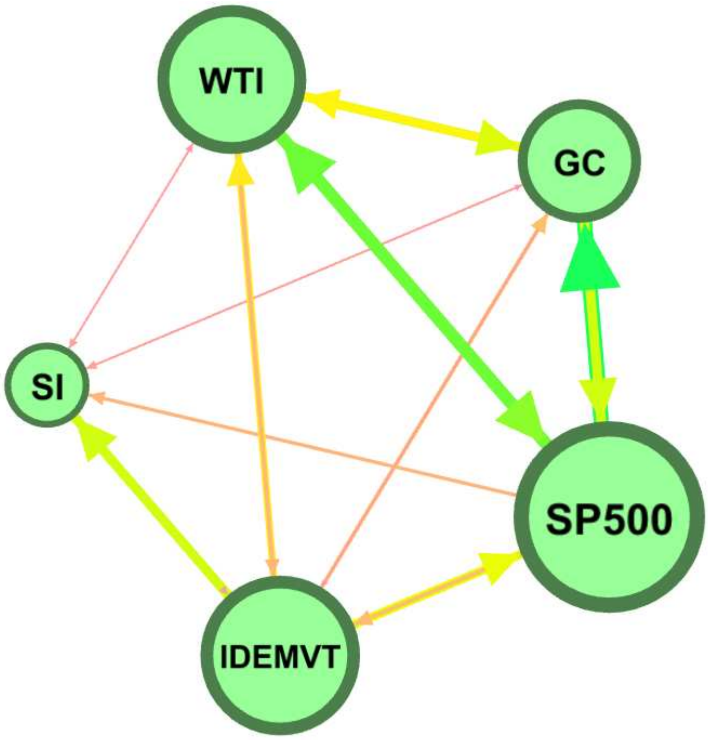

Figure 2.5. Network based on averaged pairwise directional volatility connectedness over the full sample.

Notes: SI is the sentiment index, IDEMVT is volatility tracker, WTI refers to the volatility of crude oil WTI futures, SP500 refers to the volatility of the S&P 500 Index, and GC refers to the volatility of COMEX Gold futures.

2.5.2. TVP-VAR-based connectedness over time

Although we have analyzed the averaged dynamic connectedness tables and network plots based on the averaged pairwise directional of return and volatility, we still need to observe the total connectedness dynamics over time to determine the influence of extreme events on the connectedness between the variables in our study[11]. Because the prediction of the TVP-VAR model depends on the initial value, we discard the initial one and a half years when visualizing the connectedness plots. Therefore, the sample size in the connectedness plots starts from July 2, 2007 to December 30, 2020.

Figures 2.6 and 2.7 show the total connectedness of the return and volatility series using the TVP-VAR model, respectively. In general, we can observe that the total connectedness of the return series is relatively more stable than the total connectedness of the volatility series. Furthermore, the total connectedness of the return series ranges from 0% to 45%, which is smaller than the total connectedness of the volatility series, which ranges from 0% to 60%. This result indicates that the total connectedness of volatility is more sensitive to extreme events. More precisely, in Figure 2.6, we can see that before 2020, the total connectedness of returns exhibits a relatively stable trend. Owing to the 2020 COVID-19 pandemic, the total connectedness of returns suddenly rises above 40%. The impact of 2020 COVID-19 on stock markets significantly

[11] We have done the analysis of traditional VAR model, but the result is unstable and cannot be trusted, so we do not put the result of traditional VAR in our article.

surpasses the impact of the 2008 global financial crisis and the 2010 European debt crisis on stock markets.

Figure 2.7 shows the total connectedness of volatility series. It is evident that there are two fluctuation points in the graph of the total connectedness of the volatility series, which fluctuates fiercer than the total connectedness of the return series. This finding indicates that volatility is more sensitive to extreme events. More precisely, around 2013, there is a sudden fluctuation, which is influenced by the 2013 drop in the price of gold. The most significant price drop in the gold market in the last decade occurred between October 2012 and July 2013, a nine-month stretch during which the metal lost more than a quarter of its value. Furthermore, because of the impact of the 2020 COVID-19 pandemic, the total connectedness of volatility around 2020 suddenly fluctuates over 55%, which is fiercer than the fluctuation around 2013 due to the sharp drop in gold prices in 2013.

Furthermore, we investigate the pairwise directional connectedness between the SI, IDEMVT, and the three other stock indexes. Figures 2.8 (a) and (b) show the pairwise directional connectedness between the SI, IDEMVT, and the S&P 500 Index, WTI futures, and Gold futures of the return series, respectively. Conversely, Figures 2.9 (a) and (b) show the pairwise directional connectedness between the SI, IDEMVT, and the three other stock indexes of the volatility series, respectively. In general, either in the return or volatility series, the total connectedness between the IDEMVT and the three other stock indexes is larger than the connectedness between the SI and the three other stock indexes. More precisely, in the return series, compared with the S&P 500 Index, WTI futures, and Gold futures, the connectedness between the SI and IDEMVT is stronger. In addition, the connectedness between the IDEMVT and the return of the S&P 500 Index, WTI futures, and Gold futures fluctuates fiercely around 2020 due to the 2020 COVID-19 pandemic. In the volatility series, the connectedness from the SI to the three other stock indexes fluctuates more severely than in the return series and fluctuates fiercely around 2020 because of the 2020 COVID-19 pandemic. Furthermore, the connectedness from the SI to the volatility of WTI and S&P 500 suddenly surges around mid-2014 due to the fall in the 2014 international crude oil prices; the connectedness from the SI to the volatility of GC fluctuates around 2013 because of 2013 drop in gold price. This finding indicates that the SI is sensitive to extreme events and has a corresponding impact on the volatility of markets, which is severely influenced by the events. Moreover, since the IDEMVT is related to the disease, the connectedness between it and the volatility of stock indexes also fluctuates fiercely around 2020 due to the 2020 COVID-19 pandemic.

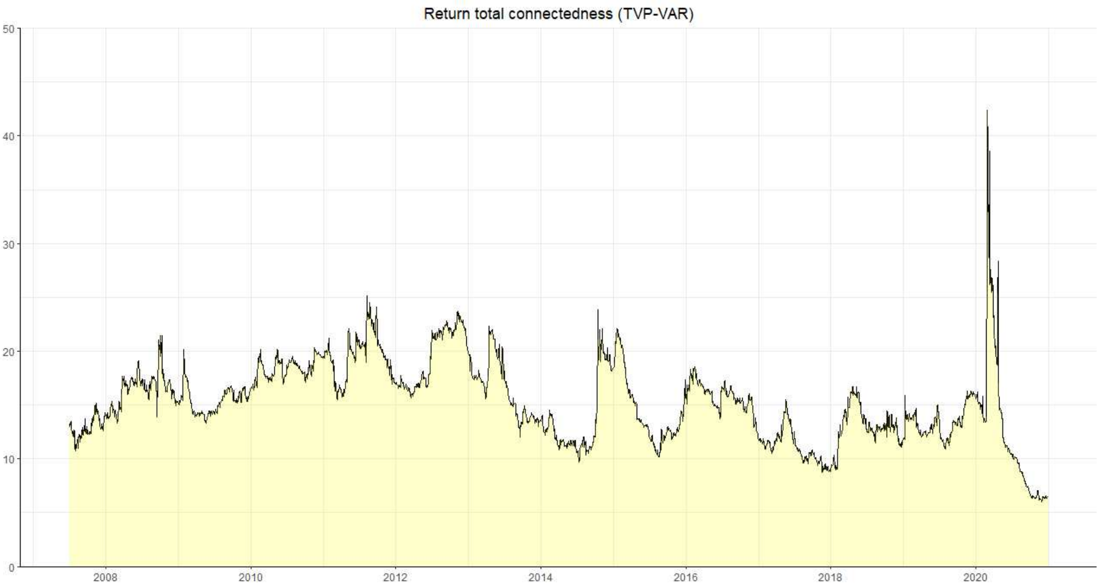

Figure 2.6. Total connectedness of return series from the TVP-VAR model.

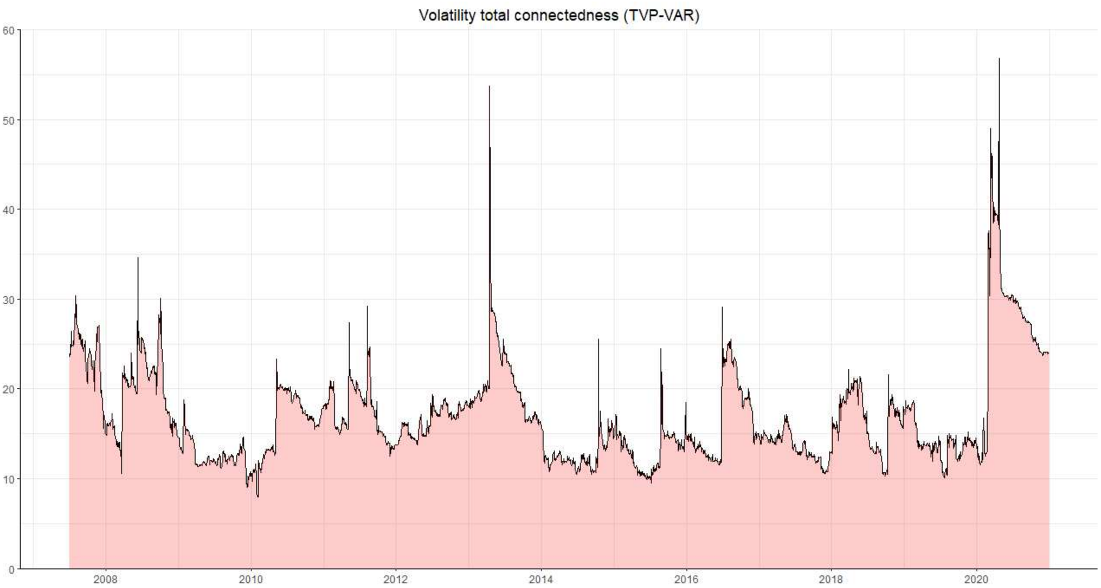

Figure 2.7. Total connectedness of volatility series from TVP-VAR model.

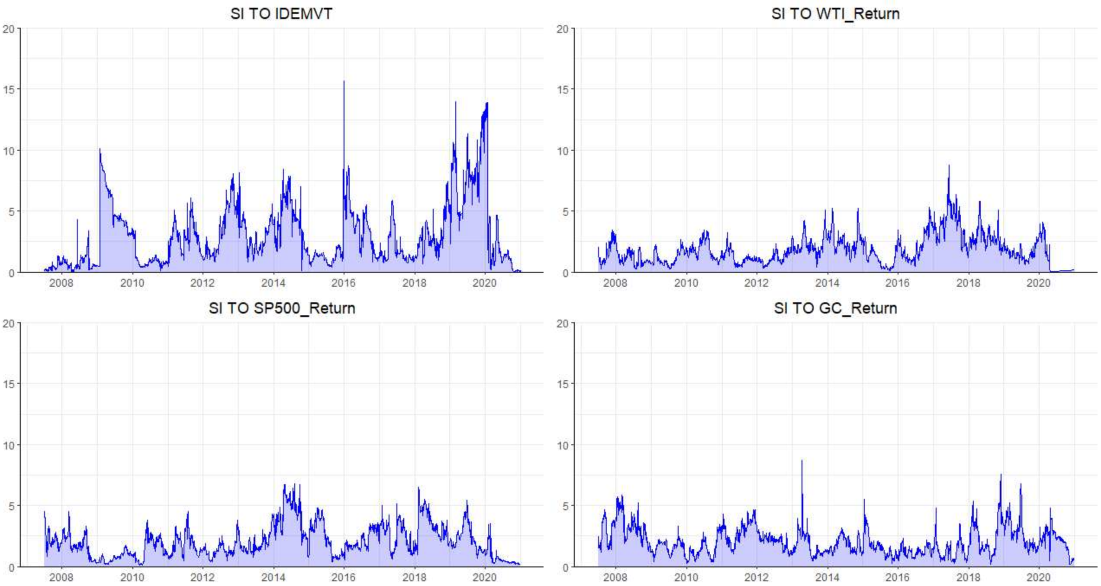

(a)

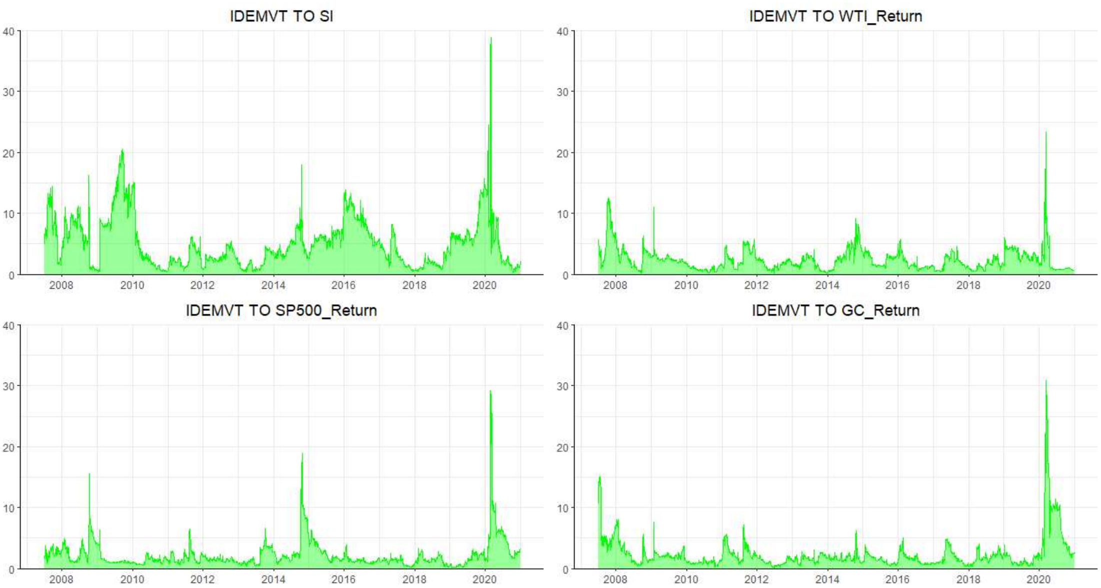

(b)

Figure 2.8. Pairwise directional connectedness of return series from the TVP-VAR model.

Notes: SI is the sentiment index, IDEMVT is volatility tracker, WTI_Return refers to the return of crude oil WTI futures; SP500_Return refers to the return of the S&P 500 Index; and GC_Return refers to the return of COMEX Gold futures.

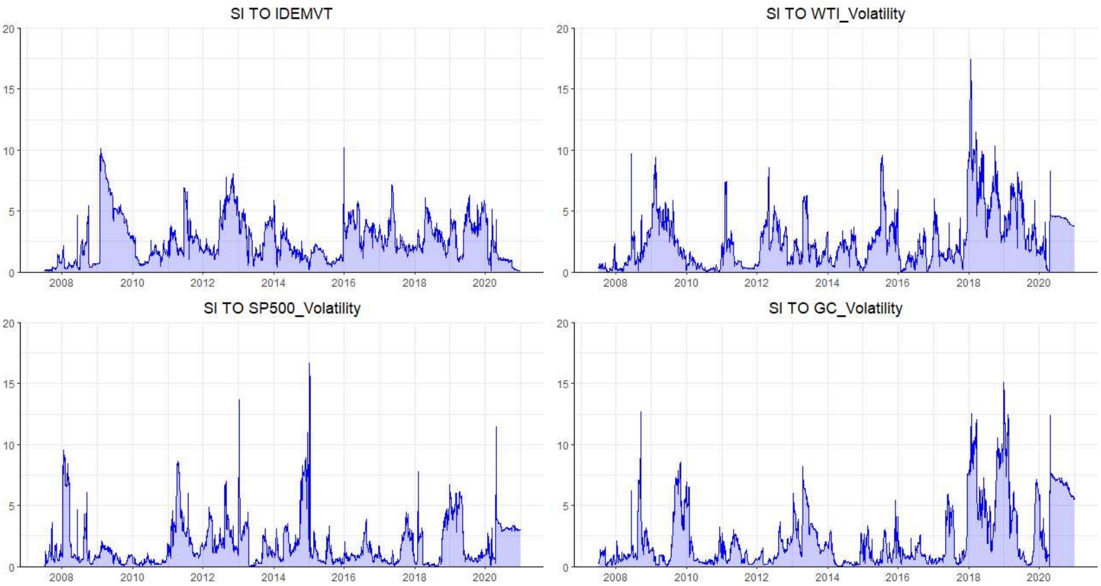

(a)

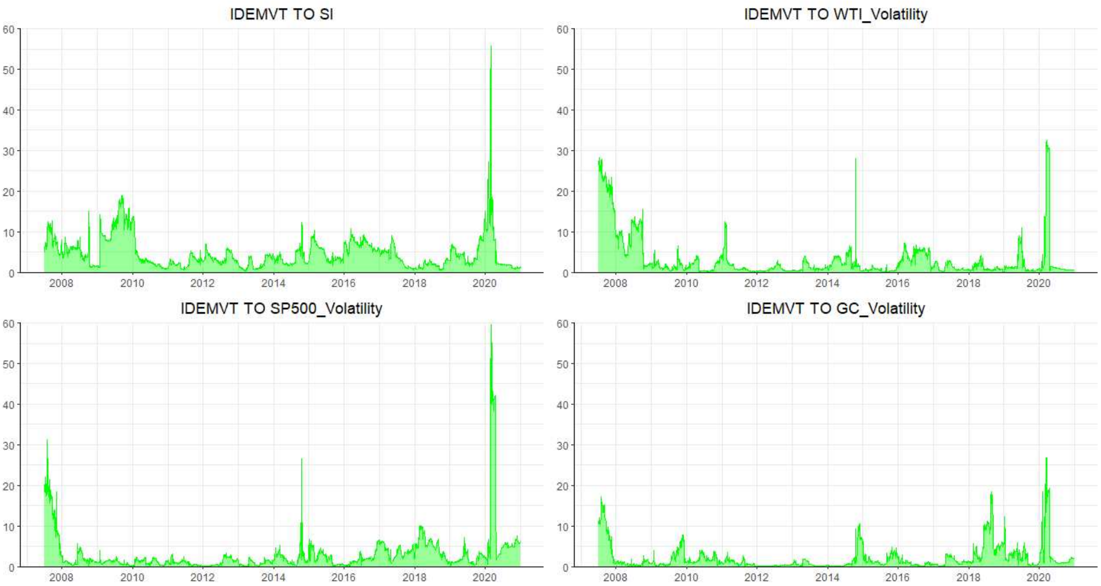

(b)

Figure 2.9. Pairwise directional connectedness of volatility series from the TVP-VAR model.

Notes: SI is the sentiment index, IDEMVT is volatility tracker, WTI_Volatility refers to the volatility of crude oil WTI futures; SP500_Volatility refers to the volatility of the S&P 500 Index; and GC_Volatility refers to the volatility of COMEX Gold futures.

2.6. Conclusions

In this study, we employ a text mining methodology to construct an SI based on the news headlines of an Australian news source, i.e., ABC. We use the TVP-VAR model to investigate the connectedness between the SI, IDEMVT, the crude oil market, the US stock market, and the gold market.

The main results of this study can be summarized in three points. First, from the averaged connectedness dynamics, it is evident that there is a strong connectedness between the SI and IDEMVT both in return and volatility series. The SI contributes the most spillover effect on the return of S&P 500 (2.1%) in the return series among the S&P 500 Index, WTI futures, and Gold futures, while SI contributes the most spillover effect to the volatility of WTI (2.4%) in the volatility series among the S&P 500 Index, WTI futures, and Gold futures. Besides, the NET directional connectedness values of the SI and IDEMVT indicate that the SI is the NPDC receiver and the IDEMVT is the NPDC transmitter in both return and volatility series.

Second, we employ Diebold and Yilmaz's (2016) network method to understand the structure of connectedness from another perspective. The results indicate that SI acts mainly as a spillover receiver, while the IDEMVT acts as a spillover transmitter. SI receives the most return and volatility spillover effect from the IDEMVT. Furthermore, there is a strong connectedness between the volatility of the S&P 500 Index, WTI futures, and Gold futures.

Third, by observing the total connectedness via the TVP-VAR model over time, we find that the total connectedness of return suddenly rises above 40% owing to the 2020 COVID-19 pandemic. The impact of the 2020 COVID-19 pandemic on stock markets significantly surpasses the impact of the 2008 global financial crisis and the 2010 European debt crisis on stock markets. Similarly, the plot of the total connectedness of volatility indicates a sudden fluctuation influenced by the drop in gold price in 2013. Besides, the influence of the 2020 COVID-19 pandemic to the total connectedness of volatility exceeds the influence of the sharp drop in the price of gold in 2013, indicating the unprecedented effect of COVID-19 epidemic.

The novelty of this article can be summarized as follows: first, our study is the first to employ the text mining method to construct the SI, and thereafter evaluate the connectedness among the SI, as well as the crude oil, stock, and gold markets under the impact of the COVID-19 pandemic. Zhang et al. (2021) employ Diebold and Yilmaz's (2012) rolling window method to investigate the spillover effect between the crude oil market and the stock market under the impact of the COVID-19 pandemic. However, we select the TVP-VAR model, which is more suitable than Diebold and Yilmaz's (2012) rolling window method, to analyze the total connectedness over time. Second, Sayim et al. (2015), Dash et al. (2013), and Rupande et al. (2019) directly employ investor sentiment data; however, in our study, we adopt the text mining method to construct the SI, which allows us to freely choose its data source, to duly realize the variable combination.

As the COVID-19 pandemic remains ongoing, we believe that our study can provide a basic guiding effect for analyzing the connectedness between the SI and stock market at a particular moment. Moreover, by analyzing the connectedness between the SI and the stock markets for investors, their investment strategy should also consider the SI when measuring the total risk. Because we employ the text mining method to construct only one kind of SI in our study, we believe that there is still much room to explore the connectedness between the various SIs and the stock market during the COVID-19 pandemic period. For example, similar to García (2013) and Tetlock (2007), employing the common source of news to construct the sentiment index; use the different dictionaries, such as Harvard IV-4 (Tetlock, 2007) and Loughran and McDonald (L&M) (Loughran and McDonald, 2011) to construct the different sentiment index; employ the composite sentiment index highly related to stock returns to compare our SI and in the comparative analysis of sentiment index, we can study the Monday effect of financial market proposed by Shiller (2003).

Appendix

We include the average dynamic connectedness results of the NRC dictionary-based sentiment index in the appendix as follows:

Table A. Averaged dynamic connectedness table of return series.

	SI	IDEMVT	WTI_Return	SP500_Return	GC_Return	FROM
SI	86.2	7.6	1.8	2.3	2	13.8
IDEMVT	2.3	92.4	1.7	2.1	1.5	7.6
WTI_Return	2.2	4.4	77.3	9.5	6.6	22.7
SP500_Return	2	5.3	9.5	79.6	3.6	20.4
GC_Return	2.1	6.7	7.1	3.7	80.4	19.6
TO	8.6	23.9	20.1	17.7	13.7	84
NET directional connectedness	−5.1	16.3	−2.5	−2.7	−5.9	TCI
NPDC transmitter	2	4	1	3	0	21

Notes: Estimation results are based on a TVP-VAR (0.99, 0.99) model with a lag length of order 5 (HQC) and a 10-step ahead forecast. SI is the sentiment index, IDEMVT is the volatility tracker, WTI_Return refers to the return of crude oil WTI futures; SP500_Return refers to the return of the S&P 500 Index; GC_Return refers to the return of COMEX Gold futures; NPDC transmitter refers to the net pairwise directional connectedness transmitter. "TO" represents the spillover effect from one market to other all markets, equal to the sum of the values in column *j* without the trace value, and "FROM" means the spillover effect received from all other markets, equal to the sum of the value in row *i* without the trace value. "TCL" is the total connectedness index which is the sum of "TO" or "FROM" and divided by the number of variables−1.

Table B. Averaged dynamic connectedness table of volatility series.

	SI	IDEMVT	WTI_Vol	SP500_Vol	GC_Vol	FROM
SI	85.6	6	2.6	3.1	2.7	14.4
IDEMVT	2	88.4	3.4	4	2.2	11.6
WTI_Vol	1.6	5.7	77.5	9.1	6.1	22.5
SP500_Vol	2	6.8	8.6	75.7	6.9	24.3
GC_Vol	2.5	3.6	6.9	10.6	76.5	23.5
TO	8.1	22.1	21.5	26.8	17.9	96.4
NET directional connectedness	−6.3	10.5	−1.1	2.5	−5.6	TCI
NPDC transmitter	0	4	2	3	1	24.1

Notes: Estimation results are based on a TVP-VAR (0.99, 0.99) model with a lag length of order 6 (HQC) and a 10-step ahead forecast. SI is the sentiment index, IDEMVT is the volatility tracker, WTI_Vol refers to the volatility of crude oil WTI futures, SP500_Vol refers to the volatility of the S&P 500 Index, GC_Vol refers to the volatility of COMEX Gold futures, and NPDC transmitter refers to the net pairwise directional connectedness transmitter. “TO” represents the spillover effect from one market to other all markets, equal to the sum of the values in column *j* without the trace value, and “FROM” means the spillover effect received from all other markets, equal to the sum of the value in row *i* without the trace value. “TCL” is the total connectedness index which is the sum of “TO” or “FROM” and divided by the number of variables−1.

Based on the AFINN dictionary-based sentiment index, we also employ the BIC to select the lags of return and volatility series, and we put the averaged dynamic connectedness table of return and volatility series whose lags selected by BIC in the appendix as follows:

Table C. Averaged dynamic connectedness table of return series.

	SI	IDEMVT	WTI_Return	SP500_Return	GC_Return	FROM
SI	85.6	8.3	1.9	2.4	1.8	14.4
IDEMVT	2.8	92.9	1.3	1.8	1.3	7.1
WTI_Return	1.5	3.5	79.2	9.5	6.3	20.8
SP500_Return	1.7	5	9.5	80.4	3.4	19.6
GC_Return	1.7	6	6.9	3.8	81.5	18.5
TO	7.7	22.9	19.5	17.5	12.7	80.3
NET directional connectedness	−6.6	15.7	−1.3	−2.1	−5.7	TCI
NPDC transmitter	4	0	1	2	3	16.1

Notes: Estimation results are based on a TVP-VAR (0.99, 0.99) model with a lag length of order 4 (BIC) and a 10-step ahead forecast. SI is the sentiment index, IDEMVT is the volatility tracker, WTI_Return refers to the return of crude oil WTI futures; SP500_Return refers to the return of the S&P 500 Index; GC_Return refers to the return of COMEX Gold futures; NPDC transmitter refers to the net pairwise directional connectedness transmitter. “TO” represents the spillover effect from one market to other all markets, equal to the sum of the values in column *j* without the trace value, and “FROM” means the spillover effect received from all other markets, equal to the sum of the value in row *i* without the trace value. “TCL” is the total connectedness index which is the sum of “TO” or “FROM” and divided by the number of variables−1.

Table D. Averaged dynamic connectedness table of volatility series.

	SI	IDEMVT	WTI_Vol	SP500_Vol	GC_Vol	FROM
SI	86.1	6.5	2.3	3.2	2	13.9
IDEMVT	2.2	88.2	3.7	3.4	2.5	11.8
WTI_Vol	1.3	6.6	76.6	8.5	7	23.4
SP500_Vol	1.5	6.9	8.5	76	7.3	24
GC_Vol	1.5	3.5	7.2	11	76.9	23.1
TO	6.5	23.4	21.6	26.1	18.7	96.4
NET directional connectedness	−7.4	11.5	−1.8	2.1	−4.4	TCI
NPDC transmitter	4	0	2	1	3	19.3

Notes: Estimation results are based on a TVP-VAR (0.99, 0.99) model with a lag length of order 4 (BIC) and a 10-step ahead forecast. SI is the sentiment index, IDEMVT is the volatility tracker, WTI_Vol refers to the volatility of crude oil WTI futures, SP500_Vol refers to the volatility of the S&P 500 Index, GC_Vol refers to the volatility of COMEX Gold futures, and NPDC transmitter refers to the net pairwise directional connectedness transmitter. "TO" represents the spillover effect from one market to other all markets, equal to the sum of the values in column j without the trace value, and "FROM" means the spillover effect received from all other markets, equal to the sum of the value in row i without the trace value. "TCL" is the total connectedness index which is the sum of "TO" or "FROM" and divided by the number of variables−1.

Table E reports the summary pf empirical results of ARMA-GARCH model of WTI, SP500, and GC.

Table E: Empirical results of ARMA-GARCH model.

	WTI		S&P 500		GC	
	Estimate	SE	Estimate	SE	Estimate	SE
μ	−0.000002***	0.000000	0.000767***	0.000127	0.000267**	0.000133
AR (1)			−0.067027***	0.019112	0.097633**	0.042854
AR (2)					0.832536***	0.009230
MA (1)	−0.0972***	0.000020			−0.090305**	0.038441
MA (2)					−0.856534***	0.011206
ω	0.000000	0.000000	0.000003***	0.000001	0.000001	0.000001
α_1	0.064208***	0.000013	0.147272***	0.012423	0.042171***	0.010157
β_1	0.912959***	0.000219	0.831525***	0.012955	0.949824***	0.010860
$Q(20)$	3.370		3.347		3.396	
p-value	0.344		0.349		0.385	
$Q^2(20)$	0.134		2.796		2.132	
p-value	1.000		0.792		0.683	

Note: "***" and "**" represent statistical significance at 1% and 5%, respectively. $Q\ (20)$ and $Q^2\ (20)$ are the Ljung–Box statistics with 20th lags for the standard residuals and standard residuals squared, respectively.

Table F(a) and Table F(b) reports the correlation matrix of return and volatility series respectively in appendix as follows:

Table F(a): Correlation matrix of return series.

	SI	IDEMVT	WTI_Return	SP500_Return	GC_Return
SI	1	−0.009	0.000	0.001	−0.013
IDEMVT	−0.009	1	−0.031	−0.002	0.016
WTI_Return	0.000	−0.031	1	0.169	0.117
SP500_Return	0.001	−0.002	0.169	1	0.015
GC_Return	−0.013	0.016	0.117	0.015	1

Notes: SI is the sentiment index, IDEMVT is the volatility tracker, WTI_Return refers to the return of crude oil WTI futures; SP500_Return refers to the return of the S&P 500 Index; GC_Return refers to the return of COMEX Gold futures.

Table F(b): Correlation matrix of volatility series.

	SI	IDEMVT	WTI_Vol	SP500_Vol	GC_Vol
SI	1	−0.009	−0.033	−0.046	0.079
IDEMVT	−0.009	1	0.442	0.405	0.205
WTI_Vol	−0.033	0.442	1	0.311	0.302
SP500_Vol	−0.046	0.405	0.311	1	0.618
GC_Vol	0.079	0.205	0.302	0.618	1

Notes: SI is the sentiment index, IDEMVT is the volatility tracker, WTI_Vol refers to the volatility of crude oil WTI futures, SP500_Vol refers to the volatility of the S&P 500 Index, GC_Vol refers to the volatility of COMEX Gold futures.

References

Al-Awadhi, AM, K Al-Saifi, A Al-Awadhi and S Alhammadi (2020). Death and contagious infectious diseases: Impact of the COVID-19 virus on stock market returns. *Journal of Behavioral and Experimental Finance*, 27, 100326.

Antonakakis, N, D Gabauer, R Gupta and V Plakandaras (2018). Dynamic connectedness of uncertainty across developed economies: A time-varying approach. *Economics Letters*, 166, 63–75.

Antweiler, W and MZ Frank (2004). Is all that talk just noise? The information content of internet stock message boards. *The Journal of Finance*, 59(3), 1259–1294.

Baker, SR, N Bloom, SJ Davis and SJ Terry (2020a). COVID-induced economic uncertainty. NBER Working Paper No. 26983.

Baker, SR, N Bloom, SJ Davis, K Kost, M Sammon and T Viratyosin (2020b). The unprecedented stock market reaction to COVID-19. *The Review of Asset Pricing Studies*, 10, 742–758.

Barro, RJ, JF Ursua and J Weng (2020). The coronavirus and the great influenza. pandemic –Lessons from the 'Spanish Flu' for the coronavirus's potential effects on mortality and economic activity. NBER Working Paper No. 26866.

Bekiros, S (2014). Forecasting with a state space time-varying parameter VAR model: Evidence from the Euro area. *Economic Modelling*, 38, 619–626.

Chatziantoniou, I and D Gabauer (2021). EMU risk-synchronisation and financial fragility through the prism of dynamic connectedness. *The Quarterly Review of Economics and Finance*, 79, 1–14.

Crone, SF and C Koeppel (2014). Predicting exchange rates with sentiment indicators: An empirical evaluation using text mining and multilayer perceptrons. *In 2014 IEEE Conf. Computational Intelligence for Financial Engineering & Economics (CIFEr)*, pp. 114–121. London, UK: IEEE.

Dahir, AM, F Mahat, BAA Noordin and NHA Razak (2019). Dynamic connectedness between bitcoin and equity market information across BRICS countries: Evidence from TVP-VAR connectedness approach. *International Journal of*

Managerial Finance, 16(3), 357–371.

Dash, SR and J Mahakud (2013). Impact of investor sentiment on stock return: Evidence from India. *Journal of Management Research*, 13(3), 131–144.

Diebold, FX and K Yilmaz (2009). Measuring financial asset return and volatility spillovers, with application to global equity markets. *The Economic Journal*, 119(534), 158–171.

Diebold, FX and K Yilmaz (2012). Better to give than to receive: Predictive directional measurement of volatility spillover. *International Journal of Forecasting*, 28(1), 57–66.

Diebold, FX and K Yilmaz (2014). On the network topology of variance decompositions: Measuring the connectedness of financial firms. *The Economic Journal*, 182(1), 119–134.

Diebold, FX and K Yilmaz (2016). Trans-Atlantic equity volatility connectedness: US and European financial institutions, 2004–2014. *Journal of Financial Econometrics*, 14(1), 81–127.

Donadelli, M, R Kizys and M Riedel (2017). Dangerous infectious diseases: Bad. News for Main Street, good news for Wall Street? *Journal of Financial Markets*, 35, 84–103.

Feldman, R, S Govindaraj, J Livnat and B Segal (2010). Management’s tone change, post earnings announcement drift and accruals. *Review of Accounting Studies*, 15(4), 915–953.

Gabauer, D and R Gupta (2018). On the transmission mechanism of country-specific.

and international economic uncertainty spillovers: Evidence from a TVP-VAR connectedness decomposition approach. *Economics Letters*, 171, 63–71.

García, D (2013). Sentiment during recessions. *The Journal of Finance*, 68(3), 1267–1300.

Geraci, MV and JY Gnabo (2018). Measuring interconnectedness between financial. institutions with Bayesian time-varying vector autoregressions. *Journal of Financial and Quantitative Analysis*, 53(3), 1371–1390.

Gil-Alana, LA and M Monge (2020). Crude oil prices and COVID-19: Persistence of. the shock. *Energy Research Letters*, 1(1), 13200.

Gondaliya, C, A Patel and T Shah (2021). Sentiment analysis and prediction of Indian stock market amid COVID-19 pandemic. *IOP Conference Series: Materials Science and Engineering*, 1020, 012023.

Hu, M and B Liu (2014). Mining and summarizing customer reviews. *In ACM SIGKDD Int. Conf. Knowledge Discovery and Data Mining*, pp. 168–177. New York: Association for Computing Machinery.

Jebabli, I, M Arouri and F Teulon (2014). On the effects of world stock market and oil price shocks on food prices: An empirical investigation based on TVP-VAR models with stochastic volatility. *Energy Economics*, 45, 66–98.

Jiang, F, J Lee, X Martin and G Zhou (2019). Manager sentiment and stock returns. *Journal of Financial Economics*, 132(1), 126–149.

Johnman, M, BJ Vanstone and A Gepp (2018). Predicting FTSE 100 returns and volatility using sentiment analysis. *Accounting & Finance*, 58(S1), 253–274.

Koop, G, MH Pesaran and SM Potter (1996). Impulse response analysis in nonlinear multivariate models. *Journal of Economics*, 74(1), 119–147.

Koop, G and D Korobilis (2014). A new index of financial conditions. *European. Economic Review*, 71, 101–116.

Korobilis, D and K Yilmaz (2018). Measuring dynamic connectedness with large Bayesian VAR models. https://ssrn.com/abstract=3099725 or http://dx.doi.org/10.2139/ssrn.3099725.

Kulkarni, R (2018). A Million News Headlines [CSV data file]. doi: 10.7910/DVN/SYBGZL. https://www.kaggle.com/therohk/million-headlines.

Liu, T and X Gong (2020). Analyzing time-varying volatility spillovers between the crude oil markets using a new method. *Energy Economics*, 87, 104711.

Liu, T and S Hamori (2021). Does investor sentiment affect clean energy stock? Evidence from TVP-VAR-based connectedness approach. *Energies*, 14(12), 3442.

Loughran, T and B McDonald (2011). When is a liability not a liability? Textual. analysis, dictionaries, and 10-Ks. *The Journal of Finance*, 66(1), 35–65.

McKibbin, W and R Fernando (2020). The economic impact of COVID-19. *In Economics in the Time of COVID-19*. London: CEPR Press.

Mohammad, SM and PD Turney (2013). Crowdsourcing a Word-Emotion. Association Lexicon. *Computational Intelligence*, 29(3), 436–465.

Nakajima, J (2011). Time-varying parameter VAR model with stochastic volatility: An overview of methodology and empirical applications. *Monetary and*

Economic Studies, 29, 107–142.

Nielsen, FA (2011). A new ANEW: Evaluation of a word list for sentiment analysis in microblogs. arXiv preprint, arXiv:1103.2903.

Onali, E (2020). COVID-19 and stock market volatility. https://ssrn.com/abstract=3571453.

Pesaran, HH and Y Shin (1998). Generalized impulse response analysis in linear. multivariate models. *Economics Letters*, 58, 17–29.

Price, SMK, JS Doran, DR Peterson and BA Bliss (2012). Earnings conference calls and stock returns: The incremental informativeness of textual tone. *Journal of Banking & Finance*, 36(4), 992–1011.

Primiceri, GE (2005). Time varying structural vector autoregressions and monetary. policy? *Review of Economic Studies*, 72(3), 821–852.

Rupande, L, HT Muguto and PF Muzindutsi (2019). Investor sentiment and stock return volatility: Evidence from the Johannesburg Stock Exchange. *Cogent Economics & Finance*, 7(1), 1600233.

Said, SE and DA Dickey (1984). Testing for unit roots in autoregressive-moving. average models of unknown order, *Biometrika*, 71(3), 599–607.

Sayim, M and H Rahman (2015). The relationship between individual investor. sentiment, stock return and volatility: Evidence from the Turkish market. *International Journal of Emerging Markets*, 10(3), 504–520.

Shaikh, I (2020). Impact of COVID-19 pandemic disease outbreak on the global. equity markets. *Economic Research-Ekonomska Istraživanja*, 34(1), 2317–

2336.

Shiller, RJ (2003). From efficient markets theory to behavioral finance. *Journal of. Economic Perspectives*, 17(1), 83–104.

Silge, J and D Robinson (2016). tidytext: Text mining and analysis using tidy data. principles in R. *Journal of Open Source Software*, 1(3), 37. doi: 10.21105/joss.00037.

Sun, Y, Q Bao and Z Lu (2021). Coronavirus (COVID-19) outbreak, investor. sentiment, and medical portfolio: Evidence from China, Hong Kong, Korea, Japan, and U.S. *Pacific-Basin Finance Journal*, 65, 101463.

Tetlock, PC (2007). Giving content to investor sentiment: The role of media in the stock market. *The Journal of Finance*, 62(3), 1139–1168.

Wang, YH, A Keswani and SJ Taylor (2006). The relationships between sentiment, returns and volatility. *International Journal of Forecasting*, 22(1), 109–123.

Wen, F, M Zhang, M Deng, Y Zhao and J Ouyang (2019). Exploring the dynamic effects of financial factors on oil prices based on a TVP-VAR Model. *Physica A: Statistical Mechanics and Its Applications*, 532, 121881.

Zhang, W and S Hamori (2021). Crude oil market and stock markets during the. COVID-19 pandemic: Evidence from the US, Japan, and Germany. *International Review of Financial Analysis*, 74, 101702.

Chapter 3. Volatility spillover and investment strategies among sustainability-related financial indexes: Evidence from the DCC-GARCH-based dynamic connectedness and DCC-GARCH t-Copula approach

3.1. Introduction

[12]Since the COVID-19 outbreak, we have recognized that the future of economic development will require addressing the threats and challenges posed by the outbreak to promote sustainable economic development. Especially with the spread of the COVID-19 epidemic, the prices of traditional energy stocks such as oil have taken a huge hit, and people are becoming aware of the importance of protecting the environment and focusing on climate change. Against this background, sustainable investment is becoming the preferred investment option. ESG stands for Environmental, Social, and Governance, whose investment philosophy focuses on the environment, social responsibility, and sustainable development. In recent years, ESG-related stocks have received a lot of attention from investors as their role in financial markets has become critical. The total US domestic assets managed using sustainable investment strategies have grown from USD 12 trillion in early 2018 to USD 17.1 trillion in early 2020. As of July 2020, 90% of the companies in the S&P 500 Index have adopted them as a standard by publishing an annual corporate sustainability/ESG report (Chang et al., 2021). In principle, higher stock returns should correspond to good management of ESG factors. A company is believed to improve its market position by avoiding short-sighted decisions related to ESG choices (Bénabou and Tirole, 2010). Companies with strong ESG performance indicators are more likely to attract ecologically and socially conscious investors, especially younger investors. Although the COVID-19 epidemic has greatly impacted investment in the past two years, it has not slowed down investors' growing interest in ESG investment. On the contrary, it draws more attention to environmental protection. The current shortage of the supply chain and the crisis brought about by climate change have accelerated investors to further consider the right investment choice. Therefore, ESG investment will become a popular trend in future investment practices.

The large-scale development and utilization of primary energy, especially fossil energy, has caused increasingly serious environmental damage and had a great negative impact on human life. At the same time, the use of fossil fuels as the main energy source has always been the largest contributor to greenhouse gas (GHG) emissions. Natural renewable energy sources such as solar energy, wind power, tidal energy, etc., are inexhaustible. As an alternative to fossil fuels, renewable energy significantly reduces carbon emissions and achieves a sustainable economy, as shown in the 2015 Paris Climate Agreement and the United Nations Sustainable Development Goals. Renewable energy has attracted the attention of many investors to the renewable energy market (Tiwari et al., 2022). Under the European Union Emissions Trading Scheme (EU ETS), companies will have allowances that indicate how much carbon dioxide they

[12] Chapter 3 is based on the published paper: Zhang, W., He, X., & Hamori, S. (2022). Volatility spillover and investment strategies among sustainability-related financial indexes: Evidence from the DCC-GARCH-based dynamic connectedness and DCC-GARCH t-copula approach. *International Review of Financial Analysis*, 83, 102223. https://doi.org/10.1016/j.irfa.2022.102223

can emit. This arrangement will lead to higher production costs for companies that use coal and other fuels, making renewable energy more attractive (Hanif et al., 2021). Therefore, the spillover and nonlinear correlation dynamics between the renewable energy index and carbon emission index are worth studying, and we also employ the carbon emission futures in our study.

Green bonds refer to debt securities used to raise funds for various projects to alleviate climate change issues. The main purpose of issuing green bonds is to finance various climate change mitigation projects. These projects are all-encompassing, ranging from reducing greenhouse gas emissions to energy efficiency projects. In recent years, the issuance of green bonds has increased. As of 2019, the global green bond issuance had reached a new record of USD 257.7 billion. Therefore, more and more researchers are studying the volatility spillover relationship between the green bond market and the financial market (Pham, 2021; Reboredo et al., 2020; Mensi et al., 2021). Furthermore, as Agliardi and Agliardi (2019) emphasized, the characteristics of green bonds are not limited to the "green" aspects directly related to the promotion and implementation of green development initiatives. Still, they include the government's responsibility to accelerate climate action and create a geopolitical situation conducive to green transactions. Therefore, some researchers have also set out to study the relationship between green bonds and geopolitical risks, economic policy, carbon market risk, etc. (Lee et al., 2021; Pham and Nguyen, 2021; Jin et al., 2020).

The sustainability index is designed and constructed to provide information to institutional and retail investors. There are basically three sustainability indexes that have the most influence and are the most representative in the international arena: the Dow Jones Sustainability Index, the FTSE4Good Index, and the Domini 400 Social Index. In the last decade, Socially Responsible Investment (SRI) has grown faster than traditional investment (Maraqa et al., 2020; Cortez et al., 2012), and the number of investors including SRI in their portfolios has also increased. SRI does not include investment activities related to tobacco, weapons, and gambling. Many investors believe that investing in companies that comply with sustainability standards will create new long-term value. This type of investment is considered safer because it avoids environmental and social development risks, and sustainability indexes such as the Dow Jones Sustainability Index, the FTSE4Good Index, etc., can become investors' investment wind indicators.

In 1997, to solve the problem of global warming, more than 100 countries in the world signed the Kyoto Protocol. The treaty stipulates the emission reduction obligations of developed countries and proposes three flexible emission reduction mechanisms. Carbon emissions trading is one of them. Under the agreement's restrictions, carbon dioxide emission rights have become a new asset different from commodity futures and financial assets (Medina and Pardo, 2013). The construction of the carbon emission trading system has spread to Europe, North America, South America, and Asia. Carbon markets are globally recognized tools for mitigating climate change because they provide cost-effective solutions (Zeng et al., 2021). So far, the most effective system is the EU Emissions Trading System (EU ETS). The entire EU ETS covers more than 12,000 power stations, factories, and other industrial facilities.

They account for nearly half of the EU's total carbon dioxide emissions, and their quota market share accounts for more than 90% of the global quota market share (Sun et al., 2020). Since carbon emissions have such good investment prospects, people may ask: How does the dynamic spillover effect between the carbon market and the sustainable stock market perform? How is the risk-hedging performance between them?

To answer these questions, the present study investigates the dynamic connectedness between the ESG stock index, the renewable energy stock index, the green bond stock index, the sustainability stock index, and the carbon emission futures by employing a novel method: the DCC-GARCH-based connectedness approach developed by Gabauer (2020). To better understand the structure of the volatility spillover effect among these indexes, this study uses the network approach based on Diebold and Yilmaz (2016) to visualize the volatility spillover table. Moreover, the present study uses both the optimal hedging ratios and the optimal portfolio weights based on the DCC-GARCH t-copula model to measure the degree of the risk hedging (Kroner and Sultan, 1993; Kroner and Ng, 1998) and the hedging effectiveness to measure the effectiveness of risk hedging (Ederington, 1979).

The significance of this study can be summarized in the following points: First, our study is the first to use the brand-new DCC-GARCH-based dynamic connectedness model and the DCC-GARCH t-copula model to investigate the volatility spillover effect and the risk-hedging manifestation between the ESG stock index, the renewable energy stock index, the green bond stock index, the sustainability stock index, and the carbon emission futures. Previous studies have shown high and strong spillovers between carbon prices and renewable energy indexes in the short and long terms (Hanif et al., 2021), and this spillover effect is also reflected in carbon prices and green bonds (Tiwari et al., 2022). Because the renewable energy stock index and the green bond index are closely related to sustainability, we also use the indexes related to sustainable investing: the ESG index and the sustainability index. We not only study the dynamic relationship and risk-hedging performance between sustainability-related indexes and carbon emissions, but we also evaluate the dynamic relationship and risk-hedging performance among sustainability-related indexes. We find that there is a strong conditional correlation among sustainability indexes that is consistent with Zhang et al. (2021).

Second, the DCC-GARCH-based dynamic connectedness approach, a newly created method by Gabauer (2020), differs from the traditional model for estimating dynamic connectedness. This novel method can overcome the main drawbacks of rolling window analysis: the arbitrary choice of window size and loss of observations in most cases. It also lets us test whether the contagion mechanism is time-varying.

Third, given that the volatility spillover effect among sustainability indexes and the conditional correlation between sustainability indexes and carbon emissions are found to be strong, we need to consider whether they can be used as a portfolio of risk-hedging investment strategies. Our empirical results indicate that asset risk hedging, especially after COVID-19, has had a massive impact on financial markets, thus providing investors with an investment direction when creating a portfolio.

The main findings of this study are as follows: First, we provide new evidence for the dynamic connectedness among sustainability-related indexes by employing the new

DCC-GARCH-based dynamic connectedness approach. The results show that carbon emission futures are the volatility transmitter, and the green bond is the volatility receiver among the five sustainability-related indexes. Second, the results of network analysis indicate that the green bond is the one-way volatility spillover receiver. Furthermore, the volatility connectedness from the renewable energy stock index to ESG and sustainability indexes also has a relatively high level. Third, the results of dynamic total connectedness show that the dynamic connectedness fluctuated between 45 and 92% during 2010 and 2021 because of the influence of political, economic, cultural, and other international events, especially around 28 October 2011, February–June 2013, and December 2019. These results illustrate that the eurozone (debt) crisis, the drop in the international carbon market price, and the COVID-19 pandemic have had a profound impact on sustainable development investments. Finally, among the five indexes, the carbon emission futures index should take a long position, and the renewable energy index should take a short position. Except for the green bond index, the carbon emission market has a good risk-hedging performance with other indexes.

The rest of this study is organized as follows: Section 3.2 briefly reviews previous relevant literature. Section 3.3 is dedicated to the model theory used in this study. Section 3.4 describes the data used in the study and their descriptive statistics. Section 3.5 presents and discusses the empirical findings of this study. Section 3.6 includes the conclusions and implications, and prospects for future research.

3.2. Literature review

Excellent ESG performance can play a role in reducing costs, increasing value, reducing systemic risks, improving operational efficiency, and providing legal protection. As ESG has received attention from the governments and regulatory authorities of various countries, ESG investment has gradually become the mainstream trend in the international investment community. More and more researchers have investigated the application of the ESG index in investment portfolios. Giese et al. (2019) focused on how asset owners can achieve ESG integration by indexing portfolios that seek to replicate ESG indexes. La Torre et al. (2020) investigated how ESG components affect stock returns and found that ESG strategies had a positive impact on returns for a few firms, mostly in specific industries such as energy and utilities. Using event study methodology, Cui and Docherty (2020) examined stock returns after ESG news announcements and calculated the cumulative abnormal return to 21 trading days after each news release. They discovered evidence that the market overreacts to ESG news, which could have negative implications for market efficiency and investor behavior. In the context of carbon neutrality, the international community is increasingly encouraging the promotion of sustainable investment. Therefore, more researchers are investigating the relationship between the ESG index, renewable energy stock indexes, and green finance. They think that investing in stocks of companies with the highest environmental, social, and governance (ESG) ratings may be a potentially enhanced investment in renewable energy stocks (Liu and Hamori, 2020; He et al., 2021).

As global warming intensifies, the emission of greenhouse gases will be subject to stricter restrictions. Investors have also begun to realize that the increasingly frequent abnormal weather caused by global warming is becoming more and more threatening to the human living environment. Since the end of the 20th century, the necessity of focusing green investment on environmental protection and social responsibility has gradually been recognized by financial investors. Renewable energy is a type of green finance, and its commercialization is promoted by governments in many countries. In recent years, the development of the renewable energy market has become more mature, and more investors and researchers are devoting themselves to researching the new energy market (Zeng et al., 2017; Egli, 2020; He et al., 2019; Shahbaz et al., 2021).

Furthermore, in addition to the renewable energy market, Reboredo (2018) investigated the co-movement between the green bond market and financial markets. He found that the green bond market was coupled with the corporate and treasury bond markets, but the co-movement with the stock and energy commodity markets was weak. Park et al. (2020) analyzed the volatility dynamics and spillover effects between equity and green bond markets. They found that green bonds displayed asymmetric volatility, but their volatility was sensitive to positive return shocks, unlike equity.

The dynamic connectedness approach based on the DCC-GARCH model was developed by Gabauer (2020) to provide an alternative framework to first estimate the volatility transmission mechanism. This method is different from the traditional method of calculating dynamic connectedness, and it does not have to adhere to the window size of the moving window. Unlike that of Diebold and Yilmaz (2012, 2014), another advantage of using this approach is that only one model is needed to obtain the conditional volatility transmission mechanism. Some researchers have employed this approach to calculate the dynamic connectedness among the gold market, oil market, and five representative stock markets under the COVID-19 epidemic and found that gold is the volatility receiver and oil is the transmitter (Benlagha and EI Omari, 2021). Nawazish (2021) also applied this method to estimate the time-varying correlations between gold futures and crude oil futures and concluded that gold could not effectively hedge the uncertainty of crude oil.

Furthermore, the dynamic connectedness method based on the DCC-GARCH model is not only used in correlation analysis among stock markets. It can also be applied to investigate the asymmetric spillovers in sustainable investment (Iqbal et al., 2021); the connectedness between virtual currency–Bitcoin and the stock market (Kamran et al., 2021); the connectedness in the exchange rate markets (Funke et al., 2020); and the dynamic transmission mechanism among 2Y, 5Y, and 10Y interest rate swaps (Chatziantoniou et al., 2021). Moreover, Lesame et al. (2021) estimated the dynamic connectedness in the international Real Estate Investment Trust (REIT) markets to capture the systemic risks and impact transmission across REIT markets and found that the interdependence of the REIT markets is dynamic, with a significant increase during the COVID-19 pandemic.

A group of researchers focused on estimating the hedging ratio, the portfolio weights, and the hedging effectiveness among financial markets. Broadstock et al. (2022) employed the "minimum connectedness" portfolio method to estimate the manifestation of the green bond in an international fixed-income investor's portfolio. They found that the portfolio weight of the green bond ranged from 40 to 80%, indicating that the green bond had an extraordinary performance. Furthermore, Wang et al. (2021) compared the risk-hedging ability of Bitcoin in the stock market, commodity market, and exchange rate market. They concluded that the connectedness between Bitcoin and the stock market is the smallest for all hedges in the short horizons.

Moreover, some researchers have investigated the leading–lag relationship between housing prices and home sales in the US and found that portfolio managers and investors should consider the dynamic relationship among various regions in the United States when making investment decisions and creating a persuasive portfolio (Antonakakis et al., 2020a). Moreover, Akhtaruzzaman et al. (2021) investigated how financial contagion occurred between financial and non-financial companies in China and G7 countries during the COVID-19 epidemic and estimated the hedging performance. They found that the optimal hedging ratio between China and G7 stock returns (financial and non-financial) had increased significantly in most cases during the COVID-19 pandemic. Similar to ours, there are also papers studying the hedging performance of green investments such as green bonds and renewable energy (Yousaf et al., 2021; Saeed et al., 2020; Janda et al., 2021).

3.3. Methodology

3.3.1. DCC-GARCH and Volatility Impulse Response Functions

Following Gabauer (2020), we employed the Volatility Impulse Response Functions (VIRFs) for Dynamic Conditional Correlation–Generalized Autoregressive Conditional Heteroskedasticity (DCC-GARCH) to analyze the dynamic connectedness among sustainability-related indexes. Compared with the traditional method (using a moving window to calculate the dynamic connectedness), one advantage of the dynamic connectedness approach based on DCC-GARCH is that it does not require selecting an arbitrary window size to retrieve dynamic connectedness measures (Bouri et al., 2021). Antonakakis (2012) and Hoesli and Reka (2013) employed the DCC-GARCH model developed by Engle (2002) and generalized the Vector Autoregression (VAR) methodology proposed by Diebold and Yilmaz (2009) to construct the conditional volatility transmission mechanism. While they needed two models, another advantage of the dynamic connectedness approach based on DCC-GARCH is that we needed only one model to derive the conditional volatility transmission mechanism.

The GARCH model calculates the volatility as a deterministic variable, which is essential for the DCC-GARCH model. The SV model, on the other hand, calculates volatility as a stochastic variable. Following Jones and Olson (2013); Singhal and Ghosh (2016); Hou et al. (2019), we employ the GARCH model to forecast the volatility.

The advantages of the DCC-GARCH model over the BEKK model are summarized in three points. First, the DCC-GARCH model directly calculates the dynamic conditional correlation over time. Second, using the DCC-GARCH model allows the calculation of dynamic connectedness without using the moving window approach, thus avoiding missing observation samples (Gabauer, 2020). Third, the DCC-GARCH model estimates the correlation coefficients of the standardized residuals and, therefore, directly accounts for heteroskedasticity. Because of this, the time-varying correlation (DCC) is free of volatility bias (Celık, 2012). For the comparison between the BEKK model and the DCC-GARCH model, see Caporin and McAleer (2008), Caporin and McAleer (2012), and Huang et al. (2010).

To investigate the time-varying conditional volatility, we applied the DCC-GARCH model constructed by Engle (2002). The DCC-GARCH model to calculate the time-varying conditional variance and covariance is shown as follows:

$$\boldsymbol{y}_t = \boldsymbol{c}_t + \boldsymbol{\varepsilon}_t, \quad \boldsymbol{\varepsilon}_t|\boldsymbol{M}_{t-1} \sim N(\boldsymbol{0}, \boldsymbol{H}_t), \tag{3.1}$$

$$\boldsymbol{\varepsilon} = \boldsymbol{H}_t^{1/2}\boldsymbol{u}_t, \ \boldsymbol{u}_t \sim N(\boldsymbol{0}, \boldsymbol{I}), \tag{3.2}$$

$$\boldsymbol{H}_t = \boldsymbol{D}_t\boldsymbol{R}_t\boldsymbol{D}_t, \tag{3.3}$$

$$\boldsymbol{D}_t = diag\left(h_{11t}^{1/2}, \dots, h_{KKt}^{1/2}\right), \tag{3.4}$$

where $\boldsymbol{M}_{t-1}$ represents all information available from 1 to $t-1$. $\boldsymbol{y}_t$, $\boldsymbol{c}_t$, $\boldsymbol{\varepsilon}_t$ and $\boldsymbol{u}_t$ are $(K \times 1)$-dimensional vectors standing for the analyzed time series, conditional mean, error term, and standardized error term, respectively. Moreover, $\boldsymbol{R}_t$, $\boldsymbol{D}_t$ and $\boldsymbol{H}_t$ are $(K \times K)$-dimensional matrices that represent the dynamic conditional correlations, the time-varying conditional correlations, and time-varying conditional variance–covariance, respectively.

In the first step, the components were estimated by the GARCH model for each series (Bollerslev, 1986). According to the research of Hansen and Lunde (2005), we can define the one shock and the one persistency parameter as follows:

$$h_{ii,t} = \omega + \alpha\varepsilon_{i,t-1}^2 + \beta h_{ii,t-1}, \tag{3.5}$$

where α and β are non-negative shock and persistency parameters. α, β satisfy this condition: $\alpha + \beta < 1$.

In the second step, the dynamic conditional correlations can be calculated as follows:

$$\boldsymbol{R}_t = diag\left(q_{iit}^{-1/2}, \dots, q_{KKt}^{-1/2}\right)\boldsymbol{Q_t}diag\left(q_{iit}^{-1/2}, \dots, q_{KKt}^{-1/2}\right), \tag{3.6}$$

$$\boldsymbol{Q_t} = (1 - a - b)\overline{\boldsymbol{Q}} + a\boldsymbol{u}_{t-1}\boldsymbol{u}_{t-1}' + b\boldsymbol{Q}_{t-1}, \tag{3.7}$$

where $\boldsymbol{Q_t}$ and $\overline{\boldsymbol{Q}}$ are $(K \times K)$-dimensional positive-definite matrices standing for the variance–covariance matrices of the conditional and unconditional standardized residuals, respectively. Similarly, a and b are non-negative shock and persistency parameters. a, b satisfy this condition: $a + b < 1$. So long as $a + b < 1$ is satisfied, $\boldsymbol{Q_t}$ and $\boldsymbol{R}_t$ can vary over time; otherwise, this model will change to the Constant Conditional Correlation–Generalized Autoregressive Conditionally Heteroscedastic (CCC-GARCH) model where $\boldsymbol{R}_t$ is constant over time (Bollerslev, 1990).

The dynamic connectedness methodology developed by Diebold and Yilmaz (2012, 2014) based on the Generalized Impulse Response Functions (GIRFs) is commonly used in traditional volatility spillover analysis. In their study, GIRF was defined as the J-step-ahead influence of a shock in each variable of $\boldsymbol{y}_t$ on variable j :

$GIRF(J, \gamma_{j,t}, \boldsymbol{M}_{t-1}) = E(\boldsymbol{y}_{t+J} | \varepsilon_{j,t} = \gamma_{j,t}, \boldsymbol{M}_{t-1}) - E(\boldsymbol{y}_{t+J} | \varepsilon_{j,t} = 0, \boldsymbol{M}_{t-1})$, where $\gamma_{j,t}$ is a shock at the *j*th variable. Note that *J*-step-ahead means predicting the result after *J* days, and we set *J* to be ten days in our dynamic analysis. Unlike the traditional VAR model, the advantage of GIRF is that it is unaffected by variable ordering.

Inspired by GIRF, the VIRF developed by Gabauer (2020) stands for a shock in each variable of $\boldsymbol{H}_t$ on variable *j*'s conditional volatilities at *J*-step-ahead and can be stated as follows:

$$\boldsymbol{\Phi}^g = VIRF(J, \gamma_{j,t}, \boldsymbol{M}_{t-1}) = E(\boldsymbol{H}_{t+J} | \varepsilon_{j,t} = \gamma_{j,t}, \boldsymbol{M}_{t-1}) - E(\boldsymbol{H}_{t+J} | \varepsilon_{j,t} = 0, \boldsymbol{M}_{t-1}), \tag{3.8}$$

where $\boldsymbol{M}_{t-1}$ represents all information available from 1 to $t-1$. $\boldsymbol{H}_{t+J}$ represents the time-varying conditional variance-covariance of the *J*-period forecast.

The core of VIRF is using the DCC-GARCH model (Engle & Sheppard, 2001) to predict conditional variance–covariance, which can be done iteratively in three steps. In the first step, the conditional volatilities ($\boldsymbol{D}_{t+h} | \boldsymbol{M}_t$) will be forecasted by the univariate GARCH (1, 1) model as follows:

$$E(h_{ii,t+h} | \boldsymbol{M}_t) = \sum_{i=0}^{h-1} \omega(\alpha+\beta)^i + (\alpha+\beta)^{h-1} E(h_{ii,t+h-1} | \boldsymbol{M}_t), \quad h = 1, 2, \dots, n \tag{3.9}$$

whereas, in the second step, we can predict $E(\boldsymbol{Q}_{t+h} | \boldsymbol{M}_t)$ by:

$$E(\boldsymbol{Q}_{t+h} | \boldsymbol{M}_t) = (1 - a - b)\bar{\boldsymbol{Q}} + aE(\boldsymbol{u}_{t+h-1}\boldsymbol{u}'_{t+h-1} | \boldsymbol{M}_t) + bE(\boldsymbol{Q}_{t+h-1} | \boldsymbol{M}_t), \quad h = 1,2, \dots, n \tag{3.10}$$

where $E(\boldsymbol{u}_{t+h-1}\boldsymbol{u}'_{t+h-1} | \boldsymbol{M}_t) \approx E(\boldsymbol{Q}_{t+h-1} | \boldsymbol{M}_t)$ (Engle & Sheppard, 2001), which can help to forecast the dynamic conditional correlations and the conditional variance–covariance in the final step:

$$E(\boldsymbol{R}_{t+h} | \boldsymbol{M}_t) \approx diag[E(q_{iit+h}^{-1/2} | \boldsymbol{M}_t), \dots, E(q_{KKt+h}^{-1/2} | \boldsymbol{M}_t)] E(\boldsymbol{Q}_{t+h}) diag[E(q_{iit+h}^{-1/2} | \boldsymbol{M}_t), \dots, E(q_{KKt+h}^{-1/2} | \boldsymbol{M}_t)], \tag{3.11}$$

$$E(\boldsymbol{H}_{t+h} | \boldsymbol{M}_t) \approx E(\boldsymbol{D}_{t+h} | \boldsymbol{M}_t) E(\boldsymbol{R}_{t+h} | \boldsymbol{M}_t) E(\boldsymbol{D}_{t+h} | \boldsymbol{M}_t), \tag{3.12}$$

3.3.2. Dynamic Connectedness Approach based on DCC-GARCH

The Generalized Forecast Error Variance Decomposition (GFEVD) $\Psi_{ij.t}^{g}(J)$ was calculated based on VIRF. The GFEVD can be explained as the pairwise directional connectedness from variable *j* to variable *i*. In other words, the pairwise directional connectedness can be accounted for by the impact of the shock in variable *j* on the variance share of the forecast error of variable *i*. These variance shares are normalized so that the sum of each row is 1, which means that all variables together interpret 100%

of the variance of the prediction error of variable i (Diebold and Yilmaz 2012, 2014). The calculation process is as follows:

$$\textit{Pairwise Directional Connectedness}: \; \tilde{\Psi}^{g}_{ij.t}(J) = \frac{\sum_{t=1}^{J} \Phi^{2,g}_{ij,t}}{\sum_{j=1}^{K}\sum_{t=1}^{J-1} \Phi^{2,g}_{ij,t}} \tag{3.13}$$

where $\sum_{j=1}^{K} \tilde{\Psi}^{g}_{ij.t}(J) = 1$ and $\sum_{i,j=1}^{K} \tilde{\Psi}^{g}_{ij.t}(J) = K$. The denominator represents the aggregate cumulative effect of all shocks, while the numerator represents the cumulative effect of the ith shock.

Next, by using the GFEVD, the total connectedness index (TCI) can be calculated as follows:

$$\textit{Total Connectedness Index (TCI)}: \; C^{g}_{t}(J) = \frac{\sum_{i,j=1,i\neq j}^{K} \tilde{\Psi}^{g}_{ij.t}(J)}{K} \tag{3.14}$$

In general, the TCI reflects the average amount of one variable's forecast error variance share is explained by all other variables, or, in other words, how much a shock in one variable affects all others on average.

After we derive the TCI, we can define the total directional connectedness TO other variables, which means the spillovers transmitted from variable i to variable j, by:

$$\textit{Total Directional Connectedness (TO)}: \; C^{g}_{i\to j,t}(J) = \frac{\sum_{j=1,i\neq j}^{K} \tilde{\Psi}^{g}_{ji.t}(J)}{\sum_{j=1}^{K} \tilde{\Psi}^{g}_{ji.t}(J)} \tag{3.15}$$

Then, the total directional connectedness FROM other variables, which represents the spillovers variable i receives from variable j, can be defined by:

$$\textit{Total Directional Connectedness (FROM)}: \; C^{g}_{i\leftarrow j,t}(J) = \frac{\sum_{j=1,i\neq j}^{K} \tilde{\Psi}^{g}_{ij.t}(J)}{\sum_{i=1}^{K} \tilde{\Psi}^{g}_{ij.t}(J)} \tag{3.16}$$

Finally, the net total directional connectedness of variable i is the difference between the total directional connectedness (TO) and the total directional connectedness (FROM). If variable i has a positive (negative) value of net total directional connectedness, it signifies that variable i is a net shock transmitter (receiver). This can be calculated by:

$$\textit{Net Total Directional Connectedness}: \; C^{g}_{i.t} = C^{g}_{i\to j,t}(J) - C^{g}_{i\leftarrow j,t}(J) \tag{3.17}$$

3.3.3. Optimal Hedging and Portfolio Strategies based on DCC-GARCH t-Copula

Following Antonakakis et al. (2020b) and Mandacı et al. (2020), we employed the DCC-GARCH t-copula model to calculate the conditional variance–covariance and dynamic conditional correlations that are applied to compute the optimal hedging ratio and the optimal portfolio weights. Because we explained the structure of the DCC-GARCH model in detail in Section 3.1, we will not repeat the DCC-GARCH model here. We employed the dynamic connectedness based on the fundamental DCC-GARCH model by Engle (2002) with standardized error following the multivariate Student's t-distribution. To estimate the optimal hedging ratio and the optimal portfolio weights, we employed the model with copula functions (Sklar, 1959) rather than Student's t-distribution. Patton (2006) proposed the copula theory as a flexible tool for modeling the dependency among N random variables, demonstrating that the N-marginal distribution function and a copula combine to generate an N-dimensional joint distribution function. $F_{X_1,\dots,X_N}$ is defined as the joint distribution function of the random variables $X_1,\dots,X_N$ with continuous marginal distribution functions $F_{X_1}(x_1),\dots,F_{X_N}(x_N)$. In this situation, the unique *N*-dimensional copula distribution function *C* can be defined as:

$$F_{X_1,\dots,X_N} = C\left(F_{X_1}(x_1),\dots,F_{X_N}(x_N)\right), \tag{3.18}$$

$$C(u_1,\dots,u_N) = F_{X_1,\dots,X_N}(F_{X_1}^{-1}(u_1),\dots,F_{X_N}^{-1}(u_N), \tag{3.19}$$

Patton (2006) applied the theory of copulas to the multivariate conditional case, allowing for asymmetric modeling of time-varying conditional dependence between time series. The density of Student's *t*-copula function with shape parameter θ is used to construct the DCC-GARCH t-copula model as follows:

$$C(u_1,\dots,u_N|\boldsymbol{R}_t,\theta) = t_\theta\left(F_{X_1}^{-1}(u_1|\bullet_1),\dots,F_{X_N}^{-1}(u_N|\bullet_N)\right)$$

$$= \int_{-\infty}^{F_1^{-1}(u_1)}\dots\int_{-\infty}^{F_N^{-1}(u_N)} \frac{\Gamma(\theta+N/2)}{\Gamma(\theta/2)(\theta\pi)^{N/2}|\boldsymbol{R}_t|^{1/2}}\left((1+\frac{1}{\theta}\boldsymbol{z}_t'\boldsymbol{R}_t^{-1}\boldsymbol{z}_t)\right)^{(\theta+N)/2} dz_1,\dots,dz_N \tag{3.20}$$

where $F_{X_i}^{-1}(u_i|\bullet_i)$ stands for the conditional distribution, and $\bullet_i$ denotes the estimated parameters of the univariate GARCH model. This indicates that there are different marginal distributions in the fundamental univariate GARCH models within the DCC-GARCH t-copula model.

Next, we employed the fundamental DCC-GARCH model constructed by Engle (2002) to estimate the conditional variance and covariance (because we already introduced the DCC-GARCH model in Section 3.1, we will not elaborate on it here). Here, following Kroner and Sultan (1993), we employed the estimated conditional variance and covariance from DCC-GARCH to calculate the optimal hedging ratio (β_{ijt}) as follows:

$$\beta_{ijt} = h_{ijt}/h_{jjt} \tag{3.21}$$

where h_{ijt} and h_{jjt} represent the conditional covariance of variable *i* and variable *j* and the conditional variance of *i*, respectively. The cost of hedging a 1 dollar long position in variable *i* with a β_{ijt} dollar short position in variable *j* is calculated by the optimal hedging ratio. This indicates that the higher conditional variance of *i* will lead to lower long position hedging costs, while the higher conditional covariance of *i* and *j* will cause higher long position hedging costs.

Following Kroner and Ng (1998), the optimal portfolio weights (W_{ijt}) can be denoted by:

$$W_{ijt} = \frac{h_{jjt}-h_{ijt}}{h_{iit}-2h_{ijt}+h_{jjt}} \tag{3.22}$$

Because we are only interested in long position, we imposed the restrictions on the optimal portfolio weights as follows:

$$W_{ijt} = \begin{cases} 0 & if\ W_{ijt} < 0 \\ W_{ijt} & if\ 0 \le W_{ijt} \\ 1 & if\ W_{ijt} > 1 \end{cases} \tag{3.23}$$

where W_{ijt} represents the weight of variable i in a 1 dollar portfolio of two variables *i* and j at time *t*. The weight of variable j is $W_{jit} = 1 - W_{ijt}$.

After we derived the optimal hedging ratio and the optimal portfolio weights, we calculated the effectiveness of the hedging and portfolio. Following Ederington (1979), the hedging effectiveness (HE_{ijt}) can be defined as:

$$r_{\beta ijt} = x_{it} - \beta_{jit} x_{jt} \tag{3.24}$$

$$r_{wijt} = W_{ijt} x_{it} + W_{jit} \tag{3.25}$$

$$HE_{ijt} = 1 - \left[(Var(r_{\beta ijt}), Var(r_{wijt})) / Var(r_{unhedged}) \right] \tag{3.26}$$

where $(Var(r_{\beta ijt}), Var(r_{wijt}))$ represents either the optimal hedging ratio or the optimal portfolio weight strategy's hedged portfolio variance. $Var(r_{unhedged})$ stands for the variance of the unhedged position between variable *i* and variable j. In fact, the HE measures the percent reduction in the variance of the unhedged position. A higher HE indicates a larger reduction. Following Antonakakis et al. (2020b), we found that the Brown and Forsythe (1974) test performed outstandingly in examining the significance of the HE, so we employed the Brown and Forsythe (1974) test to check the significance of the HE and determine if one of our investment approaches was successful in reducing variation.

3.4. Data

We employed the daily (from 1 November 2010 to 28 October 2021) futures prices of the ESG index and the index related to green finance, MSCI World ESG Leaders Index (WESG), WilderHill New Energy Global Innovation Index (NEX), S&P Green Bond Index Total Return (SPGB), Dow Jones Sustainability World Composite Index (DJS), and Carbon Emissions Futures (CEF). To remove the influence of the exchange rate on the analysis results, we unified the currency unit of all futures price indexes to US dollars. The official names, acronyms, and data sources of variables are reported in Table 3.1[13].

[13] In order to check whether there is multicollinearity in the model, following Mansfield and Helms (1982); Franke (2010), we used the VIF function which stands for variance inflation factor. In general, when the VIF score exceeds 5, there is multicollinearity in this model. When the VIF score exceeds 10, there is strong multicollinearity in the model and the problematic variable should be dropped from the regression model. In our model, the VIF scores are smaller than 5 (WESG: 3.48; NEX: 3.66; SPGB: 2.92; DJS: 4.46; CEF: 2.92), so there is no longer any big problem of multicollinearity in our model.

Table 3.1. Data description.

Acronym	Data	Source
WESG	MSCI World ESG Leaders Index	Bloomberg
NEX	WilderHill New Energy Global Innovation Index	Bloomberg
SPGB	S&P Green Bond Index Total Return	Bloomberg
DJS	Dow Jones Sustainability World Composite Index	Bloomberg
CEF	Carbon Emissions Futures	Bloomberg

The WESG index is a capital-weighted index composed of the MSCI Pacific ESG Leaders index, MSCI Europe and Middle East ESG Leaders index, and other regional ESG indexes. It provides comprehensive information on companies that outperform their industry peers in terms of environmental, social, and governance (ESG). The WESG index is intended for investors seeking a broad and diverse sustainability benchmark with relatively low tracking errors in the relevant stock market. Therefore, this index is very representative of the world, and it was also a very good choice for us to investigate the volatility among the relevant indexes of the global sustainable stock market and their analyses of investment portfolio strategies[14]. The NEX index is primarily made up of companies involved in solar and wind power, as well as other businesses dealing in renewable energy such as biomass and biofuels, hydro, geothermal, marine, and so on; it also includes companies involved in energy storage, emerging new energy innovation such as electric vehicles, hydrogen and fuel cells, and decarbonization, broadly defined. The technologies of these companies that address climate change can help reduce emissions relative to the use of traditional fossil fuels. Since the Kyoto Protocol, clean energy has grown significantly outside of the United States, with many activities currently underway in Europe, the Asia–Pacific region, and other locations. Therefore, since its construction in 2006, the NEX has become the most famous index in this industry and has been used as a diversification tool in green finance-related investment portfolio strategies[15]. The SPGB index aims to track the global green bond market and includes green bonds issued by multilateral, government, and corporate issuers from around the world. This index adheres to strict criteria, including only bonds whose proceeds are used to fund environmental protection projects. Based on long-term environmental, social, and governance standards, the DJS index represents the top 10% of the 2500 largest companies in the S&P Global Broad Market Index. Many investors seek socially conscious investments, making the DJS index a popular benchmark for private wealth management institutions. The CEF index used in our paper refers to the carbon emission futures index under the European Union Greenhouse Gas Emission Trading Scheme (EU ETS). Since the United States is not a member of the Kyoto Protocol, only the EU ETS and the UK Emissions Trading System (UK ETS) are international exchanges. Moreover, the EU ETS is the world's largest carbon market and the most complete system that includes the largest large-scale carbon

[14] The factsheet of MSCI World ESG Leaders Index: https://www.msci.com/documents/10199/db88cb95-3bf3-424c-b776-bfdcca67d460

[15] The factsheet of WilderHill New Energy Global Innovation Index. https://cleanenergyindex.com/about_nex.php

market.

Figure 3.1 shows the plot of the raw data series in our paper. Among the five indexes, only SPGB was very stable, and there was almost no fluctuation from 2010 to 2021, basically maintaining the level of USD 120 to USD 150. However, because of COVID-19, prices in the other four indexes had an upward trend after the end of 2019. To calculate the return series, we employed the logarithmic method: $\ln(p_t) - \ln(p_{t-1})$.

Table 3.2 represents the descriptive statistics for the return series. Regarding the mean of the return series, the average return of all indexes was positive. The average return of SPGB was the smallest, while the average return of the CEF was the largest. This result was consistent in that the original price trend of SPGB was shown as stable, while the original price trend of the CEF fluctuated greatly in Figure 3.1. Meanwhile, SPGB had the smallest maximum value and the largest minimum value, while the CEF had the largest maximum value and the smallest minimum value. Through the above statistical results, SPGB was shown to be a relatively low-risk index, while the CEF was a relatively high-risk index. The skewness value of all index returns was negative, indicating that their return distribution was left-skewed. However, since the kurtosis of the return of all variables was positive, this meant that the leptokurtic was a regression of four attributes, and the returns of these five variables will see more peakedness and fat tails. We applied the Jarque and Bera (1980) test to examine the normality for the return of these five variables, and the JB test statistics rejected normality for each variable at the 1% significance level. To check the stationarity of the return series, we adopted the Augmented Dickey–Fuller (ADF) test of Said et al. (1984) to check the unit root process of the return series and found the ADF test to show that the null hypothesis for each variable with a unit was rejected, indicating that no unit root existed for each variable. ARCH-LM refers to Engle's (1982) ARCH-LM test, which was used for Autoregressive Conditional Heteroskedasticity effects. The result of the ARCH-LM test showed ARCH errors at the 1% significance level, indicating that modeling the multivariate GARCH model was appropriate.

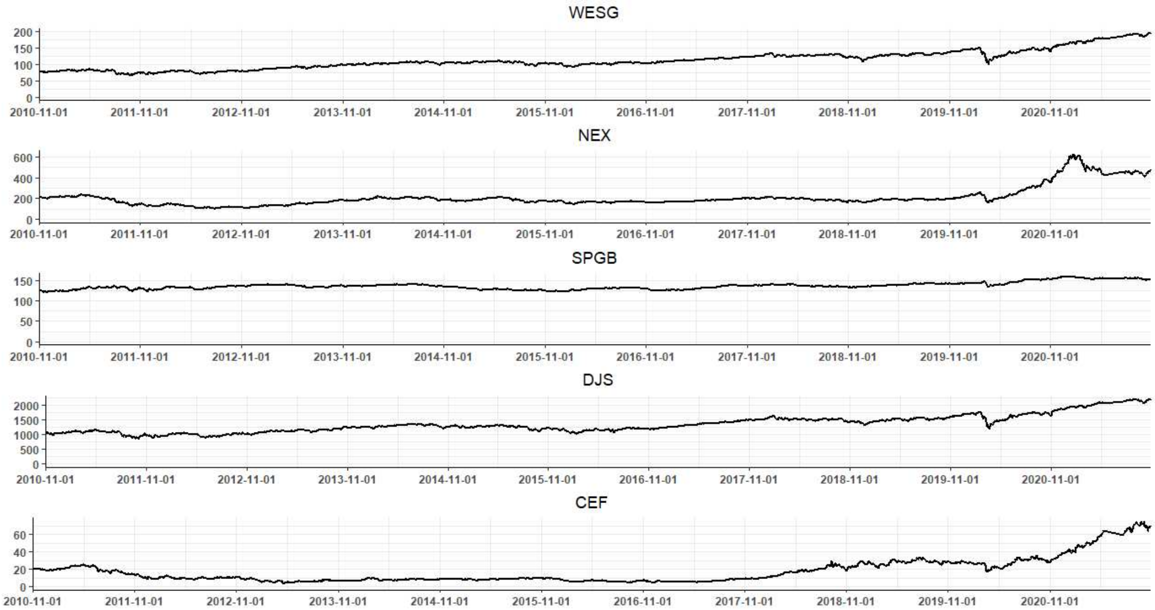

Figure 3.1. Time variations of raw data series.

Notes: WESG represents MSCI World ESG Leaders Index; NEX represents WilderHill New Energy Global Innovation Index; SPGB represents S&P Green Bond Index Total Return; DJS represents Dow Jones Sustainability World Composite Index; CEF represents Carbon Emissions Futures.

Table 3.2. Summary statistics for return series.

Descriptive Statistics for Return					
	WESG	NEX	SPGB	DJS	CEF
Mean	0.035	0.031	0.008	0.028	0.045
Median	0.071	0.087	0.015	0.059	0.082
Maximum	8.627	9.396	2.573	7.694	24.561
Minimum	−10.271	−12.541	−3.079	−10.605	−42.457
Std. Deviation	0.939	1.309	0.392	0.986	3.357
Skewness	−1.091***	−0.582***	−0.329***	−0.993***	−0.856***
Kurtosis	17.636***	8.675***	6.159***	12.699***	13.905***
JB	35685***	8656***	4336***	18668***	22181***
ADF	−14.404***	−12.472***	−14.866***	−14.665***	−15.278***
ARCH-LM	957.55***	579.87***	427.76***	712.82***	206.72***

Notes: All values are measured in percentile units. JB represents Jarque and Bera (1980) test for normality; ADF represents Augmented Dickey and Fuller Unit Root Test; ARCH-LM represents Engle's (1982) ARCH-LM test; *** denotes rejection of the null hypothesis at 1% significance levels.

3.5. Empirical results

3.5.1. Dynamic Connectedness Analysis

Table 3.3 exhibits the averaged dynamic connectedness of the volatility series.[16] The value in the ith row and jth column is the pairwise directional connectedness, which

[16] We use the R code provided by Prof. David Gabauer on Github (https://github.com/GabauerDavid) in our study.

means the spillover effect transmitted from variable j to variable i, and vice versa. FROM represents the spillover effect that a market receives from all other markets and is equal to the sum of the values in row i, excluding the diagonal values. On the other hand, TO stands for the spillover effects transmitted from one market to other markets and is equal to the sum of the values in column j, excluding the diagonal values. "NET directional connectedness" refers to the difference between the TO value and the FROM value of a variable. "NPDC transmitter" refers to the net pairwise directional connectedness transmitter, which stands for the number of variables to which variable i transmits more spillover effects than the number of variables from which it receives spillover effects. TCI represents the total connectedness index, which is the sum of the TO value or FROM value and is divided by $N-1$ (number of variables minus one).

From Table 3.3, we can see the TCI of the volatility series was 64.62%, indicating a high interconnectedness between the volatility of sustainability-related indexes. In terms of the pairwise connectedness, the largest volatility spillover effect was from the CEF to the SPGB, at 39.52%. Meanwhile, the smallest volatility effect was from the SPGB to the CEF, at 0.25%, but the volatility spillover effect from the CEF to the SPGB had a violent level that was the highest among the five variables (39.52%), illustrating a one-way risk transfer relationship from the CEF to the SPGB. For the results of the TO value, the CEF had the largest TO value (86.88%), and the SPGB had the smallest TO value (3.7%). For the results of the FROM value, the WESG had the largest FROM value (73.95%) and the CEF had the smallest FROM value (3.4%). Although the FROM value of the SPGB was not the highest, it still had a relatively high value (66.66%). Therefore, the net directional connectedness of the CEF had the largest value (83.48%) and the CEF was an absolute volatility transmitter. Meanwhile, the SPGB had the smallest net directional connectedness (−62.96%), indicating that it was a complete volatility receiver among these five sustainability-related indexes[17].

Table 3.3. Averaged dynamic connectedness table of volatility series.

	WESG_Vol	NEX_Vol	SPGB_Vol	DJS_Vol	CEF_Vol	FROM
WESG_Vol	26.05	30.61	1.1	27.03	15.22	73.95
NEX_Vol	13.11	55.46	0.86	16.15	14.42	44.54
SPGB_Vol	5.37	11.57	33.34	10.21	39.52	66.66
DJS_Vol	21.38	29.31	1.5	30.1	17.71	69.9
CEF_Vol	0.64	1.58	0.25	0.93	96.6	3.4
TO	40.49	73.07	3.7	54.31	86.88	258.46
NET directional connectedness	−33.47	28.53	−62.96	−15.59	83.48	TCI
NPDC transmitter	1	3	0	2	4	64.62

Note: WESG_Vol represents the volatility of WESG; NEX_Vol represents the volatility of NEX; SPGB_Vol represents the volatility of SPGB; DJS_Vol represents the volatility of DJS; CEF_Vol represents the volatility of CEF.

To further visualize our dynamic connectedness table of volatility series, we

[17] We put the result of robustness check in the appendix.

referred to Diebold and Yilmaz (2016) and Bilgin and Yilmaz (2018) to network the dynamic connectedness table as shown in Figure 3.2.[18] We used the node size, arrow direction, etc., to convey information about the estimated network characteristics that could help us to better show the structure of the dynamic connectedness. Node size represents the value of TO; the larger the value of TO, the larger the size of the node. Arrow direction stands for the transmission direction of the pairwise directional connectedness between two variables. The size of the arrow represents the value level of the pairwise connectedness transferred between the two variables, and the number shown above the arrow represents the specific value of pairwise connectedness: the larger the value, the thicker the arrow. The variable displayed by the node label next to the number is the receiver, and the variable displayed by the other node label is the transmitter. In Figure 3.2 we can observe that the node of the CEF is the largest while the node of the SPGB is the smallest, indicating that the CEF contributed the most volatility spillover effect to other variables while the SPGB contributed the least, which was consistent with the result in the dynamic connectedness table. The thickness of the arrow and the number on the arrow reveal that the CEF contributed the highest volatility connectedness to the SPGB (39.52%). The volatility connectedness from the NEX to the WESG and DJS also had relatively high levels, 30.61 and 29.31%, respectively. However, except for the SPGB, the other four variables had values of more than 10% for the volatility spillover transmitted to other variables. Only the volatility spillover effect transferred from the SPGB to other variables did not exceed 5%, and the SPGB had the smallest node, indicating that the SPGB was a monodirectional receiver of the volatility spillover effect and will fluctuate with the impact of other indexes.

[18] We employed the free software: Gephi (https://gephi.org/) to network the dynamic connectedness table.

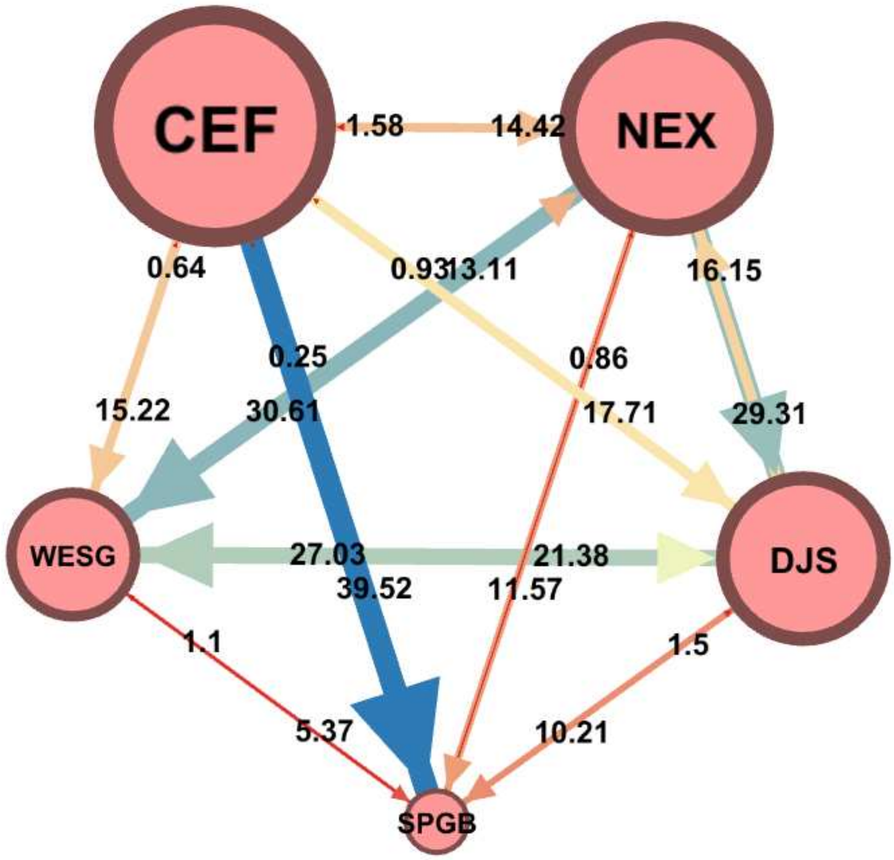

Figure 3.2. Network based on the averaged dynamic connectedness table of volatility series for the full sample.

Notes: WESG represents the volatility of WESG; NEX represents the volatility of NEX; SPGB represents the volatility of SPGB; DJS represents the volatility of DJS; CEF represents the volatility of CEF. Node size represents the value of TO. Arrow direction stands for the direction of volatility spillover. The size of the arrow represents the level of volatility spillover between the two variables. The number on the arrow represents the specific value of the volatility spillover between the two variables.

Because the dynamic connectedness table and network cannot display the impact of specific events on volatility connectedness fluctuations, we visualized the volatility dynamic total connectedness to observe the long-term or cyclical impact of some crisis events on volatility connectedness. Figure 3 shows the dynamic total connectedness of the volatility series. There are nine obvious fierce fluctuations in the volatility dynamic total connectedness. These violent fluctuations were influenced by the major economic, political, financial, and cultural events that greatly affected the world for 10 years, from 2010 to 2021. Following Korobilis and Yilmaz (2018), we ordered these fluctuations by number and highlighted them with pink shades, and we sorted the events corresponding to these nine fluctuations into Table 3.4 following the chronology.

In Figure 3.3, we can observe that the volatility total dynamic connectedness took a value between 45% and 92%, indicating that the connectedness among the sustainability-related indexes was very relevant and time-varying. This fact is usually concealed by the nature of static TCI. Around July 2011, because of the sovereign debt problems of Italy and Spain, the TCI had high volatility approaching 88%. As of 28 October 2011, as pointed out by Kamalodin et al. (2012), the euro crisis had led to a decline in lending credit in countries within the eurozone, such as Greece, Italy, and Spain. The gap in bond yield spreads and credit default swaps became more significant, causing alarms in the financial markets. We also saw the high volatility, 90% influenced by the euro crisis. At the end of 2012, the relevant countries continued to implement fiscal austerity policies to solve the European debt crisis, and many European countries are now seeing anti-austerity strikes, which also influence the TCI. A high fluctuation of more than 90% around February 2013 can be explained as affected by the value of global carbon dioxide dropping 38%. The declining trend of oil prices in April 2014 and the turbulence in China's financial market around 29 June–28 August 2015 caused the TCI to have slightly higher volatility around April 2014 and June 2015. Around June 2016, influenced by Brexit, there was a high fluctuation of over 85% in the TCI. In September 2018, the further intensification of the trade war between China and the United States caused a significant fluctuation in the TCI in the second half of 2018. Because of the COVID-19 pandemic, global financial markets encountered an unprecedented crisis. Therefore, the TCI suddenly experienced violent fluctuations in early 2020, and the value of TCL is more than 75%. Central banks, ministries of finance, and international financial institutions worldwide have introduced unprecedented policy support measures for economic growth. After 2020, TCI generally shows a declining trend with fluctuations.

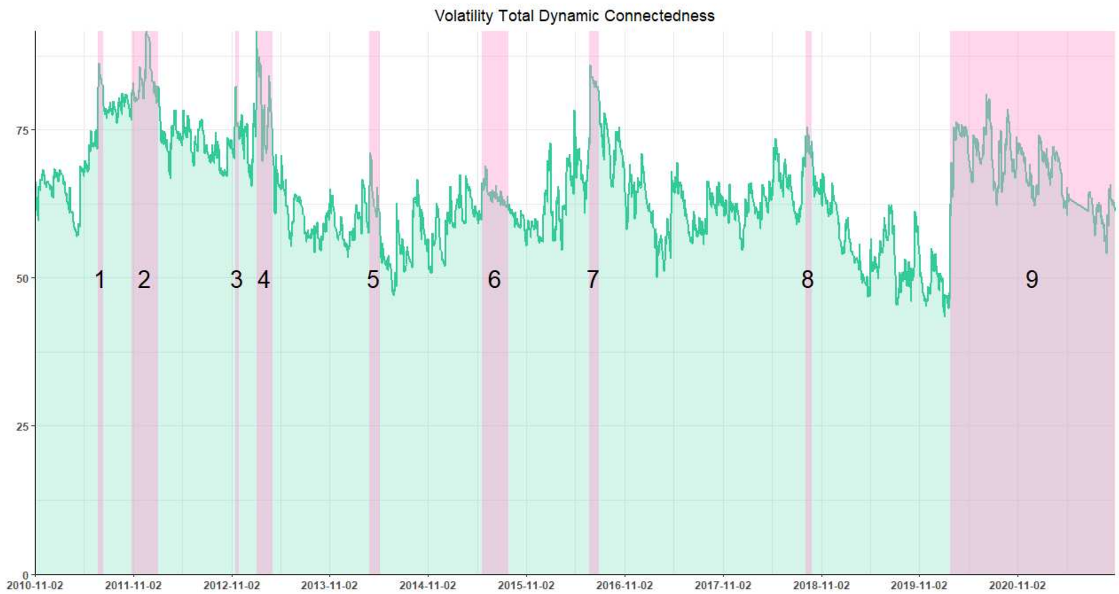

Figure 3.3. Volatility total dynamic connectedness.

Notes: The green shaded part represents the moderate fluctuation; the pink shades represent the fierce fluctuations. The numbers in the pink shaded area correspond to the events in Table 3.4.

Table 3.4. Chronology of volatility-related events affecting sustainability-related indexes.

No.	Event details
1	July–August 2011: The sovereign debt troubles of Italy and Spain.
2	28 October 2011: The eurozone (debt) crisis (Kamalodin et al. 2012).
3	November 2012: The "penetration effect" of the European debt crisis, many European countries are now anti-austerity strikes.
4	February–June 2013: Global carbon markets' value dropped 38% to EUR 38.4 billion (USD 52.9 billion).
5	April 2014: Oil market prices show a downward trend.
6	29 June–28 August 2015: The turmoil in China's financial market led to a sharp drop in global stock market indexes (Korobilis and Yilmaz, 2018).
7	23 June 2016: Brexit: the withdrawal of the United Kingdom (UK) from the European Union (EU).
8	September 2018: China–United States trade war: The US announced its 10% tariff on USD 200 billion worth of Chinese goods would begin on 24 September 2018.
9	December 2019: COVID-19 pandemic.

3.5.2 Hedging Strategies

Having already calculated the volatility dynamic connectedness, we found that there was indeed a strong time-varying volatility relationship among sustainability-related indexes. Therefore, it was essential to investigate the investment diversification strategies and risk management. In this study, we mainly employed two tools, namely, the hedging ratio and the portfolio weights, to estimate the risk-hedging ability of assets. We assumed that investors should hold a long position in an index when the future volatility of this index is expected to be higher than the current volatility level. On the contrary, when the future volatility of an index is expected to decline, the investor should take the short position in this index.

Table 3.5 shows the results of the optimal hedging ratios among the sustainability-related indexes. The value of β_{ijt} in Table 3.5 is the averaged median value of the dynamic hedging ratio for a long position of 1 dollar in an index's volatility and a short position of β_{ijt} dollar for another index's volatility. The HE in Table 3.5 is the hedging effectiveness employed to measure the risk reduction in the variance of the unhedged position. The value of the HE is the average of the dynamic hedging effectiveness. The p-value is defined as the lowest significance level at which the null hypothesis is rejected: the two indexes cannot be effectively risk hedged against each other. The values of the hedging ratio ranged from 0.03 to 1.89. The value of the HE implied that risk reduction ranged from 0.04 to 0.93. As is clear from the table, the cheapest hedging was that a 1 dollar long position in the volatility of the SPGB was obtained with a 3 cents short position in the volatility of the CEF. In contrast, the most expensive hedging was that a 1 dollar long position in the volatility of the CEF was obtained with a 1.89

dollar short position in the volatility of the SPGB. However, the result of the HE indicated that hedging the WESG, the NEX, the SPGB, and the DJS by putting the short position of the CEF volatility was statistically insignificant. Compared with other indexes in a short position, a 53 cents short position in the VEX volatility hedged against a 1 dollar long position in the WESG volatility, whose hedging cost was cheapest. On the contrary, an 87 cents short position in the DJS volatility hedged against a 1 dollar long position in the WESG volatility, whose hedging cost was most expensive. The volatility of the NEX was hedged with an 85 cents short position of the SPGB, which was the cheapest. The cheapest cost in hedging the volatility of the SPGB was hedged by the 10 cents short position of the NEX volatility. We needed 58 cents in the short position of the NEX volatility to hedge against the 1 dollar long position of the DJS volatility as well as 52 cents in the short position of the NEX to hedge against the 1 dollar long position of the CEF volatility, which was cheapest. These results indicated that the NEX volatility was very suitable as a short position to hedge against the volatility of the other four indexes.

The highest HE value reached 93%, representing the risk of investments in the WESG, and was reduced by 93% when taking a short position in the DJS volatility, and vice versa. However, when the WESG volatility was in a short position to hedge a long position in the DJS volatility, it was more expensive than when the DJS volatility was in a short position to hedge a long position in the WESG volatility. Therefore, when the WESG and DJS are in a portfolio, the DJS is better as a short position to hedge a long position in the WESG. We found that the higher the hedging effectiveness, the higher the hedging cost tendency. For instance, when we took a 1 dollar long position in the WESG volatility, the NEX volatility, the SPGB volatility, the DJS volatility, and the CEF volatility, the risk of investment was reduced by 93% (87 cents short position in the DJS), 67% (1.13 dollar short position in the WESG), 21% (17 cents short position in the DJS), 93% (1.05 dollar short position in the WESG), and 16% (78 cents short position in the WESG), respectively.

Table 3.5. Dynamic optimal hedging ratio and hedging effectiveness.

Long position/Short position	β_{ijt}	St.dev.	HE	p-value
WESG/NEX	0.53	0.15	0.61***	0.00
WESG/SPGB	0.59	0.49	0.29***	0.00
WESG/DJS	0.87	0.11	0.93***	0.00
WESG/CEF	0.06	0.07	0.04	0.27
NEX/WESG	1.13	0.32	0.67***	0.00
NEX/SPGB	0.85	0.67	0.22***	0.00
NEX/DJS	1.01	0.30	0.67***	0.00
NEX/CEF	0.09	0.10	0.04	0.25
SPGB/WESG	0.16	0.14	0.11***	0.00
SPGB/NEX	0.10	0.08	0.13***	0.00
SPGB/DJS	0.17	0.12	0.21***	0.00
SPGB/CEF	0.03	0.03	0.04	0.34
DJS/WESG	1.05	0.13	0.93***	0.00
DJS/NEX	0.58	0.16	0.59***	0.00
DJS/SPGB	0.83	0.56	0.35***	0.00
DJS/CEF	0.08	0.08	0.05	0.22
CEF/WESG	0.78	0.60	0.16***	0.00
CEF/NEX	0.52	0.37	0.14***	0.00
CEF/SPGB	1.89	1.29	0.12***	0.00
CEF/DJS	0.79	0.47	0.16***	0.00

Notes: *** denotes rejection of the null hypothesis at 1% significance levels. β_{ijt} is the optimal hedging ratio for the cost of hedging a 1 dollar long position in the variable *i* with a β_{ijt} dollar short position in variable *j* at time *t*. HE represents the hedging effectiveness, and the value of HE is the average of the dynamic hedging effectiveness. The p-value is defined as the lowest significance level at which the null hypothesis is rejected: the two indexes cannot be effectively risk hedged against each other. St.dev. represents the standard deviation.

Table 3.6 shows the result of the dynamic portfolio weights and the hedging effectiveness. The value of W_{ijt} in Table 3.6 is the averaged median value of the dynamic portfolio weights of variable *i* in a 1 dollar portfolio of the two variables *i* and *j* at time *t*. The values of portfolio weights ranged from 0 to 1. However, judging by the result of the HE, it was insignificant when the portfolio weights took a value of 1. More precisely, only the NEX and the CEF were put into a 1 dollar long position; the values of the HE were all significant. The values of the HE for the 1 dollar long position of the SPGB were all insignificant. These conclusions further demonstrated that the CEF is suitable as a long position and the SPGB is not suitable for a long position. Furthermore, the HE statistics were relatively high for the portfolios with the SPGB volatility; the portfolio weights of the SPGB volatility ranged from 0 to 0.11. The lowest HE for the SPGB volatility was 0.83, whose portfolio weights indicated that when constructing a 1 dollar portfolio with the WESG volatility, 11 cents were invested in the WESG volatility and the remaining 89 cents were invested in the SPGB volatility. The highest HE for the CEF/SPGB volatility was 0.99, whose portfolio weights indicated that when constructing a 1 dollar portfolio with the CEF volatility, the entire 1 dollar should be invested in the SPGB volatility.

Table 3.6. Dynamic optimal portfolio weights and hedging effectiveness.

Long position/Short position	W_{ijt}	St.dev.	HE	p-value
WESG/NEX	0.90	0.18	−0.02	0.63
WESG/SPGB	0.11	0.11	0.83***	0.00
WESG/DJS	0.79	0.36	0.06	0.13
WESG/CEF	0.96	0.08	−0.01	0.73
NEX/WESG	0.10	0.18	0.48***	0.00
NEX/SPGB	0.05	0.06	0.91***	0.00
NEX/DJS	0.16	0.21	0.43***	0.00
NEX/CEF	0.89	0.12	0.07**	0.04
SPGB/WESG	0.89	0.11	0.03	0.45
SPGB/NEX	0.95	0.06	0.02	0.67
SPGB/DJS	0.94	0.07	0.02	0.62
SPGB/CEF	1.00	0.00	0.00	0.92
DJS/WESG	0.21	0.36	0.14***	0.00
DJS/NEX	0.84	0.21	−0.01	0.81
DJS/SPGB	0.06	0.07	0.84***	0.00
DJS/CEF	0.96	0.07	−0.01	0.75
CEF/WESG	0.04	0.08	0.92***	0.00
CEF/NEX	0.11	0.12	0.86***	0.00
CEF/SPGB	0.00	0.00	0.99***	0.00
CEF/DJS	0.04	0.07	0.91***	0.00

Notes: *** and ** denote rejection of the null hypothesis at 1% and 5% significance levels, respectively. W_{ijt} denotes the weight of variable i in a 1 dollar portfolio of the two variables i and j at time t. HE represents the hedging effectiveness, and the value of HE is the average of the dynamic hedging effectiveness. The p-value is defined as the lowest significance level at which the null hypothesis is rejected: the two indexes cannot be effectively risk hedged against each other. St.dev. represents the standard deviation.

Figures 3.4 and 3.5 exhibit the dynamic hedging ratio and portfolio weights, respectively. Compared with a static hedging strategy, the dynamic hedging ratio and portfolio weights can better capture the dynamic fluctuations of the assets.

In Figure 3.4, we can observe that compared with other asset portfolios, the dynamic hedging ratio of WESG/DJS was relatively stable and not affected by financial and political events. When the COVID-19 pandemic has a significant impact on the global economy, WESG and DJS can serve as risk-hedging effective assets to counteract the economic impact of the COVID-19 epidemic on investors. However, there were obvious fluctuations in certain periods for other investment portfolios. Especially when CEF is invested as a long position, the fluctuations are particularly sharp. A study of hedging ratios between other assets and carbon emission futures shows that hedging ratios vary within a time-varying framework and are event-dependent. For instance, roughly during February-June 2013: Global carbon markets' value dropped 38%, CEF had a high hedge rate volatility regardless of whether they hedged any of the other four assets as a long position. Besides, we can observe that some major global events, such as the Greek debt crisis, the Brexit, and the COVID-19 pandemic, have had a volatile impact on the dynamic hedging ratio.

In Figure 3.5, the dynamic portfolio weights of SPGB/CEF hardly changed over time. Thus, we confirm the insignificance of the hedging effectiveness for green bond and carbon emission futures, indicating that SPGB and CEF are not suitable as risk-hedging portfolios. We can see that the dynamics portfolio weights of other asset portfolios also fluctuate over time, especially with peaks in certain time periods. For example, in the NEX/CEF portfolio, there are three distinct peak fluctuations around November 2011, around November 2015, and after December 2019. These can be explained by a series of economic events, including the conclusion of the European debt crisis, the UK's resolution to leave the EU, and the COVID-19 epidemic. The dynamic nature of the hedging ratio and portfolio weights further confirms the need for active portfolio rebalancing. Dynamics allow investors to know when to buy or sell and to be aware of the impact of economic and political events on their investments, which is not possible in a static approach.

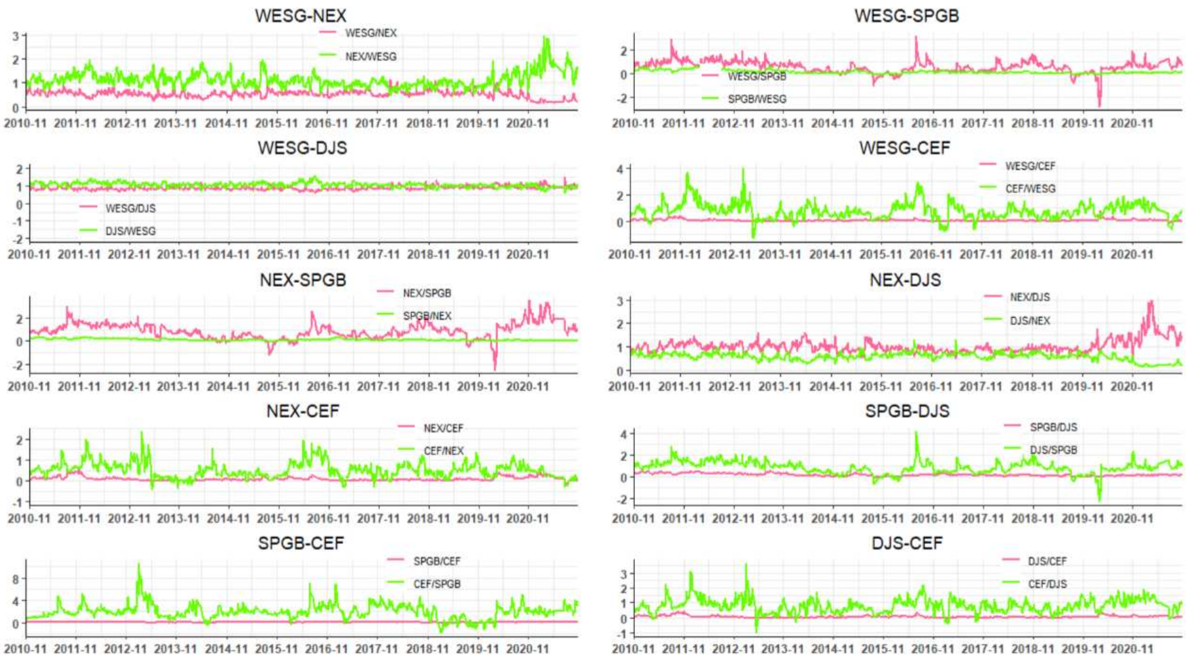

Figure 3.4. Dynamic optimal hedging ratios.

Notes: WESG represents the volatility of WESG; NEX represents the volatility of NEX; SPGB represents the volatility of SPGB; DJS represents the volatility of DJS; CEF represents the volatility of CEF.

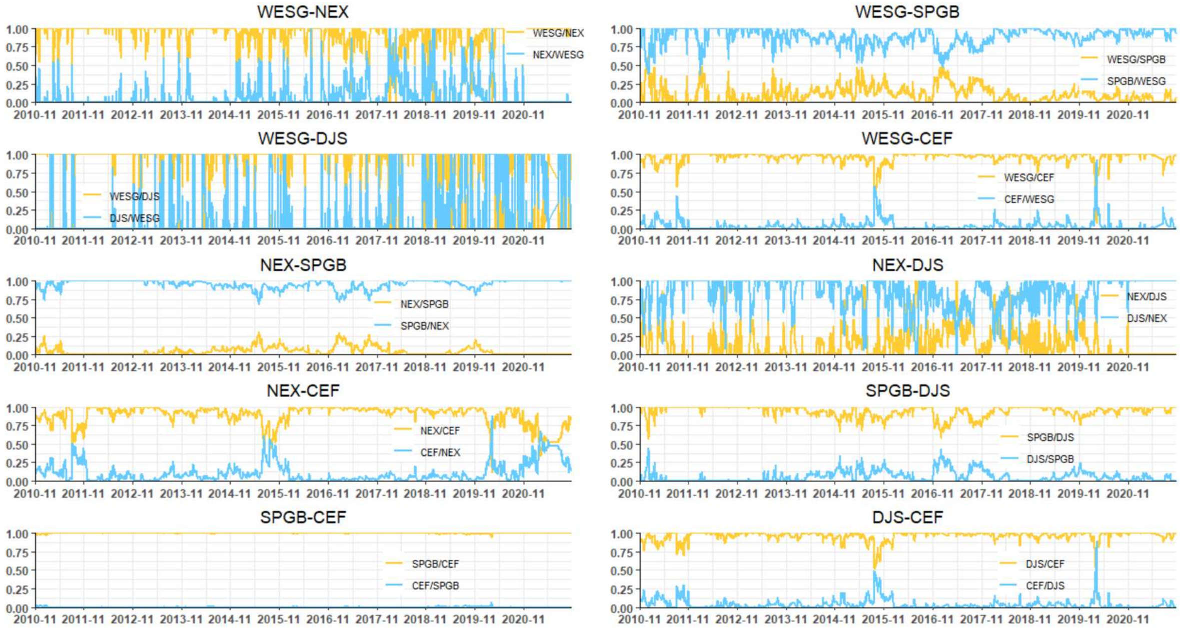

Figure 3.5. Dynamic optimal portfolio weights.

Notes: WESG represents the volatility of WESG; NEX represents the volatility of NEX; SPGB represents the volatility of SPGB; DJS represents the volatility of DJS; CEF represents the volatility of CEF.

3.6. Conclusions

In recent years, the world has experienced many crises in terms of climate change and public health. Human beings have never felt the impact of unsystematic risks on society as clearly as today. Countries around the world and global investors are beginning to pay attention to the risks and losses that climate change will bring to the economy and financial system. In this context, sustainable investment products are gaining favor from global investors. This study focused on dynamic volatility spillovers across a broad range of asset classes, including the ESG stock index, the renewable energy stock index, the green bond stock index, the sustainability stock index, and the carbon emission futures.

Furthermore, this present study aimed to provide investors and portfolio managers with optimal hedging ratios and portfolio weights. More precisely, we used time-series daily data from 1 November 2010 to 28 October 2021, and we employed the new DCC-GARCH-based dynamic connectedness method to investigate the time-varying volatility spillover effect and used the network to visualize the level and the direction of dynamic connectedness among our indexes. Furthermore, we estimated the DCC-GARCH t-copula model to construct many bivariate and multivariate portfolios for all series to inform our hedging effectiveness and possible financial rewards.

The conclusions of this study can be summarized as follows:

First, in the full sample dynamic connectedness analysis of volatility, we found that the total connectedness of the volatility series was 64.62%, which indicated strong conditional correlations among the five sustainability-related indexes. More precisely, among the five indexes, the largest volatility spillover was from the carbon emission futures to the green bond index, which was 39.25%, but vice versa was the smallest volatility spillover, 0.25%. This finding indicated that carbon emission has an obvious one-way risk contagion to green bonds, and Leitao et al. (2021) also confirmed this conclusion. Moreover, the carbon emission futures contributed the most volatility spillovers to others (86.88%), and the green bond index contributed the fewest (3.7%). On the contrary, the ESG index received the most volatility spillovers from others (73.95%), and the carbon emission futures received the fewest (3.4%). This result demonstrated that the carbon emission futures index is a volatility transmitter and the green bond index is a volatility receiver, which was further confirmed in the net directional connectedness because the carbon emission futures had the largest net directional volatility spillover (83.48%) and the green bond had the smallest (62.96%).

Second, using the network of Diebold and Yilmaz (2016) to visualize the dynamic connectedness, we observed the intensity and direction of volatility spillover transmission. The network graph shows that the carbon emission futures were the volatility transmitter, and the green bond was the volatility receiver, which was consistent with the conclusion in the averaged dynamic connectedness table. The volatility connectedness from the renewable energy stock index to the ESG and sustainability indexes also had a relatively high level, 30.61 and 29.31%, respectively. Among the five indexes, only the volatility spillover from the green bond to other indexes did not exceed 5%. The green bond was a monodirectional receiver for the volatility spillover among the five indexes, which was also demonstrated in Zhang et al. (2021).

Third, the total dynamic connectedness of volatility for the five indexes ranged from 45 to 92%. This conclusion indicated that the connectedness among the sustainability-related indexes was time-varying, and the fierce fluctuations in the total connectedness were impacted by major economic, political, financial, and cultural events from 2010 to 2021. These events included: 28 October 2011—the eurozone (debt) crisis; February–June 2013—global carbon markets' value dropping 38% to EUR 38.4 billion (USD 52.9 billion); and December 2019—the COVID-19 pandemic. These events were also confirmed in Kamalodin et al. 2012; Zhang et al. (2021); Korobilis and Yilmaz (2018); Zhang and Hamori (2021), and Liu et al. (2021).

Finally, we made several interesting findings on the performance of risk hedging. Overall, we found suggestive evidence that portfolio construction can significantly reduce investment risk across all assets. The result of the hedging effectiveness indicated that hedging the ESG index, the renewable energy stock index, the green bond, and the sustainability index by putting the short position of the carbon emission futures volatility was statistically insignificant. Taking the long position for the carbon emission futures hedged risk effectively in this asset. The renewable energy stock index was suitable as a short position to hedge against the volatility of the other four indexes. However, the hedging effectiveness of the portfolio weights in the long position of the green bond was insignificant, which meant that the green bond was not suitable for taking the long position. Moreover, the highest hedging effectiveness for the SPGB volatility was 0.99, which indicated that we constructed a 1 dollar portfolio with the CEF volatility by investing 0 cents in the SPGB volatility. This showed that the carbon emission futures could not effectively hedge against the green bond, which was consistent with Tiwari et al. (2022).

The results of this study provided some insights. Because of carbon emission futures' high efficiency in risk hedging on long positions, policy makers should consider carbon futures and the other four sustainability-related indexes as interrelated assets in their policy frameworks, except for green bonds. The good performance of the NEX in risk hedging on short positions also suggested that policy decisions on the energy transition to a decarbonized economy should consider other sustainability indicators that are also essential for the transition to a climate-resilient economy. As investors, we should also pay attention to the stability of the hedging function of sustainability-related indexes and construct a hedging strategy considering the different dynamics and characteristics of the stock market and its interaction with the financial market.

We believe our study offers a certain guiding role for future research on sustainable investment. There is still much room to study the relationship among sustainability-related indexes, and we intend to add factors that may affect sustainable investment in future research, such as investor sentiment indexes, economic uncertainty indexes, etc. In addition, we plan to combine the SV model with the dynamic connectedness approach to study the dynamic spillover between stock markets in our future research.

Appendix

To check the robustness of the dynamic linkage results, we replace the order of the GARCH model in the DCC-GARCH model from (1, 1) to (3, 1). The result of averaged dynamic connectedness table of volatility series based on GARCH (3, 1) is exhibited in Table A. The empirical results obtained from Table A and the empirical results obtained from Table 3 are basically the same.

Table A. Averaged dynamic connectedness table of volatility series.

	WESG_Vol	NEX_Vol	SPGB_Vol	DJS_Vol	CEF_Vol	FROM
WESG_Vol	28.03	28.83	0.99	25.78	16.37	71.97
NEX_Vol	14.81	51.69	0.68	16.75	16.07	48.31
SPGB_Vol	5.45	8.33	45.15	7.44	33.63	54.85
DJS_Vol	22.43	28.01	1.16	28.73	19.67	71.27
CEF_Vol	0.74	1.48	0.19	0.96	96.62	3.38
TO	43.43	66.65	3.03	50.93	85.74	249.79
NET directional connectedness	−28.54	18.34	−51.82	−20.34	82.36	TCI
NPDC transmitter	1	3	0	2	4	62.45

Note: The results of Table A is based on GARCH (3, 1). WESG_Vol represents the volatility of WESG; NEX_Vol represents the volatility of NEX; SPGB_Vol represents the volatility of SPGB; DJS_Vol represents the volatility of DJS; CEF_Vol represents the volatility of CEF.

References

Agliardi, E., & Agliardi, R. (2019). Financing environmentally-sustainable projects. with green bonds. *Environment and Development Economics*, *24*(6), 608–623. https://doi.org/10.1017/s1355770x19000020

Akhtaruzzaman, M., Boubaker, S., & Sensoy, A. (2020). Financial contagion during COVID–19 crisis. *Finance Research Letters*, *38*, 101604. https://doi.org/10.1016/j.frl.2020.101604

Antonakakis, N. (2012). Exchange return comovements and volatility spillovers before and after the introduction of euro. *Journal of International Financial Markets, Institutions and Money*, *22*(5), 1091–1109. https://doi.org/10.1016/j.intfin.2012.05.009

Antonakakis, N., Chatziantoniou, I., & Gabauer, D. (2020a). A regional decomposition of US housing prices and volume: market dynamics and Portfolio diversification. *The Annals of Regional Science*, *66*(2), 279–307. https://doi.org/10.1007/s00168-020-01021-2

Antonakakis, N., Cunado, J., Filis, G., Gabauer, D., & de Gracia, F. P. (2020b). Oil and asset classes implied volatilities: Investment strategies and hedging effectiveness. *Energy Economics*, *91*, 104762. https://doi.org/10.1016/j.eneco.2020.104762

Benlagha, N., & Omari, S. E. (2021). Connectedness of stock markets with gold and oil: New evidence from COVID-19 pandemic. *Finance Research Letters*, 102373. https://doi.org/10.1016/j.frl.2021.102373

Bilgin, M., & Yilmaz, K. (2018). Producer Price Inflation Connectedness and Input-

Output Networks. *SSRN Electronic Journal*. https://doi.org/10.2139/ssrn.3244645

Bollerslev, T. (1986). Generalized autoregressive conditional heteroskedasticity. *Journal of Econometrics*, *31*(3), 307–327. https://doi.org/10.1016/0304-4076(86)90063-1

Bollerslev, T. (1990). Modelling the Coherence in Short-Run Nominal Exchange Rates: A Multivariate Generalized Arch Model. *The Review of Economics and Statistics*, *72*(3), 498. https://doi.org/10.2307/2109358

Bouri, E., Gabauer, D., Gupta, R., & Tiwari, A. K. (2021). Volatility connectedness of major cryptocurrencies: The role of investor happiness. *Journal of Behavioral and Experimental Finance*, *30*, 100463. https://doi.org/10.1016/j.jbef.2021.100463

Broadstock, D. C., Chatziantoniou, I., & Gabauer, D. (2022). Minimum Connectedness Portfolios and the Market for Green Bonds: Advocating Socially Responsible Investment (SRI) Activity. *Applications in Energy Finance*, 217–253. https://doi.org/10.1007/978-3-030-92957-2_9

Brown, M. B., & Forsythe, A. B. (1974). Robust Tests for the Equality of Variances. *Journal of the American Statistical Association*, *69*(346), 364–367. https://doi.org/10.1080/01621459.1974.10482955

Caporin, M., & McAleer, M. (2008). Scalar BEKK and indirect DCC. *Journal of Forecasting*, *27*(6), 537–549. https://doi.org/10.1002/for.1074

Caporin, M., & McAleer, M. (2012). DO WE REALLY NEED BOTH BEKK AND DCC? A TALE OF TWO MULTIVARIATE GARCH MODELS. *Journal of Economic Surveys*, *26*(4), 736–751. https://doi.org/10.1111/j.1467-6419.2011.00683.x

Celık, S. (2012). The more contagion effect on emerging markets: The evidence of DCC-GARCH model. *Economic Modelling*, *29*(5), 1946–1959. https://doi.org/10.1016/j.econmod.2012.06.011

Chatziantoniou, I., Gabauer, D., & Stenfors, A. (2021, May 25). Independent Policy, Dependent Outcomes: A Game of Cross-Country Dominoes across European Yield Curves. Retrieved January 10, 2022, from ideas.repec.org website: https://ideas.repec.org/p/pbs/ecofin/2021-06.html

Cortez, M. C., Silva, F., & Areal, N. (2011). SOCIALLY RESPONSIBLE INVESTING IN THE GLOBAL MARKET: THE PERFORMANCE OF US AND EUROPEAN FUNDS. *International Journal of Finance & Economics*, *17*(3), 254–271. https://doi.org/10.1002/ijfe.454

Cui, B., & Docherty, P. (2020). Stock Price Overreaction to ESG Controversies. *SSRN Electronic Journal*. https://doi.org/10.2139/ssrn.3559915

Diebold, F. X., & Yilmaz, K. (2008). Measuring Financial Asset Return and Volatility Spillovers, with Application to Global Equity Markets. *The Economic Journal*, *119*(534), 158–171. https://doi.org/10.1111/j.1468-0297.2008.02208.x

Diebold, F. X., & Yilmaz, K. (2012). Better to give than to receive: Predictive directional measurement of volatility spillovers. *International Journal of Forecasting*, *28*(1), 57–66. https://doi.org/10.1016/j.ijforecast.2011.02.006

Diebold, F. X., & Yilmaz, K. (2016). Trans-Atlantic Equity Volatility Connectedness: US and European Financial Institutions, 2004–2014. *Journal of Financial Econometrics*, *14*(1), 81–127. https://doi.org/10.1093/jjfinec/nbv021

Diebold, F. X., & Yılmaz, K. (2014). On the network topology of variance decompositions: Measuring the connectedness of financial firms. *Journal of Econometrics*, *182*(1), 119–134. https://doi.org/10.1016/j.jeconom.2014.04.012

Ederington, L. H. (1979). The Hedging Performance of the New Futures Markets. *The Journal of Finance*, *34*(1), 157–170. https://doi.org/10.1111/j.1540-6261.1979.tb02077.x

Egli, F. (2020). Renewable energy investment risk: An investigation of changes over time and the underlying drivers. *Energy Policy*, *140*, 111428. https://doi.org/10.1016/j.enpol.2020.111428

Engle, R. (2002). Dynamic Conditional Correlation: A Simple Class of Multivariate Generalized Autoregressive Conditional Heteroskedasticity Models. *Journal of Business & Economic Statistics*, *20*(3). https://doi.org/10.1198/073500102288618487

Engle, R., & Sheppard, K. (2001). Theoretical and Empirical properties of Dynamic Conditional Correlation Multivariate GARCH. *National Bureau of Economic Research Working Paper Series*, *No. 8554*. https://doi.org/10.3386/w8554

Evrim Mandacı, P., Cagli, E. Ç., & Taşkın, D. (2020). Dynamic connectedness and portfolio strategies: Energy and metal markets. *Resources Policy*, *68*, 101778. https://doi.org/10.1016/j.resourpol.2020.101778

Franke, G. R. (2010). Multicollinearity. *Wiley International Encyclopedia of Marketing*. https://doi.org/10.1002/9781444316568.wiem02066

Funke, M., Loermann, J., & Tsang, A. (2020). Volatility transmission and volatility impulse response functions in the main and the satellite Renminbi exchange rate markets. Retrieved from http://urn.fi/URN:NBN:fi:bof-202010062433

Gabauer, D. (2020). Volatility impulse response analysis for DCC-GARCH models: The role of volatility transmission mechanisms. *Journal of Forecasting*. https://doi.org/10.1002/for.2648

Giese, G., Lee, L.-E., Melas, D., Nagy, Z., & Nishikawa, L. (2019). Performance and Risk Analysis of Index-Based ESG Portfolios. *The Journal of Index Investing*, *9*(4), 46–57. https://doi.org/10.3905/jii.2019.9.4.046

Hanif, W., Arreola Hernandez, J., Mensi, W., Kang, S. H., Uddin, G. S., & Yoon, S.-M. (2021). Nonlinear dependence and connectedness between clean/renewable energy sector equity and European emission allowance prices. *Energy Economics*, *101*, 105409. https://doi.org/10.1016/j.eneco.2021.105409

Hansen, P. R., & Lunde, A. (2005). A forecast comparison of volatility models: does anything beat a GARCH(1,1)? *Journal of Applied Econometrics*, *20*(7), 873–889. https://doi.org/10.1002/jae.800

He, L., Zhang, L., Zhong, Z., Wang, D., & Wang, F. (2019). Green credit, renewable energy investment and green economy development: Empirical analysis based on 150 listed companies of China. *Journal of Cleaner Production*, *208*, 363–372. https://doi.org/10.1016/j.jclepro.2018.10.119

He, X., Liu, G., & Hamori, S. (2021). Measuring Tail Dependencies Between ESG and Renewable Energy Stocks: A Copula Approach. *SpringerBriefs in Economics*, 37–52. https://doi.org/10.1007/978-981-16-2990-7_3

Hoesli, M., & Reka, K. (2011). Volatility Spillovers, Comovements and Contagion in Securitized Real Estate Markets. *The Journal of Real Estate Finance and Economics*, *47*(1), 1–35. https://doi.org/10.1007/s11146-011-9346-8

Hou, Y., Li, S., & Wen, F. (2019). Time-varying volatility spillover between Chinese fuel oil and stock index futures markets based on a DCC-GARCH model with a semi-nonparametric approach. *Energy Economics*, *83*, 119–143. https://doi.org/10.1016/j.eneco.2019.06.020

Huang, Y., Su, W., & Li, X. (2010). Comparison of BEKK GARCH and DCC GARCH Models: An Empirical Study. *Advanced Data Mining and Applications*, 99–110. https://doi.org/10.1007/978-3-642-17313-4_10

Iqbal, N., Abubakr Naeem, M., & Tahir Suleman, M. (2021). Quantifying the asymmetric spillovers in sustainable investments. *Journal of International Financial Markets, Institutions and Money*, 101480. https://doi.org/10.1016/j.intfin.2021.101480

Janda, K., Kristoufek, L., & Zhang, B. (2021). Return and Volatility Spillovers between Chinese and US Clean Energy Related Stocks: Evidence from Var-Mgarch Estimations. *SSRN Electronic Journal*. https://doi.org/10.2139/ssrn.3972013

Jin, J., Han, L., Wu, L., & Zeng, H. (2020). The hedging effect of green bonds on carbon market risk. *International Review of Financial Analysis*, *71*, 101509. https://doi.org/10.1016/j.irfa.2020.101509

Jones, P. M., & Olson, E. (2013). The time-varying correlation between uncertainty, output, and inflation: Evidence from a DCC-GARCH model. *Economics Letters*, *118*(1), 33–37. https://doi.org/10.1016/j.econlet.2012.09.012

Kamalodin,S., Boonstra, W., Bruinshoofd, A., Visser, H., & Mooij, J. (2012).Financial crisis investigation. Rabobank Working Paper Series, 2012/01,Utrecht: Rabobank Nederland.

Kamran, M., Butt, P., Abdel-Razzaq, A., & Djajadikerta, H. G. (2021). Is Bitcoin a safe haven? Application of FinTech to safeguard Australian stock markets. *Studies in Economics and Finance*, *ahead-of-print*(ahead-of-print). https://doi.org/10.1108/sef-05-2021-0201

Korobilis, D., & Yilmaz, K. (2018). Measuring Dynamic Connectedness with Large Bayesian VAR Models. *SSRN Electronic Journal*. https://doi.org/10.2139/ssrn.3099725

Kroner, K. F., & Ng, V. K. (1998). Modeling Asymmetric Comovements of Asset Returns. *Review of Financial Studies*, *11*(4), 817–844. https://doi.org/10.1093/rfs/11.4.817

Kroner, K. F., & Sultan, J. (1993). Time-Varying Distributions and Dynamic Hedging with Foreign Currency Futures. *The Journal of Financial and Quantitative Analysis*, *28*(4), 535. https://doi.org/10.2307/2331164

La Torre, M., Mango, F., Cafaro, A., & Leo, S. (2020). Does the ESG Index Affect Stock Return? Evidence from the Eurostoxx50. *Sustainability*, *12*(16), 6387. https://doi.org/10.3390/su12166387

Lee, C.-C., Lee, C.-C., & Li, Y.-Y. (2021). Oil price shocks, geopolitical risks, and green bond market dynamics. *The North American Journal of Economics and Finance*, *55*, 101309. https://doi.org/10.1016/j.najef.2020.101309

Leitao, J., Ferreira, J., & Santibanez-Gonzalez, E. (2021). Green bonds, sustainable development and environmental policy in the European Union carbon market. *Business Strategy and the Environment*, *30*(4), 2077–2090. https://doi.org/10.1002/bse.2733

Lesame, K., Bouri, E., Gabauer, D., & Gupta, R. (2021). On the Dynamics of International Real-Estate-Investment Trust-Propagation Mechanisms: Evidence from Time-Varying Return and Volatility Connectedness Measures. *Entropy*, *23*(8), 1048. https://doi.org/10.3390/e23081048

Liu, G., & Hamori, S. (2020). Can One Reinforce Investments in Renewable Energy Stock Indices with the ESG Index? *Energies*, *13*(5), 1179. https://doi.org/10.3390/en13051179

Liu, T., Nakajima, T., & Hamori, S. (2021). The impact of economic uncertainty caused by COVID-19 on renewable energy stocks. *Empirical Economics*.

https://doi.org/10.1007/s00181-021-02087-3

Mansfield, E. R., & Helms, B. P. (1982). Detecting Multicollinearity. *The American Statistician*, *36*(3a), 158–160. https://doi.org/10.1080/00031305.1982.10482818

Maraqa, B., & Bein, M. (2020). Dynamic Interrelationship and Volatility Spillover among Sustainability Stock Markets, Major European Conventional Indices, and International Crude Oil. *Sustainability*, *12*(9), 3908. https://doi.org/10.3390/su12093908

Medina, V., & Pardo, A. (2013). Is the EUA a new asset class? *Quantitative Finance*, *13*(4), 637–653. https://doi.org/10.1080/14697688.2012.691985

Mensi, W., Naeem, M. A., Vo, X. V., & Kang, S. H. (2022). Dynamic and frequency spillovers between green bonds, oil and G7 stock markets: Implications for risk management. *Economic Analysis and Policy*, *73*, 331–344. https://doi.org/10.1016/j.eap.2021.11.015

Nawazish, S. (2021). Does gold future hedge global uncertainty in crude oil futures? Evidence from DCC-GARCH model. *Asian Finance Research Journal*, *3*(1).

Park, D., Park, J., & Ryu, D. (2020). Volatility Spillovers between Equity and Green Bond Markets. *Sustainability*, *12*(9), 3722. https://doi.org/10.3390/su12093722

Patton, A. J. (2006). MODELLING ASYMMETRIC EXCHANGE RATE DEPENDENCE. *International Economic Review*, *47*(2), 527–556. https://doi.org/10.1111/j.1468-2354.2006.00387.x

Pham, L. (2021). Frequency connectedness and cross-quantile dependence between green bond and green equity markets. *Energy Economics*, *98*, 105257. https://doi.org/10.1016/j.eneco.2021.105257

Pham, L., & Nguyen, C. P. (2021). How do stock, oil, and economic policy uncertainty influence the green bond market? *Finance Research Letters*, 102128. https://doi.org/10.1016/j.frl.2021.102128

Reboredo, J. C. (2018). Green bond and financial markets: Co-movement, diversification and price spillover effects. *Energy Economics*, *74*, 38–50. https://doi.org/10.1016/j.eneco.2018.05.030

Reboredo, J. C., Ugolini, A., & Aiube, F. A. L. (2020). Network connectedness of green bonds and asset classes. *Energy Economics*, *86*, 104629. https://doi.org/10.1016/j.eneco.2019.104629

Saeed, T., Bouri, E., & Tran, D. K. (2020). Hedging Strategies of Green Assets against Dirty Energy Assets. *Energies*, *13*(12), 3141. https://doi.org/10.3390/en13123141

Shahbaz, M., Topcu, B. A., Sarıgül, S. S., & Vo, X. V. (2021). The effect of financial development on renewable energy demand: The case of developing countries. *Renewable Energy*, *178*, 1370–1380. https://doi.org/10.1016/j.renene.2021.06.121

Singhal, S., & Ghosh, S. (2016). Returns and volatility linkages between international crude oil price, metal and other stock indices in India: Evidence from VAR-

DCC-GARCH models. *Resources Policy*, *50*, 276–288. https://doi.org/10.1016/j.resourpol.2016.10.001

Sklar, M.(1959). Fonctions De Repartition An Dimensions Et Leurs Marges. *8. Publ. Inst.Statist. Univ. Paris*, pp. 229–231.

Sun, L., Xiang, M., & Shen, Q. (2020). A comparative study on the volatility of EU and China's carbon emission permits trading markets. *Physica A: Statistical Mechanics and Its Applications*, *560*, 125037. https://doi.org/10.1016/j.physa.2020.125037

Tiwari, A. K., Aikins Abakah, E. J., Gabauer, D., & Dwumfour, R. A. (2022). Dynamic spillover effects among green bond, renewable energy stocks and carbon markets during COVID-19 pandemic: Implications for hedging and investments strategies. *Global Finance Journal*, *51*, 100692. https://doi.org/10.1016/j.gfj.2021.100692

Wang, P., Zhang, H., Yang, C., & Guo, Y. (2021). Time and frequency dynamics of connectedness and hedging performance in global stock markets: Bitcoin versus conventional hedges. *Research in International Business and Finance*, *58*, 101479. https://doi.org/10.1016/j.ribaf.2021.101479

Yousaf, I., Suleman, T., & Demirer, R. (2021). Green Investments: A Luxury Good or a Financial Necessity? *SSRN Electronic Journal*. https://doi.org/10.2139/ssrn.3855125

Zeng, S., Jia, J., Su, B., Jiang, C., & Zeng, G. (2021). The volatility spillover effect of the European Union (EU) carbon financial market. *Journal of Cleaner*

Production, *282*, 124394. https://doi.org/10.1016/j.jclepro.2020.124394

Zeng, S., Liu, Y., Liu, C., & Nan, X. (2017). A review of renewable energy investment in the BRICS countries: History, models, problems and solutions. *Renewable and Sustainable Energy Reviews*, *74*, 860–872. https://doi.org/10.1016/j.rser.2017.03.016

Zhang, W., & Hamori, S. (2021). Crude oil market and stock markets during the COVID-19 pandemic: Evidence from the US, Japan, and Germany. *International Review of Financial Analysis*, *74*, 101702. https://doi.org/10.1016/j.irfa.2021.101702

Zhang, W., Nakajima, T., & Hamori, S. (2021). Does ESG Index Have Strong Conditional Correlations with Sustainability Related Stock Indices? In: ESG Investment in the Global Economy. SpringerBriefs in Economics. Springer, Singapore. https://doi.org/10.1007/978-981-16-2990-7_2.

Chapter 4. The Impact of the COVID-19 Pandemic and Russia-Ukraine War on Multiscale Spillovers in Green Finance Markets: Evidence from Lower and Higher Order Moments

4.1. Introduction

[19]Green bonds play a significant role in promoting the development of a global green low-carbon economy in the green financial market. They are bonds whose revenues are largely used to finance environmental initiatives, such as clean energy, energy efficiency, bioenergy, and low-carbon transportation (Campiglio, 2016; Gao et al., 2021). The green bond market has stood out since the signing of the Paris Climate Agreement in 2015 and the proposal of the UN Sustainable Development Goals (SDGs), allowing a significant number of countries to commit to and support the transformation to a climate-resilient economy, resulting in a thriving green bond market (Naeem, Adekoya and Oliyide, 2021; Reboredo and Ugolini, 2020).

The Dow Jones World Sustainability Index is the first sustainability index in the world launched by Dow Jones & Company, which evaluates the sustainability of companies from the perspective of investment in three aspects: economic, social, and environmental. The index closely tracks large companies that have demonstrated excellence in sustainable progress, and its constituents are selected from the top 10% of the Dow Jones Global Index of 2,500 of the world's largest companies. Considered one of the global reference benchmarks for socially responsible investments, sustainability indices offer diversification options and hedging against global uncertainty for traditional asset portfolios, in addition to reaching green investment targets (de Oliveira et al., 2020; Iqbal et al., 2022). As a result, investors are increasingly using sustainability indices to allocate their portfolios (Schaeffer et al., 2012).

The COVID-19 outbreak has plunged the world into the most severe economic recession since World War II, triggering a sharp rise in uncertainty and causing serious threats and shocks to the global community from social, financial, and economic perspectives (Liu et al., 2022; Sharif et al., 2020). Although the global economy has now begun to recover, the outbreak is a warning for us. It is well known that the impact of COVID-19 on the oil market was unprecedented. In March 2020, circuit breakers for the price of oil were triggered four times in just ten days, and global investors experienced one of the most volatile months in the history of the U.S. stock market. Theoretically, the spread of the COVID-19 pandemic dampened crude oil demand, leading to lower crude oil prices and returns (Liu et al., 2020). Therefore, many investors are turning their attention to the green finance market. Figure 4.1 indicates that the average annual trading volume of green bonds, clean energy, wind, solar, and sustainability index stocks is not affected by the outbreak of the COVID-19 pandemic in 2020 or the Russia-Ukraine war in 2022. Additionally, the average annual trading volume of these green finance indices has been consistently increasing year by year.

In addition, the outbreak of the Russia-Ukraine conflict in 2022 has increased the

[19] Chapter 4 is based on the published paper: Zhang, W., He, X., & Shigeyuki Hamori. (2023). The impact of the COVID-19 pandemic and Russia-Ukraine war on multiscale spillovers in green finance markets: Evidence from lower and higher order moments. *International Review of Financial Analysis*, 89, 102735–102735. https://doi.org/10.1016/j.irfa.2023.102735

uncertainty of energy supply in Europe. The instability of oil and gas markets has made the EU, Asia, and other regions realize the urgency of finding alternative energy sources. This policy shift will accelerate the development of renewable energy, and future policy design and funding are likely to be tilted toward renewable energy. The high prices of oil and natural gas also make renewable energy investments more attractive.

As reported by the International Renewable Energy Agency (Irena, 2020), 72% of all electricity growth in 2019 was due to renewable energy development, with wind and solar growth of 60 GW and 90 GW, respectively, together accounting for 90% of renewable energy additions. The British Petroleum Company (2021) predicts that after 2015, the installed capacity of wind power will continue to grow at a rate of approximately 14% per year, and solar power will grow by approximately 18% per year. These results show that wind and solar energy play a significant role in the renewable energy market.

Global natural disasters and climate extremes have occurred frequently in recent years. The physical risks posed by natural disasters and climate change to economic agents have led to the destruction of capital stocks, loss of life, and disruption of economic activity. There are growing concerns that climate change issues could hit financial markets hard, and resilience is also being tested (Adams and Abhayawansa, 2022). In this context, the market for sustainability bonds issued to finance or refinance the green finance market continues to expand, and the flow of funds for sustainable investments has reached a new height. Companies with high Environmental, Social and Governance (ESG) ratings achieve relatively high equity returns (Albuquerque et al., 2020; Broadstock et al., 2021). Funds focused on low sustainability, on the other hand, perform poorly (Ferriani and Natoli, 2021).

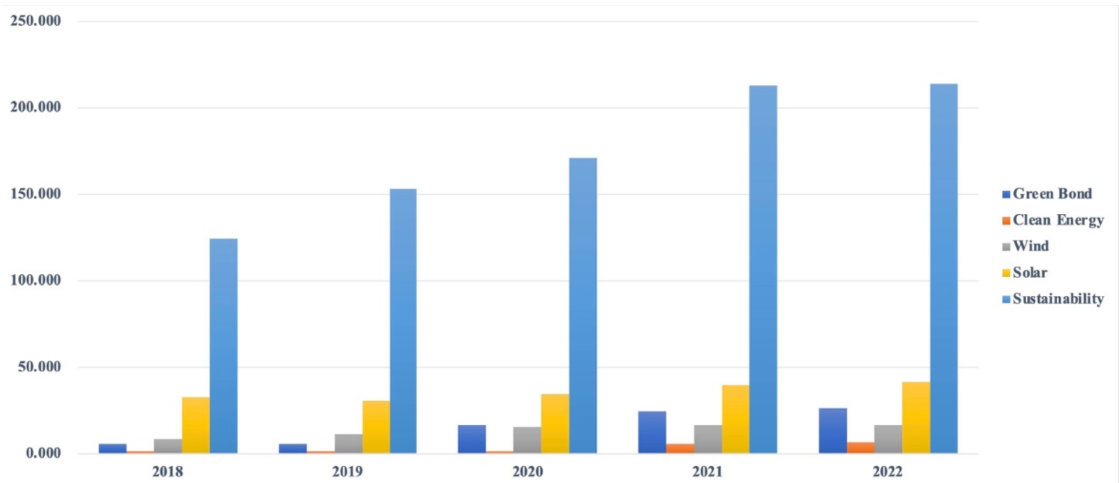

Figure 4.1. Average annual transaction volume.

Notes: Green Bond represents the return of the S&P Green Bond Index, Clean Energy represents the return of the S&P Global Clean Energy Index, Wind represents the return of the ISE Global Wind Energy Index, Solar represents the return of the MAC Global Solar Energy Index, Sustainability represents the return of the Dow Jones Sustainability World Index.

With the advancement of economic globalization and financial market integration, financial activities between countries (regions) are interpenetrating and mutually influencing, and the links between different financial markets are becoming increasingly close. There is an interaction between financial markets not only in terms of asset prices but also in terms of asset volatility. That is, the volatility in the financial market of one country (region) may be contagious to the financial market of another country (region), which is called the "volatility spillover effect." The economic crisis was caused by the collapse of stock and real estate prices in Thailand and Malaysia during the 1997 Asian financial crisis, and the collapse of the global real estate bubble triggered by the U.S. subprime mortgage crisis in 2008, which eventually led to a worldwide economic crisis. The outbreak of these major financial crises confirms that the frequent large fluctuations in financial asset prices and the consequent shocks to the macroeconomy have become prominent factors that affect macroeconomic stability (Nisticò, 2012). However, few studies have examined the spillover effects of COVID-19 on the green finance market. Given that the development of green finance has become a major trend for future development, exploring the impact of the COVID-19 pandemic on the spillover effect of the green finance market would benefit investors in reducing chain risk and diversifying investment assets.

At present, most researchers and investors focus on studying the spillover effects of financial markets in terms of the first and second moments. This is because the first-order moments (returns) and second-order moments (volatility) are commonly used to evaluate the risk-return balance. In financial markets, returns are used to measure general market levels, while volatility is used to measure market risk (He and Hamori, 2021). However, many empirical studies have demonstrated that the presence of higher-order moments (kurtosis and skewness) in the calculation of stock returns is not equal to 0, as assumed by many traditional financial econometric models. It is better to say that higher-order moments are not only non-zero but also time-varying. Moreover, skewness and kurtosis are important for investors' decision-making. Because skewness and kurtosis are related to the asset-pricing process, investors require a premium to take on the additional risk associated with the asymmetric distribution of returns. Thus, investors prefer assets with positive skewness and low kurtosis performance (Jurczenko and Maillet, 2006). This means that the transmission of spillovers in higher-order moments involves how markets are linked in terms of the degree of asymmetry in the distribution of returns directly related to downside (upside) risk. Therefore, researching the spillover of higher-order moments in the stock market during the COVID-19 pandemic is beneficial for investors to track the downside (upside) risk between stock markets for effective risk management investments.

We have analyzed the connectedness of lower-order moments (return and volatility) and higher-order moments (skewness and kurtosis) in green bonds, clean energy markets, wind markets, solar markets, and sustainability index markets. We used the Autoregressive Conditional Density (ACD) model developed by Hansen (1994) to evaluate the volatility, skewness, and kurtosis of the S&P Green Bond Index, S&P Global Clean Energy Index, ISE Global Wind Energy Index, MAC Global Solar Energy Index, and Dow Jones Sustainability World Index. To explore the impact of the COVID-

19 outbreak on the green finance market, we calculated the spillover effects of both lower-order moments and higher-order moments in the green finance market using the time-domain method proposed by Diebold and Yilmaz (2012) (hereafter, the "Diebold and Yilmaz method") and the frequency-domain method proposed by Baruník and Křehlík (2018) (hereafter, the "Baruník and Křehlík method"). By using these two methods, we can observe not only the strength and direction of the spillover effects over the fixed investment period but also the time-varying effects of crisis events on spillover effects.

The major contributions of this study are as follows: First, our study is the first to analyze the effects of the COVID-19 pandemic and Russia-Ukraine war on the lower-order moment and higher-order moment spillover effects of green financial markets using the framework of time-domain and frequency-domain methods and network topology. Second, the ACD model solves the limitations of the GARCH model and allows for dynamic volatility, skewness, and kurtosis, enabling extreme price fluctuations in stocks, securities, and other financial products to be effectively explained. Finally, by analyzing the dynamic spillover effect, it is not only possible to observe the dynamic influence of the COVID-19 outbreak on the green finance market but also to determine whether this impact is long-term or short-term by analyzing the spillover at different frequencies.

The main findings of this study are as follows. Firstly, the results from the static spillover effect show that the spillover effect of higher-order moments is lower than that of lower-order moments because the spillover transmission of higher-order moments is singular, while the spillover transmission of lower-order moments is diverse. Secondly, the results of the dynamic spillover effect analysis show that the impact of the Russia-Ukraine war on the spillover effect of lower- and higher-order moments is mild, while the effect from the COVID-19 pandemic is large and unprecedented. Thirdly, the COVID-19 outbreak has the most significant influence on the green bond market, a lasting effect on its higher-order spillovers, and the least impact on the sustainability index market. Fourthly, the fluctuations in the total volatility fluctuation spillover and total kurtosis spillover are more drastic than the dynamic total return spillover and total skewness spillover. Finally, total return spillover and total skewness spillover are mainly concentrated in the short term, total volatility spillover is mainly concentrated in the long term, and total kurtosis spillover is irregular before the COVID-19 outbreak and is mainly concentrated in the long term after the COVID-19 outbreak.

The remaining sections of this paper proceed as follows. Section 2 presents the literature review. Section 3 discusses the methodology of this study. Section 4 describes the study's data and provides descriptive statistics. Section 5 presents our empirical results. Finally, we present the conclusions in Section 6.

4.2. Literature review

Green bonds are designed to provide money with positive environmental or climate change benefits. Green bonds are considered stable and sustainable investments for financing permanent social projects. More researchers are examining the risk spillover effects between green bonds and other financial markets as a result of the gradual rise in the green bond market in recent years and the increased focus of regulators and investors on the effects of financial markets. (Liu et al., 2021; Mensi et al., 2022; Reboredo et al., 2020). In the background of the current widespread impact of COVID-19 on financial markets, green bonds are considered a good risk hedging tool. Le et al. (2021) indicated that green bonds have performed well in hedging cryptocurrencies since the COVID-19 outbreak. Furthermore, Naeem, Mbarki, Alharthi, Omri and Shahzad (2021) investigate how COVID-19 affects portfolios of green bonds' dynamic interconnectedness with other important financial assets (i.e., bond markets, global equity markets, the U.S. dollar index, and three hedging alternatives: oil, gold, and bitcoin) and find that green bonds are the optimal hedging tool for the U.S. dollar.

On the one hand, the significant economic impact of COVID-19 and the consequent negative WTI prices have had on the oil industry suggest that renewable energy will be seen as a reasonable alternative to meet energy demand (Corbet et al., 2020). On the other hand, clean energy fully satisfies the needs of sustainable development, effectively promotes the development of a green economy, and is currently leading the global trend in energy investment. Therefore, many researchers have examined the relationship between fossil fuels and renewable energy markets. For example, Sadorsky (2012) investigated the volatility spillover effects between oil prices, technology, and clean energy company stock prices and found a strong spillover transmission between oil and clean energy. Kumar et al. (2012) explored the relationship between oil prices, renewable energy stock prices, and carbon prices, and found that changes in renewable energy stock indices had a strong correlation with past oil prices. There have been significant milestones in the development of wind and solar power in the clean energy market. In 2021, solar, wind, and other clean energy sources generated 38% of global electricity, with wind turbines and solar panels generating 10% of the total electricity for the first time. From 2010 to 2020, the cost of solar power decreased by 85%, and the costs for onshore and offshore wind decreased by 56% and 48%, respectively.[20] Although wind and solar have a significant position in the clean energy market, there is little literature examining the spillover effects between them and other financial markets. To fill this gap, we investigate the dynamic spillover relationships between the wind, solar, and other green finance markets during the COVID-19 pandemic. Similar to our study, Tiwari et al. (2022) examined the dynamic spillover effects and risk-hedging performance of green bonds, wind energy stocks, solar energy stocks, and carbon markets during the COVID-19 pandemic and found that the wind energy market is the main recipient of the total spillover effect.

The COVID-19 pandemic has created a new global economic and financial landscape, thus imposing a severe challenge to the stability of traditional financial markets. In this background, as an alternative asset, green finance is attracting the attention of investors, researchers, etc. Investigating spillover effects between green financial markets and other financial markets during the COVID-19 pandemic could help investors diversify their portfolios more flexibly and efficiently. Dogan et al. (2022)

20 Cited from: https://www.un.org/en/climatechange/raising-ambition/renewable-energy

derived the connectedness between the Standard & Poor's Green Bond Index and five renewable energy sources (biofuels, fuel cells, geothermal, solar, and wind) by using the TVP-VAR model. They found that the green finance market was a net recipient of the renewable energy equity market during the COVID-19 pandemic period. Their conclusions were also confirmed by Streimikiene & Kaftan (2021). In addition to renewable energy markets, the spillover effects between green finance markets and traditional energy, commodity, equity, cryptocurrency, and other financial markets during the COVID-19 pandemic period have also been widely investigated (Mzoughi et al., 2022; Naeem et al., 2022; Hassan et al., 2022). These studies indicate that studying the short- and long-term dynamic connectedness between green financial markets and other financial markets is not only effective in capturing the spillover effects between green financial markets and other financial markets, but also beneficial to investors in revealing the risk hedging potential of green financial markets in other financial markets.

A sustainable investment strategy aims to bring about financial gains as well as social and environmental advantages. This strategy includes various asset classes related to environmental, social, and governance (ESG) investing (Brzeszczyński and McIntosh, 2014). Unlike traditional financial market indices, the sustainability index only includes businesses that surpass their peers in terms of an in-depth examination of economic, environmental, and social factors and categorizes them as industry sustainability leaders (Jain et al., 2019). While most of the published literature focuses on the returns of sustainability indices (De la Torre et al., 2016) or the financial performance of companies listed in the indices (Garcia and Orsato, 2020), there is little relevant literature examining the volatility spillovers of sustainability indices. However, our study not only fills this gap but also further extends the examination of spillovers in sustainability indices from lower- to higher-order moments.

A limitation of many current studies investigating spillovers between financial markets is that they only examine return and volatility spillovers, that is, spillovers of lower-order moments, while ignoring spillovers of higher-order moments. However, asset returns are not only non-normally distributed in the real world but are generally accompanied by skewed and fat-tailed distributions. Therefore, the transmission of crises between markets occurs not only through returns and volatility but also through skewness and kurtosis (Zhang, Bouri, et al., 2022). Investigating the risk spillover effects of higher-order moments is useful for capturing the asymmetric distribution associated with extreme or upside (downside) risks in financial markets (Finta and Aboura, 2020). Leverage and volatility feedback theories are sufficient to explain asymmetric return-volatility relationships at low frequencies (monthly, weekly, or quarterly) but not at high frequencies (daily or higher intraday frequencies). Behavioral theories, such as representation and investment psychology, provide better explanations for asymmetric returns at higher frequencies (e.g., daily or intraday levels) than traditional theories (Hibbert et al., 2008). Furthermore, the literature shows that negative skewness represents a high probability of asset returns falling in price, while positive skewness implies a high probability of asset returns rising in price. High kurtosis indicates a fat tail in the distribution of asset returns, implying a high probability of extremely high returns (Bevilacqua and Tunaru, 2021). Therefore, studying the spillover effects on higher-order moments has received increasing academic attention.

This study employs the parametric ACD model proposed by Hansen (1994) in conjunction with the normal inverse Gaussian (NIG) distribution defined by Barndorff-Nielsen (1997) to calculate the volatility, skewness, and kurtosis of sustainability-related financial indices. Unlike traditional models like GARCH-NIG, the ACD-NIG model allows skewness and kurtosis to vary over time. The ACD model with conditional distributions on the NIG distribution performs significantly better than the GARCH-NIG model in terms of correctly predicting conditional VaR (Wilhelmsson, 2009). Next, we use the methods proposed by Diebold and Yilmaz (2012) and Baruník and Křehlík (2018) to analyze the spillover effects of both lower-order and higher-order moments in both the time and frequency domains. The Diebold and Yilmaz method provides a framework for measuring the reciprocal transfer relationships between variables, while the Barunik and Krehlik methods decompose the spillover effect into different frequency bands, providing valid information for investors with different investment horizons. Therefore, researchers often use these two models to study the spillover relationships between financial markets, such as energy (Wang and Wang, 2019), commodities (Albulescu et al., 2019), and equity markets (Liu et al., 2022).

4.3. Methodology

4.3.1. Autoregressive Conditional Density model

Our study employs the Autoregressive Conditional Density (ACD) model developed by Hansen (1994) to estimate the conditional volatility, conditional skewness, and conditional kurtosis. The ACD model is an extension of the autoregressive moving average-generalized autoregressive conditional heteroskedasticity (ARMA-GARCH) model. The ACD model is constructed as follows:

$$r_t = \mu_t + \varepsilon_t \tag{4.1}$$

$$\mu_t = c + \sum_{i=1}^{p'} \gamma_i r_{t-i} + \sum_{j=1}^{q'} \eta_j \, \varepsilon_{t-j} \tag{4.2}$$

$$\varepsilon_t = \sigma_t z_t \tag{4.3}$$

$$z_t \sim \mathfrak{N}(0, 1, \theta_t, \tau_t) \tag{4.4}$$

$$\sigma_t^2 = \omega + \sum_{i=1}^{p} \mathrm{A}_i \, \varepsilon_{t-i}^2 + \sum_{j=1}^{q} B_j \sigma_{t-j}^2 \tag{4.5}$$

$$\theta_t = \Psi(\check{\theta}_t) \tag{4.6}$$

$$\tau_t = \Psi(\check{\tau}_t) \tag{4.7}$$

where μ_t is modeled using the mean equation: ARMA (p', q') model. ε_t is the residual. z_t is a random variable with unit variance and is subject to a special distribution $\mathfrak{N}$. The special distribution $\mathfrak{N}$ includes additional special parameters: the skew parameter θ_t and shape parameter τ_t, which are designated to capture the time-varying conditional high moments. σ_t^2 is the conditional variance, constructed using the GARCH (p, q) model. The biggest difference between the ACD and GARCH models is that the parameters μ_t and σ_t vary with time, and all other parameters in the GARCH model; however, μ_t, σ_t, θ_t, and τ_t vary over time in the ACD model. c and ω are defined as constants. Parameters $\omega > 0$, $A_1 \geq 0$, and $B_1 \geq 0$ ensure that the conditional variance is greater than 0. Unlike the modeling of the second moments (conditional variance), modeling of the third moments (skewness) and fourth moments (kurtosis) is performed through the skew parameter θ_t and the shape parameter τ_t. The skew parameter θ_t describes the distribution deviation from symmetry or skewness and the shape parameter τ_t controls the kurtosis of the tails. The unconstrained motion dynamics of the skew parameter θ_t and shape parameter τ_t are denoted by the parameters $\breve{\theta}_t$ and $\breve{\tau}_t$. The function $\Psi(\cdot)$ is an appropriate transformation function for the parameters $\breve{\theta}_t$ and $\breve{\tau}_t$. The specific formulas for parameters $\breve{\theta}_t$, $\breve{\tau}_t$ and function $\Psi(\cdot)$ are as follows:

$$\breve{\theta}_t = a_0 + a_1 z_{t-1} + a_2 z_{t-1}^2 + c_1 \breve{\theta}_{t-1} \tag{4.8}$$

$$\breve{\tau}_t = b_0 + b_1 z_{t-1} + b_2 z_{t-1}^2 + d_1 \breve{\tau}_{t-1} \tag{4.9}$$

$$\Psi(\breve{\theta}_t) = L_{\breve{\theta}_t} + \frac{(U_{\breve{\theta}_t} - L_{\breve{\theta}_t})}{1 + e^{-\breve{\theta}_t}} \tag{4.10}$$

$$\Psi(\breve{\tau}_t) = L_{\breve{\tau}_t} + \frac{(U_{\breve{\tau}_t} - L_{\breve{\tau}_t})}{1 + e^{-\breve{\tau}_t}} \tag{4.11}$$

where the lower and upper bounds of the distributional parameters $\breve{\theta}_t$ and $\breve{\tau}_t$ are represented by *L* and *U*, respectively.

4.3.2. Generalized Hyperbolic distribution and Normal Inverse Gaussian distribution

In Section 3.1, we mention that there is a special distribution $\mathfrak{N}$ in the ACD model. Barndorff-Nielsen (1977) and Barndorff-Nielsen (1997) defined this particular distribution as the generalized hyperbolic (GH) distribution and the normal inverse Gaussian (NIG) distribution. The GH distribution can be denoted as

$$GH(x|\lambda,\alpha,\beta,\delta,\mu) = a(\lambda,\alpha,\beta,\delta,\mu)[\delta^2 + (x-\mu)^2]^{\left(\lambda-\frac{1}{2}\right)/2}$$
$$\times K_{\lambda-1/2}(\alpha\sqrt{\delta^2 + (x-\mu)^2})e^{\beta(x-\mu)} \tag{4.12}$$

$$a(\lambda,\alpha,\beta,\delta,\mu) = (\alpha^2 - \beta^2)^{\lambda/2} / \left[\sqrt{2\pi}\alpha^{\lambda-1/2}\delta^\lambda K_\lambda\left(\delta\sqrt{\alpha^2 - \beta^2}\right)\right] \tag{4.13}$$

where the function $K_\lambda(\cdot)$ represents the modified Bessel function of the third kind and $x,\ \lambda,\ \alpha,\ \mu \in R$. δ is the scale parameter. The range of values of the asymmetric parameter β: $\delta \leq |\beta| \leq \alpha$. If X is subject to the GH distribution, it can be denoted as $X \sim GH(\lambda, \alpha, \beta, \delta, \mu)$.

Following Scott et al. (2011), the location and scale-invariant parameterization of the GH distribution can be denoted as follows:

$$\theta = \delta\sqrt{\alpha^2 - \beta^2} \tag{4.14}$$

$$\tau = \beta/\alpha \tag{4.15}$$

Following Scott et al. (2011), we define the central moments as $M_k = E\left[\left(X - E(X)\right)^k\right]$, for $k = 2, 3, \cdots$. We need to investigate the spillover effects of the return (moment 1: mean $E(X)$), volatility (moment 2: M_2), skewness (moment 3: M_3), and kurtosis (moment 4: M_4). Before calculating these moments, we must define the function $R_{\lambda,i}(\theta)$ for *i* as a positive integer according to

$$R_{\lambda,i}(\theta) = K_{\lambda+i}(\theta)/K_\lambda(\theta) \tag{4.16}$$

The mean $E(X)$, M_2, M_3, and M_4 of the GH distribution can then be calculated as follows:

$$E(X) = \mu + \frac{\beta\delta}{\sqrt{\alpha^2-\beta^2}} R_{\lambda,1}(\theta) = \mu + \beta\delta^2\theta^{-1}R_{\lambda,1}(\theta) \tag{4.17}$$

$$M_2 = Var(X) = \delta^4\beta^2\theta^{-2}\left[R_{\lambda,2}(\theta) - R_{\lambda,1}^2(\theta)\right] + \delta^2\theta^{-1}R_{\lambda,1}(\theta) \tag{4.18}$$

$$\begin{aligned} M_3 = {} & \delta^6\beta^3\theta^{-3}\left[R_{\lambda,3}(\theta) - 3R_{\lambda,2}(\theta)R_{\lambda,1}(\theta) + 2R_{\lambda,1}^3(\theta)\right] \\ & +3\delta^4\beta\theta^{-2}\left[R_{\lambda,2}(\theta) - R_{\lambda,1}^2(\theta)\right] \end{aligned} \tag{4.19}$$

$$\begin{aligned} M_4 = {} & \delta^8\beta^4\theta^{-4}\left[R_{\lambda,4}(\theta) - 4R_{\lambda,3}(\theta)R_{\lambda,1}(\theta) + 6R_{\lambda,2}(\theta)R_{\lambda,1}^2(\theta) - 3R_{\lambda,1}^3(\theta)\right] \\ & +6\delta^6\beta^2\theta^{-3}\left[R_{\lambda,3}(\theta) - 2R_{\lambda,2}(\theta)R_{\lambda,1}(\theta) + R_{\lambda,1}^3(\theta)\right] \end{aligned} \tag{4.20}$$

Barndorff-Nielsen (1997) proposed the NIG distribution. When $\lambda = -\frac{1}{2}$, the GH distribution changes into the NIG distribution as follows:

$$\begin{aligned} NIG(x|\alpha,\beta,\delta,\mu) = {} & a(\alpha,\beta,\delta,\mu)[\delta^2 + (x-\mu)^2]^{-1/2} \\ & \times K_1(\alpha\sqrt{\delta^2 + (x-\mu)^2})e^{\beta(x-\mu)} \end{aligned} \tag{4.21}$$

$$a(\alpha, \beta, \delta, \mu) = \pi^{-1}\delta\alpha e^{\delta\sqrt{\alpha^2-\beta^2}} \tag{4.22}$$

where the parameters are $\mu \in R$, $\delta > 0$ and $\delta \leq |\beta| \leq \alpha$. If X is subject to the NIG distribution, it can be expressed as $X \sim NIG(\alpha, \beta, \delta, \mu)$.

Then, the mean $E(X)$, M_2, M_3, and M_4 of the NIG distribution can be calculated as:

$$E(X) = \mu + \delta^2\beta\theta^{-1} \tag{4.23}$$

$$M_2 = Var(X) = \delta^4\alpha^2\theta^{-3} \tag{4.24}$$

$$M_3 = 3\delta^6\alpha^2\beta\theta^{-5} \tag{4.25}$$

$$M_4 = 3\delta^8\alpha^2(\alpha^2 + \beta^2)\theta^{-7} \tag{4.26}$$

Following Jensen and Lunde (2001), we employ the ACD model with the NIG distribution to calculate the volatility, skewness, and kurtosis.

4.3.3. The Diebold and Yilmaz (2012) method

After extracting the volatility, skewness, and kurtosis using the ACD model, we employ Diebold and Yilmaz's (2012) method to estimate the spillover effects of lower- and higher-order moments among sustainability-related stock markets under the COVID-19 pandemic in the time domain. The Diebold and Yilmaz method is constructed to measure the spillover effect based on evaluating the generalized forecast error variance decomposition (GFEVD) using the vector autoregression (VAR) model. The *M*-variable VAR model with *p* lags is defined as follows:

$$\boldsymbol{y}_t = \sum_{i=1}^{p} \boldsymbol{\varphi}_i \boldsymbol{y}_{t-1} + \boldsymbol{\varepsilon}_t \tag{4.27}$$

where $\boldsymbol{y}_t$ represents the $M\times1$ vector of the variables used at time *t*. The parameter $\boldsymbol{\varphi}$ is the $M\times M$ coefficient matrices. The error vector ε_t is independent and identically distributed ($\varepsilon_i \sim i.i.d(0, \boldsymbol{\Sigma})$), and the white noise $(0, \boldsymbol{\Sigma})$ with covariance matrix $\boldsymbol{\Sigma}$ is nondiagonal**.**

The VAR (*p*) process can be rebuilt using the vector moving average, as shown in Equation (28). Suppose that the roots of $|\varphi(z)|$ are outside the circle of a unit.

$$\boldsymbol{y}_t = \sum_{i=0}^{\infty} \boldsymbol{H}_i \boldsymbol{\varepsilon}_t \tag{4.28}$$

$$\boldsymbol{\Psi}_i = \boldsymbol{\varphi}_1\boldsymbol{\Psi}_{i-1} + \boldsymbol{\varphi}_2\boldsymbol{\Psi}_{i-2} + \cdots + \boldsymbol{\varphi}_p\boldsymbol{\Psi}_{i-p} \tag{4.29}$$

where $\boldsymbol{\Psi}_0$ represents an identity matrix and $\boldsymbol{\Psi}_i$ is a zero matrix when $i < 0$. By employing the generalized VAR framework conceived by Koop et al. (1996) and Pesaran and Shin (1998), the Diebold and Yilmaz method ensures that the variance decomposition is not influenced by the ordering of variables. The H-step-ahead

GFEVD can be conceived based on the generalized VAR framework as follows:

$$\boldsymbol{\theta}_{H,jk} = \frac{\sigma_{kk}^{-1}\sum_{h=0}^{H-1}((\boldsymbol{\Psi}_h\boldsymbol{\Sigma})_{jk})^2}{\sum_{h=0}^{H-1}(\boldsymbol{\Psi}_h\boldsymbol{\Sigma}\boldsymbol{\Psi}'_h)_{jj}} \tag{4.30}$$

where $\boldsymbol{\Psi}_h$ is the M×M moving average coefficient matrix at lag h and $\boldsymbol{\Sigma}$ is the covariance matrix for the error vector. Further, $\sigma_{kk} = (\boldsymbol{\Sigma})_{kk}$ is the standard deviation of the error term of the kth equation. $\boldsymbol{\theta}_{H,jk}$ represents the contribution of the kth variable to the h-step-ahead generalized forecast error variance of the jth variable.

Because the sum of the elements in each GFEVD row is not equal to one. To employ the information available in the GFEVD to calculate the spillover index, we normalize each entry by the sum of the rows, as follows:

$$\widetilde{\boldsymbol{\theta}}_{H,jk} = \frac{\boldsymbol{\theta}_{H,jk}}{\sum_{k=1}^{N}\boldsymbol{\theta}_{H,jk}} \tag{4.31}$$

where $\widetilde{\boldsymbol{\theta}}_{H,jk}$ stands for the pairwise spillover delivered from *k*th variable to *j*th variable at horizon *H*. Moreover, the total spillover across all variables can be aggregated from the pairwise spillover as:

$$S^H = 100 \times \left(1 - \frac{Tr\{\widetilde{\boldsymbol{\theta}}_{H,jk}\}}{\sum \widetilde{\boldsymbol{\theta}}_{H,jk}}\right) = 100 \times \frac{\sum_{\substack{j,k=1 \\ j\neq k}}^{N}\widetilde{\boldsymbol{\theta}}_{H,jk}}{N} \tag{4.32}$$

where *Tr{.}* is the trace operator.

Furthermore, the directional spillovers (from) measure the spillovers from all the other variables to *k*th variable, which can be conceived as follows:

$$S_{k\leftarrow .}^{H} = 100 \times \frac{\sum_{\substack{j=1 \\ j\neq k}}^{N}\widetilde{\boldsymbol{\theta}}_{H,kj}}{N} \tag{4.33}$$

Meanwhile, the directional spillovers (to) measure the spillovers transferred from *k*th variable to all other variables, which can be constructed as follows:

$$S_{.\leftarrow k}^{H} = 100 \times \frac{\sum_{\substack{j=1 \\ j\neq k}}^{N}\widetilde{\boldsymbol{\theta}}_{H,jk}}{N} \tag{4.34}$$

4.3.4. The Baruník and Křehlík (2018) method

After investigating the spillover effect in the time domain, we employ the method of Baruník and Křehlík (2018) to evaluate the spillover effect of lower- and higher-order moments for sustainability-related stock markets under the COVID-19 pandemic. Using Fourier transform, Baruník and Křehlík (2018) extended the Diebold and Yilmaz method from the time domain to the frequency domain. The Fourier transform process can be constructed as

$$\boldsymbol{\Psi}(e^{-i\omega}) = \sum_h e^{-i\omega h}\boldsymbol{\Psi}_h \tag{4.35}$$

where $i = \sqrt{-1}$, and $\boldsymbol{\Psi}(e^{-i\omega})$ is the Fourier transformation of the coefficients $\boldsymbol{\Psi}_h$. Then, the spectral density of $\boldsymbol{X_t}$ at frequency ω can be denoted as

$$\boldsymbol{S}_X(\omega) = \sum_{h=0}^{\infty} E(\boldsymbol{X}_t\boldsymbol{X}'_{t-h})\, e^{-i\omega h} = \boldsymbol{\Psi}(e^{-i\omega})\boldsymbol{\Sigma}\boldsymbol{\Psi}'(e^{+i\omega}) \tag{4.36}$$

The spillover derived from the Diebold and Yilmaz method at frequency $\omega \in (-\pi, \pi)$ can be expressed as:

$$\boldsymbol{F}(\omega)_{jk} = \frac{\sigma_{kk}^{-1}|(\boldsymbol{\Psi}(e^{-j\omega})\boldsymbol{\Sigma})_{jk}|^2}{(\boldsymbol{\Psi}(e^{-j\omega})\boldsymbol{\Sigma}\boldsymbol{\Psi}'(e^{+jw}))_{jj}} \tag{4.37}$$

where $\boldsymbol{F}(\omega)_{jk}$ specifies the portion of the spectrum of the *j*th variable that can be attributed to shocks in the *k*th variable at a given frequency, ω. To achieve generalized variance decomposition in frequency dynamics, we can weight $\boldsymbol{F}(\omega)_{jk}$ by the frequency share of the variance of the *j*th variable as follows:

$$\Xi_j(\omega) = \frac{(\boldsymbol{\Psi}(e^{-j\omega})\boldsymbol{\Sigma}\boldsymbol{\Psi}'(e^{+j\omega}))_{jj}}{\frac{1}{2\pi}\int_{-\pi}^{\pi}(\boldsymbol{\Psi}(e^{-j\omega})\boldsymbol{\Sigma}\boldsymbol{\Psi}'(e^{+j\omega}))_{jj}d\lambda} \tag{4.38}$$

where $\Xi_j(\omega)$ represents the power of the *j*th variable at a specific frequency, through a frequency equal to a constant value of 2π. In addition, we want to measure the spillover effect at different frequencies, such as short-, medium-, or long-term, rather than at a single frequency. Therefore, we define an arbitrary frequency band $\mathrm{d} = (\mathrm{a}, \mathrm{b})\colon \mathrm{a}, \mathrm{b} \in (-\pi, \pi), \mathrm{a} < \mathrm{b}$. The accumulated spillover under frequency band d can be defined as:

$$\boldsymbol{\theta}_{jk}(d) = \frac{1}{2\pi}\int_a^b \Xi_j(\omega)\boldsymbol{F}(\omega)_{jk}d\omega \tag{4.39}$$

Similar to Equation (31) in the Diebold and Yilmaz method, Equation (39) can be normalized as follows:

$$\widetilde{\boldsymbol{\theta}}_{jk}(d) = \frac{\boldsymbol{\theta}_{jk}(d)}{\sum_{k=1}^{N}\boldsymbol{\theta}_{jk}(\infty)} \tag{4.40}$$

where $\widetilde{\boldsymbol{\theta}}_{jk}(d)$ represents the pairwise spillover transmitted from *k*th variable to *j*th variable in the frequency band d.

Similarly, the total spillover at frequency band d also can be constructed as:

$$S^F(d) = 100 \times \left(\frac{\Sigma\widetilde{\boldsymbol{\theta}}_{jk}(d)}{\Sigma\widetilde{\boldsymbol{\theta}}_{jk}(\infty)} - \frac{Tr\{\widetilde{\boldsymbol{\theta}}_{jk}(d)\}}{\Sigma\widetilde{\boldsymbol{\theta}}_{jk}(\infty)}\right) = 100 \times \frac{\sum_{j,k=1,j\neq k}^{N}\widetilde{\boldsymbol{\theta}}_{jk}(d)}{\Sigma\widetilde{\boldsymbol{\theta}}_{jk}(\infty)} \tag{4.41}$$

where $Tr\{\cdot\}$ is the trace operator and the sum of $S^F(d)$ over band d is equivalent to the total spillover in the Diebold and Yilmaz method (S^H).

Furthermore, we can define the frequency directional spillover (from), which depicts the spillover effect from all other variables to *k*th variable at frequency band d as:

$$S_{k\leftarrow \cdot}^{F}(d) = 100 \times \frac{\sum_{\substack{j=1 \\ j\neq k}}^{N} \widetilde{\boldsymbol{\theta}}_{kj}(d)}{N} \tag{4.42}$$

Similarly, we can also denote the frequency directional spillover (to), which stands for the spillover effect transmitted from kth variable to all other variables in frequency band d as

$$S_{\cdot\leftarrow k}^{F}(d) = 100 \times \frac{\sum_{\substack{j=1 \\ j\neq k}}^{N} \widetilde{\boldsymbol{\theta}}_{jk}(d)}{N} \tag{4.43}$$

4.4. Data and descriptive statistics

For our study, we chose the daily data of S&P Green Bond Index Total Return (Green Bond), S&P Global Clean Energy Index (Clean Energy), ISE Global Wind Energy Index (Wind), MAC Global Solar Energy Index (Solar), Dow Jones Sustainability World Index (Sustainability), and Infectious Disease Equity Market Volatility Tracker (IDEMVT) to investigate the impact of the COVID-19 pandemic and Russia-Ukraine war on the lower- and higher-order moment spillovers of sustainability-related stock markets during the period from November 1, 2010, to January 30, 2023. Because differences in exchange rates between indices have an impact on our analysis, we standardized the prices of all indices in terms of US dollar currency units. The names and sources of the variables are listed in Table 4.1.

Table 4.1. Data description.

Variables	Data	Source
Green Bond	S&P Green Bond Index	Bloomberg
Clean Energy	S&P Global Clean Energy Index	Bloomberg
Wind	ISE Global Wind Energy Index	Bloomberg
Solar	MAC Global Solar Energy Index	Bloomberg
Sustainability	Dow Jones Sustainability World Composite Index	Bloomberg
IDEMVT	Infectious Disease Equity Market Volatility Tracker	Bloomberg

For the green bond stock market, we have chosen the S&P Green Bond Index, which includes only green bonds for which the issuer has declared the use of revenue or which have been verified independently in accordance with the Green Bond Principles established in January 2014. As a result, the index advocates for higher levels of transparency and accountability in the green bond market.[21]

The S&P Global Clean Energy Index is intended to track the performance of global

21 The homepage of the S&P Green Bond Index: https://www.spglobal.com/spdji/en/indices/esg/sp-green-bond-index/#overview

renewable energy companies from both developed and emerging markets. Companies involved in the production of clean energy or the provision of clean energy technologies and equipment are considered eligible for inclusion in the potential index.[22] Therefore, we believe that the S&P Global Clean Energy Index represents the global clean energy stock market.

As the global energy structure transformation process is accelerating, an increasing number of countries are actively introducing policy measures to promote the development of the renewable energy industry. The prospects of green energy industry development are promising. Among them, the wind and solar energy markets are of particular concern.

The ISE Global Wind Energy Index analyzes publicly traded firms involved in the wind energy sector, based on an examination of their goods and services. This is a modified capitalization-weighted index. The MAC Global Solar Energy Index is a rule-based stock index that attempts to track the performance of companies involved in the global solar energy industry. These two stock indices represent the global wind and solar stock markets, respectively.

The Dow Jones Sustainability World Composite Index covers the top 10% of the 2,500 largest organizations' sustainability leaders worldwide. Criteria used to select companies included climate change strategies, energy consumption, and corporate governance. Therefore, the Dow Jones Sustainability World Index is a best-in-class benchmark series for investors who recognize the importance of sustainable business practices in generating long-term shareholder value and want their sustainability beliefs reflected in their portfolios.

To investigate the impact of the COVID-19 pandemic on the lower and higher moment spillover effects of sustainability-related stock markets, we are using IDEMVT data to document and quantify the significant increase in economic uncertainty over the past few weeks. Following Baker et al. (2019) and Baker et al. (2020), the IDEMVT is constructed based on four indicators: global disease disasters, stock market volatility, newspaper-based economic uncertainty, and subjective uncertainty in business expectation surveys. The details of the four indicators are presented in Table 4.2. The construction of IDEMVT can be divided into the following steps. First, we obtain daily counts of newspaper articles from about 3,000 U.S. newspapers that contain at least one term in E, M, V, or ID. Second, we scale the number of articles published on the same day to obtain the raw EMV-ID count. Finally, we rescale the generated series multiplicatively to an EMV series scale for categorical data.

22 The homepage of the S&P Global Clean Energy Index: https://www.spglobal.com/spdji/en/indices/esg/sp-global-clean-energy-index/#overview

Table 4.2. The contents of IDEMVT.

Indicators	Contents
ID	epidemic, pandemic, virus, flu, disease, coronavirus, mers, sars, ebola, H5N1, H1N1
E	economic, economy, financial
M	"Stock market", equity, equities, "Standard and Poors"
V	volatility, volatile, uncertain, uncertainty, risk, risky

Figure 4.2 presents a plot of the raw data series used in this study. The prices of green bonds and sustainability indexes have experienced minor fluctuations after the COVID-19 outbreak. However, clean energy index prices, wind index prices, solar index prices, and IDEMVT all exhibited significant fluctuations after the outbreak. In the current situation, policymakers need to assess the economic impact of the COVID-19 pandemic on the green finance market. However, the outbreak of the Russia-Ukraine war has not had a significant impact on the prices of the financial assets we studied.

In our study, we use the logarithmic change in the daily closing price to calculate the daily returns of the stocks. Table 4.3 presents descriptive statistics for the returns of the five stock indices. We observe from Table 4.3 that green bonds have the lowest mean return value, while wind has the highest. In addition, solar energy has the highest maximum return value and the lowest minimum return value.

The daily returns of the five stock indices are all left-skewed in terms of skewness value. The daily returns of the five stock indexes are leptokurtic in terms of kurtosis value, indicating that the distributions of the five stock indices peak more and have fat tails. In the case of deviation from the mean, there is a possibility of extreme situations resulting in very large gains or losses, which is a matter of particular attention in risk control.

We use the Jarque–Bera test to check the normality of the five stock indices (Jarque and Bera, 1987), and the JB test statistics reject the null hypothesis of normality for each variable at the 1% significance level. The augmented Dickey–Fuller (ADF) unit root test is used to examine the stationarity of the return series (Said and Dickey, 1984). The result of the ADF test rejects the null hypothesis for each variable with a unit root at the 1% significance level, indicating that no unit root exists for each variable.

We use the ARCH-LM test by Engle (1982) to examine the autoregressive conditional heteroskedasticity effects in the daily return of five stock indices. The results indicate that building the multivariate GARCH model in our study is reasonable because it rejects the null hypothesis of the non-ARCH impact in the return series at the 1% level of significance.

After deriving the return series, we employ Hansen's ACD model with the NIG distribution to calculate the conditional volatility, skewness, and kurtosis (Hansen, 1994). Compared with the GH distribution, the NIG distribution is simpler to calculate and has been used more frequently in previous studies (Ghalanos et al., 2015; Wilhelmsson, 2009). According to the results reported in Table 4.3, our return series is left-skewed and has fat tails. The NIG distribution exhibits promising theoretical aspects and can accurately fit financial return data with skewed and fat tails (Chang et al., 2005; He and Hamori, 2021; Morimoto, 2004).

In this study, we utilize the Diebold and Yilmaz as well as the Barunik and Krehlik methods to examine the spillover effects of returns, volatility, skewness, and kurtosis across variables. To ensure the appropriateness of the analysis, it is necessary for each variable to be stationary. Descriptive statistics for the volatility, skewness, and kurtosis series are presented in Tables 4.4, 4.5, and 4.6, respectively. The ADF test statistics indicate that there are no unit root problems for each variable at the 1% significance level, which confirms the suitability of using the Diebold and Yilmaz and Barunik and Krehlik methods.

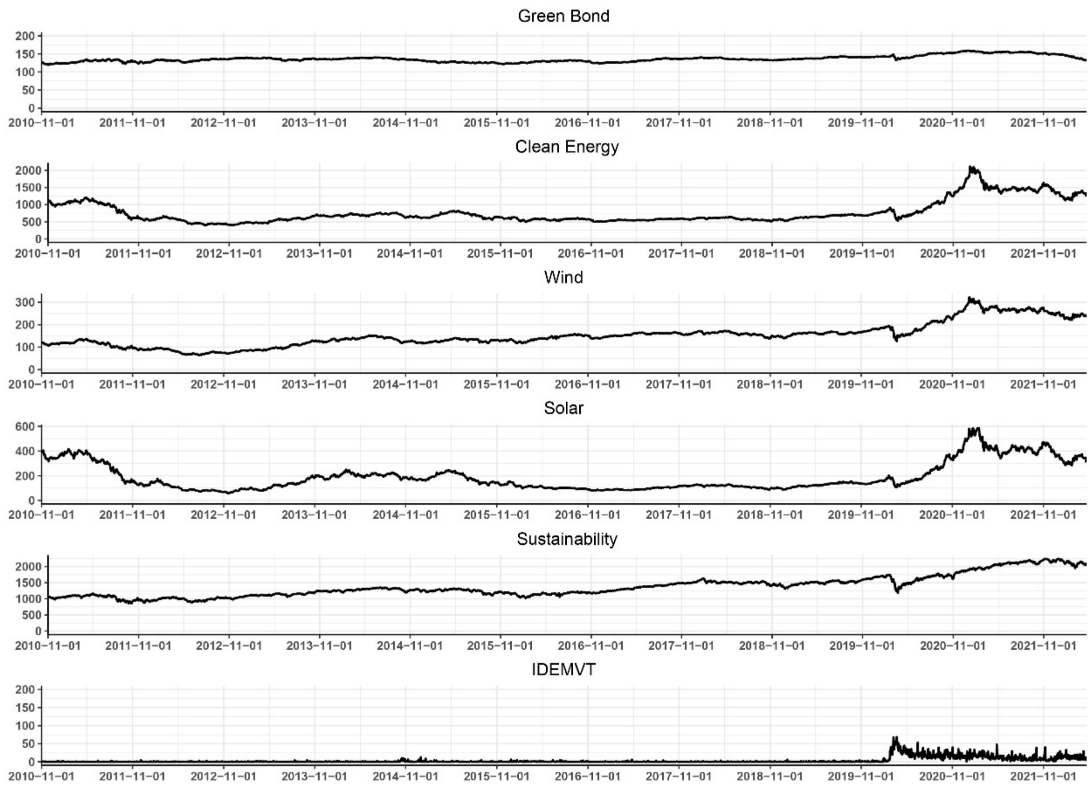

Figure 4.2. Time variations of raw data series.

Notes: Green Bond represents the S&P Green Bond Index; Clean Energy represents the S&P Global Clean Energy Index; Wind represents the ISE Global Wind Energy Index; Solar represents the MAC Global Solar Energy Index; Sustainability represents the Dow Jones Sustainability World Index; and IDEMVT represents the infectious disease equity market volatility tracker.

Table 4.3. Descriptive statistics for return series.

	Green Bond	Clean Energy	Wind	Solar	Sustainability
Mean	−2.97E−07	6.10E−05	2.05E−04	−8.00E−05	2.03E−04
Median	0.00009	0.00059	0.00066	0.00024	0.00050
Maximum	0.026	0.110	0.099	0.120	0.077
Minimum	−0.031	−0.125	−0.126	−0.150	−0.106
Std. Deviation	0.004	0.015	0.012	0.023	0.010
Skewness	−0.250	−0.391	−0.541	−0.075	−0.858
Kurtosis	5.120	6.571	7.504	3.305	11.195
JB	3418.869***	5658.647***	7426.320***	1413.864***	16574.270***
ADF	−14.394***	−12.852***	−13.760***	−13.032***	−14.811***
ARCH-LM	424.88***	710.42***	677.02***	372.11***	798.04***

Notes: This table presents descriptive statistics for the return series of the five stock indices. Because IDEMVT is volatile, we do not have to calculate its returns. JB represents Jarque and Bera (1987) test for normality; ADF stands for the Augmented Dickey and Fuller Unit Root Test developed by Said and Dickey (1984); ARCH-LM stands for ARCH-LM test developed by Engle (1982); "***" represents statistical significance at 1% level.

Table 4.4. Descriptive statistics for volatility series.

	Green Bond	Clean Energy	Wind	Solar	Sustainability	IDEMVT
Mean	0.004	0.013	0.011	0.021	0.009	3.907
Median	0.00317	0.01212	0.01041	0.02036	0.00778	0.39000
Maximum	0.011	0.066	0.050	0.062	0.053	68.370
Minimum	0.002	0.006	0.006	0.010	0.004	0.000
Std. Deviation	0.002	0.006	0.004	0.007	0.004	8.013
Skewness	1.456	2.769	3.139	1.422	3.934	3.048
Kurtosis	2.120	13.116	18.178	4.052	25.090	11.789
ADF	−3.081**	−5.183***	−5.922***	−4.482***	−6.407***	−4.380***

Notes: This table presents descriptive statistics for the volatility series of the five stock indices and IDEMVT. ADF stands for the Augmented Dickey and Fuller Unit Root Test developed by Said and Dickey (1984); "***" and "**" represent statistical significance at 1% and 5% levels, respectively.

Table 4.5. Descriptive statistics for skewness series.

	Green Bond	Clean Energy	Wind	Solar	Sustainability
Mean	−0.211	−0.042	−0.261	−0.010	−0.428
Median	−0.18401	−0.08765	−0.29078	0.00301	−0.46464
Maximum	0.632	2.877	1.960	1.012	6.992
Minimum	−3.304	−1.157	−0.921	−1.309	−1.222
Std. Deviation	0.255	0.336	0.197	0.267	0.401
Skewness	−3.592	1.947	2.234	−0.351	4.931
Kurtosis	32.845	9.581	13.374	0.937	65.571
JB	146053.756***	13818.548***	25689.567***	177.162***	568008.610***
ADF	−11.963***	−12.936***	−12.592***	−13.260***	−17.080***

Notes: This table presents descriptive statistics for the skewness series of the five stock indices. JB represents Jarque and Bera (1987) test for normality; ADF stands for the Augmented Dickey and Fuller Unit Root Test developed by Said and Dickey (1984); "***" represents statistical significance at 1% level.

Table 4.6. Descriptive statistics for kurtosis series.

	Green Bond	Clean Energy	Wind	Solar	Sustainability
Mean	1.531	1.653	1.510	1.404	2.948
Median	1.36614	1.31825	1.32044	1.30086	2.06077
Maximum	21.439	26.963	19.614	5.248	128.839
Minimum	0.603	0.263	0.423	0.483	0.122
Std. Deviation	0.979	1.489	0.935	0.538	3.575
Skewness	11.239	6.927	6.496	1.878	9.264
Kurtosis	178.229	82.760	86.227	6.943	172.811
ADF	−9.131***	−11.547***	−10.861***	−10.159***	−11.970***

Notes: This table presents descriptive statistics for the kurtosis series of the five stock indices. ADF stands for the Augmented Dickey and Fuller Unit Root Test developed by Said and Dickey (1984); "***" represents statistical significance at 1% level.

4.5. Empirical Results

4.5.1. Static spillover effects analysis

In our study, we use the Diebold and Yilmaz and Barunik and Krehlik methods to investigate the spillover effects of lower- and higher-order moments in both the time and frequency domains.[23] Specifically, we first employ the approach by Diebold and Yilmaz (2009, 2012, 2014, 2015) to build a spillover table in the time domain, which involves realizing the generalized variance decomposition of the 10-day-ahead volatility forecast errors using the VAR. Then, we apply the Barunik and Krehlik approach to divide the spillover table into three distinct frequency bands, namely, frequencies S, M, and L, to gain a better understanding of the spillover effects from various frequencies. These frequency bands are defined based on the work of Zhang and Hamori (2021) and Barunik and Krehlik (2016). Specifically, "Frequency short-term" refers to the short term, which is a period of 1 to 5 days (weekdays of one week);

[23] We used R for the analysis of our study.

"Frequency medium-term" represents the medium term, which is a period of 6 to 21 days (weekdays in one month); and "Frequency long-term" represents the long term, which is a period of 22 days to infinite days.

Furthermore, Baruník and Křehlík (2018) have shown that the Barunik and Krehilik models are not suitable for forecasting horizons H<100. Hence, we have selected 100 days as the forecasting horizon for our study. Tables 4.7, 4.8, 4.9, and 4.10 present the spillover results of lower-order moments (return and volatility) and higher-order moments (skewness and kurtosis) using the Diebold and Yilmaz and Barunik and Krehlik methods, respectively. The top half of each spillover table shows the results obtained from the Diebold and Yilmaz method, whereas the bottom half displays the results of the Barunik-Krehlic model for the three frequencies. The pairwise spillover value in row i and column j indicates the spillover effect from market j to market i and vice versa. The last row's "TO" values, representing directional spillover (to), indicate the spillover effects from one variable to all other variables. Similarly, the "FROM" values in the last column, which represent directional spillover (from), show the spillover effects from other variables to one variable. Finally, the total spillover, which is the sum of all pairwise spillovers, or the sum of all "TO" values, or the sum of all "FROM" values, is presented in the bottom right corner of each table.

Tables 4.7, 4.8, 4.9, and 4.10 display the spillover effects of return, volatility, skewness, and kurtosis, based on the Diebold and Yilmaz method and the Barunik and Krehlik methods. Let us begin by examining the total spillover effects according to the Diebold and Yilmaz method. As Figure 4.1 shows, the total volatility spillover has the highest value (60.617%), followed by the total return spillover (49.921%), total skewness spillover (36.636%), and total kurtosis spillover (29.496%). The term "volatility spillover" refers to the spread of instability from one market to another, which occurs when a volatile price change in one market has a delayed effect on the volatile price in another market, beyond the local market's impact. Such patterns are typical in financial markets and are more sensitive to political, economic, and other global events than return spillovers. Many previous studies have found that the total volatility spillover is generally greater than the total return spillover (Toyoshima and Hamori, 2018; Yilmaz, 2010; Zhang et al., 2020). Dornbusch et al. (2000) and Calvo and Reinhart (1996) introduced the concept of "fundamentals-based contagion," which refers to the spillover effects that arise from normal interdependence between market economies and are transmitted between countries' financial markets through crisis events. Another type of contagion is caused by irrational events, such as financial panic, herd behavior, loss of confidence, and heightened risk aversion, and is influenced by investors' decisions and actions. Such irrational phenomena usually have a direct impact on investor behavior. The reason why the total volatility spillover is larger than the total return spillover, total skewness spillover, and total kurtosis spillover is that volatility spillover is a "fundamentals-based contagion" between financial markets and through investor behavior, whereas return spillover, skewness spillover, and kurtosis spillover are transmitted through the actions of investors (He and Hamori, 2021; Wen et al., 2013).

In addition, considering the results obtained from the Barunik and Krehlik methods, we can see that the total return spillover (first moment) and the total skewness spillover (third moment) are the highest in the short term (35.398%, 20.152%), followed by the medium term (9.814%, 9.864%) and the long term (4.709%, 6.619%). On the other hand, the total volatility spillover (third moment) and the total kurtosis spillover (fourth moment) are the highest in the long term (58.442%, 14.172%), followed by the medium term (1.740%, 8.364%) and the short term (0.435%, 6.960%). When financial markets are processing information quickly and calmly, it is referred to as a "high-frequency connectivity" moment, and this has the most short-term effects on an asset (Baruník and Křehlík, 2018). The total return and skewness spillover effects occur precisely during the period of high-frequency connectivity, depend on past information, and follow a time-varying process (Hou and Li, 2020). Therefore, the total return and skewness spillover effects mostly occur in the short term. On the other hand, the total volatility spillover and kurtosis spillover are generated from lower frequencies, where the shock lasts longer. Thus, the total volatility and kurtosis spillover effects mostly occur in the long term.

Table 4.7 shows that IDEMVT transmits the most spillover to the return of green bonds (0.079%) and the least spillover to the return of wind (0.030%) in the time domain. In the frequency domain, IDEMVT transmits the smallest spillover to the return of wind in the short (0.029%), medium (0%), and long (0%) term, compared to the return of the other four stock indices. Notably, IDEMVT delivers zero spillover to the return of wind in the medium and long term. Therefore, it appears that the COVID-19 pandemic has not had a significant and lasting impact on the clean wind energy market. IDEMVT acquires the most spillover from the return of clean energy (2.365%) and the least spillover from the return of green bonds (0.250%). Among the five stock markets, Green Bond acquires the highest return spillover from Sustainability (13.556%), Clean Energy acquires the most return spillover from Solar (25.543%), Wind accepts the most return spillover from clean energy (22.405%), Solar accepts the most return spillover from clean energy (30.069%), and Sustainability accepts the most return spillover from wind (23.026%). These findings suggest that there is a strong mutual contagious relationship between the returns of the clean and solar energy markets.

According to Table 4.8, IDEMVT transmits the most volatility spillover to the clean energy market (11.962%) and the least to green bonds (2.634%) in the time domain. Additionally, IDEMVT receives the most volatility spillover from clean energy (16.434%) and the least from green bonds (0.559%). These findings suggest that the COVID-19 pandemic has had a greater impact on the volatility of the clean energy market compared to the other four equity markets. Moreover, among the five stock markets, Green Bond acquires the most volatility spillover from Sustainability (22.405%), Clean Energy acquires the most from Sustainability (18.361%), Wind acquires the most from Sustainability (26.185%), Solar acquires the most from clean energy (28.224%), and Sustainability acquires the most from clean energy (19.331%). These results indicate that the volatility of the clean energy market and sustainability index market is susceptible to affect other green financial markets, which is consistent with Zhang, He, et al.'s (2022) findings.

Table 4.9 indicates that IDEMVT delivers the highest skewness spillover to Green

Bond (2.874%) and the lowest skewness spillover to Sustainability (0.034%) in the time domain. Moreover, the skewness spillover from IDEMVT to sustainability is smallest in the short (0.018%) and medium (0.002%) term. These results show that the IDEMVT does not have a long-lasting excessive skewness spillover effect on the sustainability index market. The skewness spillover from IDEMVT to Green Bond increases gradually from the short (0.020%), medium (0.173%), and long (2.681%) term, indicating that the skewness spillover impact of the COVID-19 epidemic on the green bond market shows a persistent trend. Furthermore, IDEMVT receives the highest skewness spillover from Solar (0.212%) and the lowest skewness spillover from Sustainability (0.038%). Regarding the transmission of skewness spillover between sustainability-related stock markets, we can see that Green Bond receives the most skewness spillover from Wind (8.478%), Clean Energy receives the most skewness spillover from Solar (26.886%), Wind receives the most skewness spillover from clean energy (21.721%), Solar receives the most skewness spillover from Clean Energy (30.237%), and Sustainability receives the most skewness spillover from Wind (17.825%). These results indicate that the strongest skewed linkage is found between the clean energy and solar energy markets among sustainability-related financial indices.

According to Table 4.10, IDEMVT transmits the most kurtosis spillover (8.365%) to Green Bond and the least kurtosis spillover (0.016%) to sustainability in the time domain, which is similar to the results of skewness spillover. The kurtosis spillover transmitted by IDEMVT to other sustainability-related financial indices is no more than 1%. However, the kurtosis spillover passed by IDEMVT directly to Green Bond exceeds 8%. These results indicate that the COVID-19 pandemic has had a greater impact on the kurtosis spillover of the green bond market compared to other sustainability-related financial indices. In the frequency domain, we find a similar result to the skewness spillover case, in which the kurtosis spillover from IDEMVT to Sustainability is minimal, whether in the short (0.004%), medium (0.006%), or long (0.006%) term. The kurtosis spillover of Green Bond also increases gradually from the short (0.108%), medium (0.140%), and long (8.117%) term. This finding implies that the COVID-19 pandemic has a small higher-order moment spillover effect on the sustainability-related index market, while it has a significant and lasting higher moment spillover effect on the green bond market. Furthermore, when IDEMVT acts as a spillover recipient, it receives the most kurtosis spillover from Green Bond (8.146%) and the least kurtosis spillover from Sustainability (0.024%). This finding shows that the impact of the COVID-19 pandemic on the green bond market is bidirectional rather than unidirectional. Regarding the transmission of kurtosis spillover between sustainability-related stock markets, we can see that Green Bond receives the most kurtosis spillover from Sustainability (1.284%), Clean Energy receives the most kurtosis spillover from Solar (29.423%), Wind receives the most kurtosis spillover from Clean Energy (16.556%), Solar receives the most kurtosis spillover from Clean Energy (28.095%), and Sustainability receives the most kurtosis spillover from Wind (17.239%).

Table 4.7. Return spillover table.

Return spillover table of Diebold and Yilmaz (2012)

	Green Bond	Clean Energy	Wind	Solar	Sustainability	IDEMVT	FROM
Green Bond	61.032	7.544	13.852	3.937	13.556	0.079	6.495
Clean Energy	3.453	34.000	20.822	25.543	16.126	0.056	11.000
Wind	7.527	22.405	35.159	13.542	21.337	0.030	10.807
Solar	2.023	30.069	14.334	40.722	12.788	0.064	9.880
Sustainability	7.935	18.535	23.026	12.499	37.962	0.043	10.340
IDEMVT	0.250	2.365	2.220	1.006	2.562	91.597	1.400
TO	3.531	13.486	12.376	9.421	11.062	0.045	49.921

Return spillover table of Baruník and Křehlík (2018)

Frequency short-term: 1-5 days

	Green Bond	Clean Energy	Wind	Solar	Sustainability	IDEMVT	FROM
Green Bond	47.769	4.387	9.551	2.044	9.218	0.038	4.206
Clean Energy	2.649	25.492	15.865	18.481	12.473	0.047	8.253
Wind	5.790	15.752	26.592	8.801	15.859	0.029	7.705
Solar	1.426	22.488	10.711	30.184	9.853	0.050	7.421
Sustainability	6.204	13.708	17.881	8.798	29.740	0.034	7.771
IDEMVT	0.010	0.072	0.057	0.038	0.070	11.963	0.041
TO	2.680	9.401	9.011	6.360	7.912	0.033	35.398

Frequency medium-term: 6-21 days

	Green Bond	Clean Energy	Wind	Solar	Sustainability	IDEMVT	FROM
Green Bond	9.697	2.236	3.087	1.333	3.125	0.006	1.631
Clean Energy	0.600	6.277	3.681	5.175	2.739	0.001	2.033
Wind	1.283	4.862	6.307	3.431	4.050	0.000	2.271
Solar	0.441	5.589	2.682	7.723	2.203	0.003	1.820
Sustainability	1.289	3.566	3.827	2.711	6.114	0.006	1.900
IDEMVT	0.028	0.269	0.254	0.113	0.295	9.892	0.160
TO	0.607	2.754	2.255	2.127	2.069	0.003	9.814

Frequency long-term: 22-infinity days

	Green Bond	Clean Energy	Wind	Solar	Sustainability	IDEMVT	FROM
Green Bond	3.566	0.920	1.214	0.561	1.214	0.035	0.657
Clean Energy	0.204	2.231	1.276	1.888	0.914	0.008	0.715
Wind	0.454	1.791	2.260	1.310	1.428	0.000	0.831
Solar	0.156	1.992	0.940	2.815	0.732	0.012	0.639
Sustainability	0.441	1.261	1.318	0.990	2.108	0.003	0.669
IDEMVT	0.212	2.023	1.909	0.855	2.197	69.743	1.199
TO	0.245	1.331	1.109	0.934	1.081	0.010	4.709

Notes: Green Bond represents the return of the S&P Green Bond Index, Clean Energy represents the return of the S&P Global Clean Energy Index, Wind represents the return of the ISE Global Wind Energy Index, Solar represents the return of the MAC Global Solar Energy Index, Sustainability represents the return of the Dow Jones Sustainability World Index, and IDEMVT represents the Infectious Disease Equity Market Volatility Tracker.

Table 4.8. Volatility spillover table.

Volatility spillover table of Diebold and Yilmaz (2012)							
	Green Bond	Clean Energy	Wind	Solar	Sustainability	IDEMVT	FROM
Green Bond	40.571	16.858	12.095	5.437	22.405	2.634	9.905
Clean Energy	4.282	32.752	14.167	18.477	18.361	11.962	11.208
Wind	7.556	22.982	23.073	12.687	26.185	7.517	12.821
Solar	4.145	28.224	11.401	33.018	15.949	7.263	11.164
Sustainability	8.734	19.331	16.562	9.400	40.930	5.042	9.845
IDEMVT	0.559	16.434	3.387	9.103	4.565	65.952	5.675
TO	4.213	17.305	9.602	9.184	14.578	5.736	60.617
Volatility spillover table of Baruník and Křehlík (2018)							
Frequency short-term: 1-5 days							
	Green Bond	Clean Energy	Wind	Solar	Sustainability	IDEMVT	FROM
Green Bond	0.096	0.007	0.009	0.003	0.002	0.014	0.006
Clean Energy	0.040	0.421	0.192	0.295	0.119	0.011	0.109
Wind	0.090	0.170	0.587	0.081	0.226	0.006	0.096
Solar	0.010	0.144	0.043	0.332	0.024	0.017	0.040
Sustainability	0.141	0.196	0.411	0.122	0.787	0.002	0.145
IDEMVT	0.033	0.036	0.080	0.010	0.078	10.715	0.040
TO	0.052	0.092	0.122	0.085	0.075	0.008	0.435
Frequency medium-term: 6-21 days							
	Green Bond	Clean Energy	Wind	Solar	Sustainability	IDEMVT	FROM
Green Bond	0.269	0.013	0.048	0.029	0.027	0.044	0.027
Clean Energy	0.217	1.455	0.802	1.088	0.617	0.083	0.468
Wind	0.338	0.618	1.827	0.348	0.883	0.046	0.372
Solar	0.082	0.528	0.238	1.163	0.175	0.054	0.180
Sustainability	0.506	0.766	1.554	0.531	2.726	0.021	0.563
IDEMVT	0.082	0.189	0.191	0.119	0.203	7.915	0.131
TO	0.204	0.352	0.472	0.353	0.318	0.041	1.740
Frequency long-term: 22-infinity days							
	Green Bond	Clean Energy	Wind	Solar	Sustainability	IDEMVT	FROM
Green Bond	40.205	16.838	12.038	5.405	22.376	2.576	9.872
Clean Energy	4.025	30.876	13.173	17.094	17.625	11.867	10.631
Wind	7.128	22.194	20.659	12.258	25.076	7.465	12.354
Solar	4.052	27.552	11.120	31.524	15.750	7.192	10.944
Sustainability	8.087	18.369	14.597	8.747	37.418	5.019	9.137
IDEMVT	0.444	16.208	3.116	8.973	4.285	47.322	5.505
TO	3.956	16.860	9.007	8.746	14.185	5.687	58.442

Notes: Green Bond represents the volatility of the S&P Green Bond Index; Clean Energy represents the volatility of the S&P Global Clean Energy Index; Wind represents the volatility of the ISE Global Wind Energy Index; Solar represents the volatility of the MAC Global Solar Energy Index; Sustainability represents the volatility of the Dow Jones Sustainability World Index; and IDEMVT represents the Infectious Disease Equity Market Volatility Tracker.

Table 4.9. Skewness spillover table.

Skewness spillover table of Diebold and Yilmaz (2012)

	Green Bond	Clean Energy	Wind	Solar	Sustainability	IDEMVT	FROM
Green Bond	73.393	4.174	8.478	6.541	4.540	2.874	4.434
Clean Energy	1.459	45.997	17.516	26.886	7.948	0.195	9.001
Wind	4.123	21.721	47.344	14.074	12.476	0.263	8.776
Solar	1.086	30.237	9.913	53.699	4.945	0.119	7.717
Sustainability	3.902	11.432	17.825	6.455	60.353	0.034	6.608
IDEMVT	0.166	0.105	0.079	0.212	0.038	99.400	0.100
TO	1.789	11.278	8.968	9.028	4.991	0.581	36.636

Skewness spillover table of Baruník and Křehlík (2018)

Frequency short-term: 1-5 days

	Green Bond	Clean Energy	Wind	Solar	Sustainability	IDEMVT	FROM
Green Bond	15.209	0.536	1.440	0.322	1.045	0.020	0.560
Clean Energy	1.082	34.658	12.993	19.239	6.098	0.116	6.588
Wind	1.363	6.389	15.748	3.052	4.561	0.078	2.574
Solar	0.631	21.194	6.482	36.506	3.488	0.101	5.316
Sustainability	2.988	8.856	13.877	4.819	45.661	0.018	5.093
IDEMVT	0.019	0.041	0.030	0.025	0.012	12.730	0.021
TO	1.014	6.169	5.803	4.576	2.534	0.056	20.152

Frequency medium-term: 6-21 days

	Green Bond	Clean Energy	Wind	Solar	Sustainability	IDEMVT	FROM
Green Bond	29.408	1.511	3.025	2.530	1.642	0.173	1.480
Clean Energy	0.252	8.154	3.165	5.383	1.353	0.025	1.696
Wind	1.547	8.840	18.334	6.081	4.706	0.097	3.545
Solar	0.348	6.380	2.310	12.067	1.047	0.009	1.682
Sustainability	0.864	2.433	3.745	1.547	11.851	0.002	1.432
IDEMVT	0.042	0.037	0.029	0.052	0.009	10.429	0.028
TO	0.509	3.200	2.046	2.599	1.459	0.051	9.864

Frequency long-term: 22-infinity days

	Green Bond	Clean Energy	Wind	Solar	Sustainability	IDEMVT	FROM
Green Bond	28.777	2.127	4.013	3.689	1.853	2.681	2.394
Clean Energy	0.125	3.185	1.357	2.263	0.497	0.054	0.716
Wind	1.213	6.492	13.262	4.940	3.209	0.088	2.657
Solar	0.107	2.664	1.122	5.126	0.410	0.009	0.719
Sustainability	0.050	0.142	0.203	0.090	2.841	0.015	0.083
IDEMVT	0.105	0.028	0.020	0.134	0.017	76.242	0.051
TO	0.267	1.909	1.119	1.853	0.998	0.474	6.619

Notes: Green Bond represents the skewness of the S&P Green Bond Index; Clean Energy represents the skewness of the S&P Global Clean Energy Index; Wind represents the skewness of the ISE Global Wind Energy Index; Solar represents the skewness of the MAC Global Solar Energy Index; Sustainability represents the skewness of the Dow Jones Sustainability World Index; and IDEMVT represents the infectious disease equity market volatility tracker.

Table 4.10. Kurtosis spillover table.

Kurtosis spillover table of Diebold and Yilmaz (2012)							
	Green Bond	Clean Energy	Wind	Solar	Sustainability	IDEMVT	FROM
Green Bond	88.168	0.510	0.719	0.954	1.284	8.365	1.972
Clean Energy	0.193	51.169	16.057	29.423	2.731	0.427	8.138
Wind	0.115	16.556	61.699	12.724	8.152	0.753	6.384
Solar	0.384	28.095	8.712	59.548	2.960	0.300	6.742
Sustainability	0.425	5.984	17.239	4.035	72.301	0.016	4.616
IDEMVT	8.146	0.626	0.227	0.837	0.024	90.139	1.644
TO	1.544	8.629	7.159	7.996	2.525	1.644	29.496

Kurtosis spillover table of Baruník and Křehlík (2018)							
Frequency short-term: 1-5 days							
	Green Bond	Clean Energy	Wind	Solar	Sustainability	IDEMVT	FROM
Green Bond	9.155	0.002	0.014	0.034	0.068	0.108	0.038
Clean Energy	0.015	24.681	5.934	11.672	1.387	0.113	3.187
Wind	0.025	3.172	11.103	1.253	1.969	0.082	1.084
Solar	0.026	6.900	1.337	13.431	0.537	0.024	1.470
Sustainability	0.221	1.438	4.337	0.835	26.721	0.004	1.139
IDEMVT	0.062	0.086	0.061	0.032	0.012	12.432	0.042
TO	0.058	1.933	1.947	2.304	0.662	0.055	6.960
Frequency medium-term: 6-21 days							
	Green Bond	Clean Energy	Wind	Solar	Sustainability	IDEMVT	FROM
Green Bond	16.876	0.016	0.024	0.062	0.173	0.140	0.069
Clean Energy	0.041	16.050	5.337	9.463	0.881	0.100	2.637
Wind	0.030	5.073	20.068	3.213	2.549	0.188	1.842
Solar	0.052	9.262	2.590	19.100	1.028	0.040	2.162
Sustainability	0.144	2.158	5.845	1.392	24.128	0.006	1.591
IDEMVT	0.246	0.058	0.014	0.053	0.004	9.631	0.063
TO	0.085	2.761	2.302	2.364	0.772	0.079	8.364
Frequency long-term: 22-infinity days							
	Green Bond	Clean Energy	Wind	Solar	Sustainability	IDEMVT	FROM
Green Bond	62.138	0.491	0.681	0.857	1.043	8.117	1.865
Clean Energy	0.137	10.439	4.786	8.287	0.462	0.214	2.315
Wind	0.060	8.311	30.528	8.258	3.635	0.483	3.458
Solar	0.306	11.933	4.786	27.017	1.395	0.236	3.109
Sustainability	0.060	2.388	7.057	1.809	21.452	0.006	1.887
IDEMVT	7.838	0.482	0.152	0.752	0.009	68.076	1.539
TO	1.400	3.934	2.910	3.327	1.091	1.509	14.172

Notes: Green Bond represents the kurtosis of the S&P Green Bond Index; Clean Energy represents the kurtosis of the S&P Global Clean Energy Index; Wind represents the kurtosis of the ISE Global Wind Energy Index; Solar represents the kurtosis of the MAC Global Solar Energy Index; Sustainability represents the kurtosis of the Dow Jones Sustainability World Index; and IDEMVT represents the Infectious Disease Equity Market Volatility Tracker.

To gain a better understanding of the static spillover structure, we use network topology visualization techniques for Tables 4.7-4.10, following the works of Bostanci and Yilmaz (2020), Bilgin and Yilmaz (2018), and Diebold and Yilmaz (2016).[24]. Figure 4.3 displays the color spectrum of the network topology utilized in our study, where we have chosen the three classic primary colors: red, yellow, and blue. The color gradation ranges from red to blue, gradually increasing with the value of the "TO" spillover in the spillover table. Red indicates the smallest value of "TO" spillover, while blue represents the largest value.

Figures 4.4, 4.5, 4.6, and 4.7 depict the network structures of return, volatility, skewness, and kurtosis spillovers, respectively. The color of the node corresponds to the color spectrum presented in Figure 4.3, indicating that the gradation from red to blue denotes the incremental "TO" spillover of the variable. The size of the node also represents the size of the "TO" spillover; the larger the node, the larger the "TO" spillover passed by the labeled variable. The size of the arrows indicates the level of pairwise spillovers between two variables, and the arrow direction represents the direction of the spillover transition. The numbers on the arrows denote the value of the pairwise spillover, and the thicker the arrow, the larger the value of the pairwise spillover. The color of the arrows corresponds to the color spectrum shown in Figure 4.3, with the red hue indicating a smaller pairwise spillover and the blue hue indicating a larger pairwise spillover.

Figures 4.4, 4.5, 4.6, and 4.7 present the results of two methods: the Diebold and Yilmaz method in the time domain, shown in the upper left panel (a), and the Barunik and Krehlik method in the frequency domain, shown in the other panels (b), (c), and (d), representing the short, medium, and long term, respectively. In the time domain, Clean energy has the largest TO spillover for both lower- and higher-order moments of spillover in the full sample, indicating that the clean energy market is a spillover transmitter. IDEMVT, on the other hand, is a spillover receiver in the full sample, as shown by its node color and size. In the short term, Clean energy, Wind, and Solar energy deliver more spillovers than Green bond and Sustainability. Wind is the largest volatility and kurtosis spillover transmitter, while Clean energy is the largest return and skewness spillover transmitter. However, IDEMVT remains a spillover receiver. In the medium term, Clean energy is the largest return spillover, skewness spillover, and kurtosis spillover transmitter, unlike in the short term. Wind is still the largest volatility spillover transmitter, while IDEMVT continues to be a spillover receiver. In the long term, Clean energy is the largest return spillover, volatility spillover, skewness spillover, and kurtosis spillover transmitter, which is consistent with the results in the time domain. However, IDEMVT is no longer a spillover receiver in the long term, in contrast to the previous results. The node color and size of IDEMVT indicate that IDEMVT also transmits a portion of volatility spillover, skewness spillover, and kurtosis spillover to other green financial markets. These results demonstrate that the impact of the COVID-19 pandemic on sustainable financial markets is not readily apparent in the short term but is a lagged and long-lasting effect.

---

24 We use the open-source Gephi software (https://gephi.org/) to visualize the spillover tables.

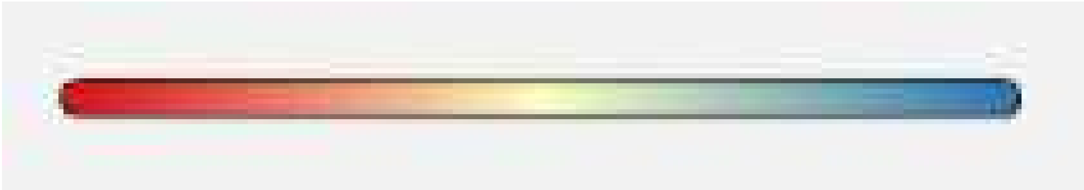

Figure 4.3. The color spectrum of the network topology.

Notes: The gradation from red to blue gradually increases according to the value of the “TO” spillover in the spillover table, which means that red represents the smallest value of "TO" spillover and blue represents the largest value.

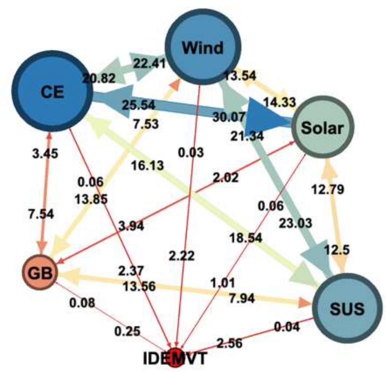

(a) The Diebold and Yilmaz method

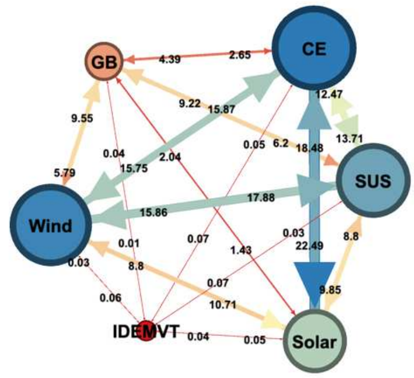

(b) The Barunik and Krehlik method: Frequency short-term: 1-5 days

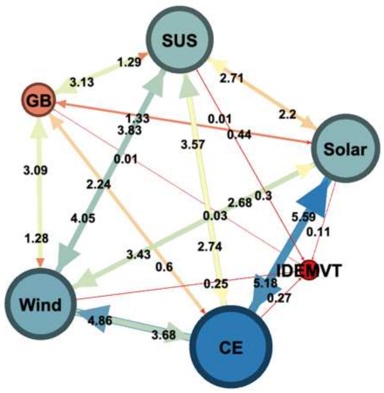

(c) The Barunik and Krehlik method: Frequency medium-term: 6-21 days

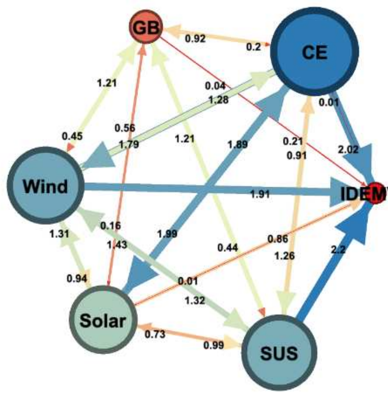

(d) The Barunik and Krehlik method: Frequency long-term: 22-infinity days

Figure 4.4. Network based on pairwise return spillover over the full sample.

Notes: Figure 4. 4 shows the network topology in Table 4.7. GB represents the return on the S&P Green Bond Index, CE represents the return on the S&P Global Clean Energy Index, Wind represents the return on the ISE Global Wind Energy Index, Solar represents the return on the MAC Global Solar Energy Index, SUS represents the return on the Dow Jones Sustainability World Index, and IDEMVT represents the Infectious Disease Equity Market Volatility Tracker. The size of each node represents the size of the "TO" spillover passed by the corresponding variable. The larger the node, the larger the "TO" spillover. The size of the arrows indicates the level of pairwise spillovers between two variables. The direction of the arrow indicates the spillover transition between the two variables. The thickness of the arrow corresponds to the value of the pairwise spillover; the larger the value, the thicker the arrow. The color of the arrow indicates the size of the pairwise spillover, with red indicating smaller spillovers and blue indicating larger spillovers.

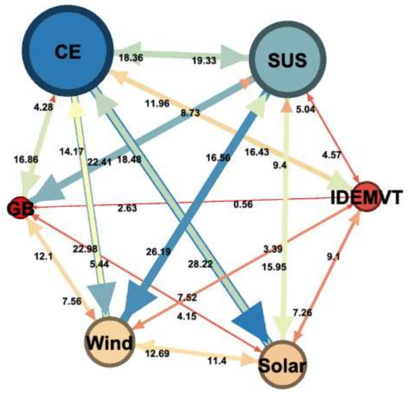

(a) The Diebold and Yilmaz method

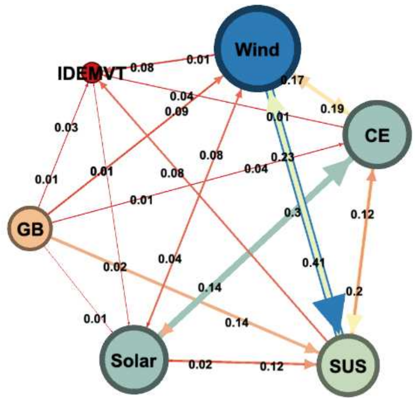

(b) The Barunik and Krehlik method:
Frequency short-term: 1-5 days

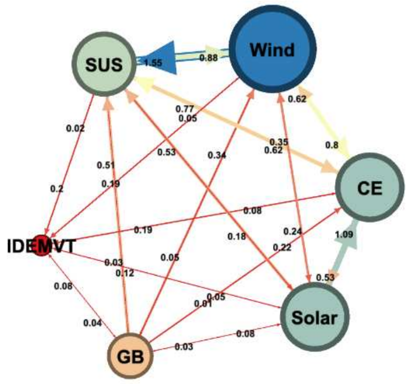

(c) The Barunik and Krehlik method:
Frequency medium-term: 6-21 days

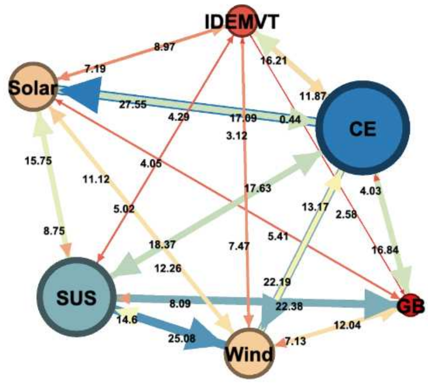

(d) The Barunik and Krehlik method:
Frequency long-term: 22-infinity days

Figure 4.5. Network based on pairwise volatility spillover over the full sample.

Notes: Figure 4.5 shows the network topology in Table 4.8. GB represents the volatility of the S&P Green Bond Index; CE represents the volatility of the S&P Global Clean Energy Index; Wind represents the volatility of the ISE Global Wind Energy Index; Solar represents the volatility of the MAC Global Solar Energy Index; SUS represents the volatility of the Dow Jones Sustainability World Index; and IDEMVT represents the infectious disease equity market volatility tracker. The size of each node represents the size of the "TO" spillover passed by the corresponding variable. The larger the node, the larger the "TO" spillover. The size of the arrows indicates the level of pairwise spillovers between two variables. The direction of the arrow indicates the spillover transition between the two variables. The thickness of the arrow corresponds to the value of the pairwise spillover; the larger the value, the thicker the arrow. The color of the arrow indicates the size of the pairwise spillover, with red indicating smaller spillovers and blue indicating larger spillovers.

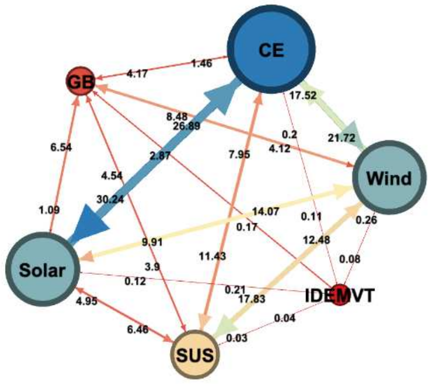

(a) The Diebold and Yilmaz method

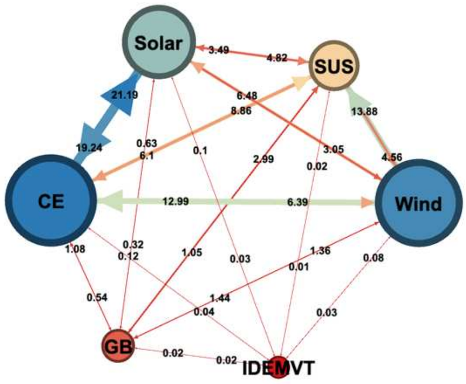

(b) The Barunik and Krehlik method: Frequency short-term: 1-5 days

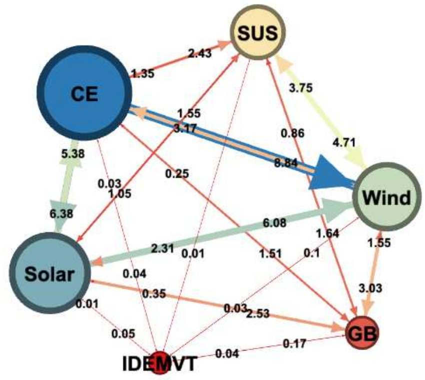

(c) The Barunik and Krehlik method: Frequency medium-term: 6-21 days

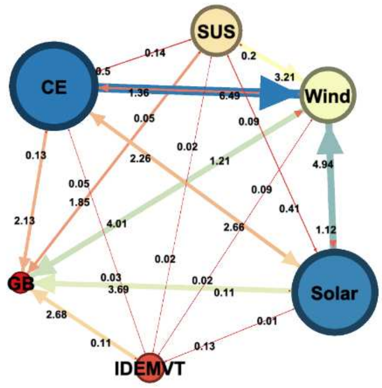

(d) The Barunik and Krehlik method: Frequency long-term: 22-infinity days

Figure 4.6. Network based on pairwise skewness spillover over the full sample.

Notes: Figure 4.6 shows the network topology in Table 4.9. GB represents the skewness of the S&P Green Bond Index; CE represents the skewness of the S&P Global Clean Energy Index; Wind represents the skewness of the ISE Global Wind Energy Index; Solar represents the skewness of the MAC Global Solar Energy Index; SUS represents the skewness of the Dow Jones Sustainability World Index; and IDEMVT represents the infectious disease equity market volatility tracker. The size of each node represents the size of the "TO" spillover passed by the corresponding variable. The larger the node, the larger the "TO" spillover. The size of the arrows indicates the level of pairwise spillovers between two variables. The direction of the arrow indicates the spillover transition between the two variables. The thickness of the arrow corresponds to the value of the pairwise spillover; the larger the value, the thicker the arrow. The color of the arrow indicates the size of the pairwise spillover, with red indicating smaller spillovers and blue indicating larger spillovers.

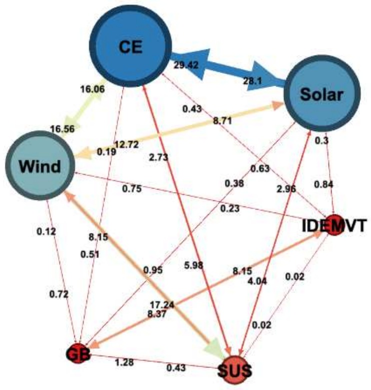

(a) The Diebold and Yilmaz method

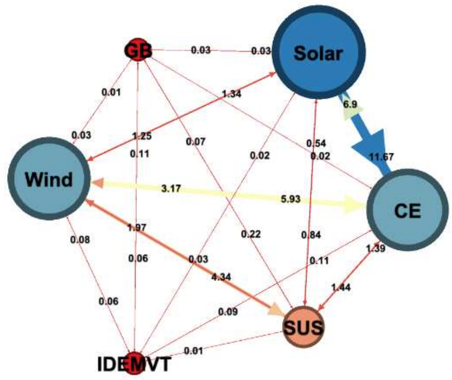

(b) The Barunik and Krehlik method: Frequency short-term: 1-5 days

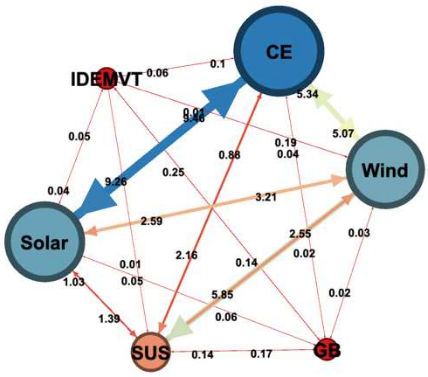

(c) The Barunik and Krehlik method: Frequency medium-term: 6-21 days

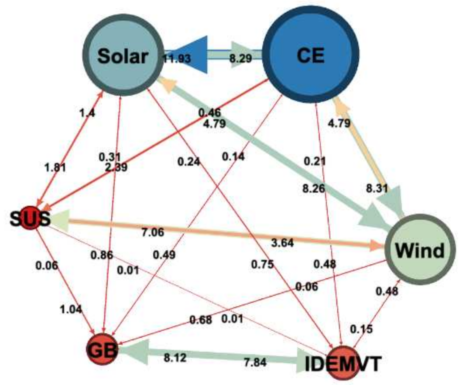

(d) The Barunik and Krehlik method: Frequency long-term: 22-infinity days

Figure 4.7. Network based on pairwise kurtosis spillover over the full sample.

Notes: Figure 4.7 shows the network topology in Table 4.10. GB represents the kurtosis of the S&P Green Bond Index, CE represents the kurtosis of the S&P Global Clean Energy Index, Wind represents the kurtosis of the ISE Global Wind Energy Index, Solar represents the kurtosis of the MAC Global Solar Energy Index, SUS represents the kurtosis of the Dow Jones Sustainability World Index, and IDEMVT represents the Market Volatility Tracker. The size of each node represents the size of the "TO" spillover passed by the corresponding variable. The larger the node, the larger the "TO" spillover. The size of the arrows indicates the level of pairwise spillovers between two variables. The direction of the arrow indicates the spillover transition between the two variables. The thickness of the arrow corresponds to the value of the pairwise spillover; the larger the value, the thicker the arrow. The color of the arrow indicates the size of the pairwise spillover, with red indicating smaller spillovers and blue indicating larger spillovers.

4.5.2. Dynamic spillover effects analysis

Although we have obtained static spillover results for lower- and higher-order moments, it is not possible to observe the time-varying effects of global political and economic crisis events on the spillover effect using static spillover results. To explore the dynamic spillover effect, we utilize the rolling window method based on the spillover results of the Diebold and Yilmaz as well as the Barunik and Krehlik methods. Similar to the calculation of the static spillover effect, we adopt 100 days ahead as the forecasting horizon. To ensure the stationarity of the VAR calculation, we follow Zhang et al. (2020) and choose a window size of 500 trading days.[25]

Figures 4.8, 4.9, 4.10, and 4.11 display the dynamic total return, volatility, skewness, and kurtosis spillover of the Diebold and Yilmaz as well as the Barunik and Krehlik methods, respectively. The dynamic spillover results of the Diebold and Yilmaz method are represented by the pink line, while the green, yellow, and blue lines show the dynamic total spillover results of the "Frequency short-term," "Frequency medium-term," and "Frequency long-term" in the Barunik and Krehlik method, respectively.

After analyzing Figures 4.8-4.11, we have found some interesting conclusions. Compared to the dynamic total return spillover (first moment) and the total skewness spillover (third moment), the total volatility spillover (second moment) and the total kurtosis spillover (fourth moment) exhibit more violent fluctuations over time. These fluctuations are caused by international political and economic events. Therefore, we have identified some crisis events that have caused large fluctuations in the graphs. We observe that while the dynamic total return spillover, dynamic total volatility spillover, dynamic total skewness spillover, and dynamic total kurtosis spillover are affected by events and fluctuate to varying degrees, the COVID-19 epidemic has had a much greater impact than other crisis events. This finding suggests that the economic influence of the COVID-19 pandemic on sustainability-related financial markets is substantial and unprecedented. The outbreak of the Russia-Ukraine war did not create a huge impact on the spillover effects of the lower-order and higher-order moments of green finance.

The spillover effects of the dynamic total return from Figure 4.8 and the dynamic total skewness from Figure 4.10 exhibit a relatively stable trend before the COVID-19 pandemic outbreak. Mild fluctuations occurred in the dynamic total return spillover in mid-2013 and mid-2018 due to the European debt crisis and the US-China trade war, respectively. Meanwhile, the dynamic total skewness spillover also experienced slight fluctuations in mid-2013 due to the European debt crisis. However, the impact of these events on the spillover effects of return and skewness is far less compared to that of the COVID-19 pandemic. In early 2020, the dynamic total return spillover and the dynamic total skewness spillover soared by more than 80% due to the pandemic outbreak. The dynamic total return spillover remained persistent above 60% after the pandemic outbreak until early 2022, while the dynamic total skewness spillover rapidly returned to approximately 40% before the outbreak. These results suggest that the effect of the COVID-19 pandemic on the dynamic total return spillover is persistent, while the effect

25 The results of dynamic total return, volatility, skewness, and kurtosis spillover in time domain of different window size are reported in Appendix.

on the dynamic total skewness spillover is transient. However, the outbreak of the Russia-Ukraine war around February 2022 caused only a negligible fluctuation in the total return spillover and the total skewness spillover. This fluctuation is insignificant compared to the impact of the COVID-19 outbreak on the spillover effects of the green finance market.

The dynamic total volatility spillover and dynamic total kurtosis spillover are more sensitive to international political and financial crisis events compared to the dynamic total return spillover and dynamic total skewness spillover, resulting in more significant fluctuations. Before the COVID-19 pandemic, the dynamic total volatility spillover exhibited varying degrees of fluctuation due to the European debt crisis in 2013, outbreaks of Ebola and Middle East respiratory syndrome in 2016, the US-China trade war in 2018, and the decline of the three major US stock markets in early 2019. Additionally, the dynamic kurtosis spillover was influenced not only by the European debt crisis, outbreaks of Ebola and Middle East respiratory syndrome, and decline in the three major U.S. stock markets in early 2019, but also by the turbulence in the Chinese stock market around 2015 and the framework agreement on Brexit reached by the UK and EU around 2017.

The impact of the COVID-19 pandemic on the dynamic total volatility spillover and dynamic total kurtosis spillover is enormous, much like the dynamic total return spillover and dynamic total skewness spillover. Following the outbreak of the pandemic, both the dynamic total volatility spillover and dynamic total kurtosis spillover surged by more than 80% in early 2020. The dynamic total volatility spillover shows a decreasing trend over time after being significantly impacted by the COVID-19 pandemic. However, the dynamic total kurtosis spillover experienced a surge of 80% following the outbreak of the pandemic, and then dropped sharply to approximately 50%. Due to the impact of the surge in infections caused by the coronavirus mutant strain, there was a sharp fluctuation in the dynamic total kurtosis spillover to 80% in mid-2021. The Russia-Ukraine war that broke out in February 2022 does not have a significant impact on the total volatility spillover and the total kurtosis spillover, similar to the total return spillover and the total skewness spillover. This finding suggests that although the outbreak of the Russia-Ukraine war did not significantly affect the green finance market, the dynamic total return, volatility, skewness, and kurtosis spillover have an overall downward trend of fluctuation after 2021. This result shows that although the emergence of COVID-19 led to a global economic crisis and a severe decline in stock markets, some effective policies were enacted in response to the outbreak, leading to a gradual recovery in financial markets over time (Chowdhury et al., 2022; Szczygielski et al., 2021).

From the frequency domain perspective, the dynamic total return spillover (first moment) and total skewness spillover (third moment) mainly occur in the short term, while the total volatility spillover (second moment) is primarily concentrated in the long term. Before the COVID-19 pandemic, the dynamic total kurtosis spillover effect was not mainly focused on the short, medium, or long term. However, after the COVID-19 outbreak, it is apparent that the dynamic total kurtosis spillover effect occurs in the long term. This indicates that the COVID-19 pandemic directly changes the speed of contagion of the dynamic total kurtosis spillover effect in the sustainability-related financial market, and the impact of a crisis event on the dynamic total kurtosis spillover will take at least one month to manifest.

To analyze the impact of the COVID-19 pandemic on each sustainability-related financial index separately, we visualize the dynamic pairwise return, volatility, skewness, and kurtosis spillover between IDEMVT and each sustainability-related financial index in Figures 4.12, 4.13, 4.14, and 4.15. These four plots show that the spillover effect transmitted by IDEMVT to each sustainability financial index is almost 0% before the COVID-19 pandemic. However, after the outbreak of the pandemic, the return and volatility spillover effect from IDEMVT on each sustainability financial index is over 60%, and the skewness and kurtosis spillover is over 75% and 80%, respectively. We observe that the dynamic pairwise return spillover between IDEMVT and sustainability-related financial indices explodes over 2 to 3 months after the outbreak of the COVID-19 pandemic, after which it quickly returns to the previous normal state. On the other hand, the dynamic pairwise volatility spillover between IDEMVT and sustainability-related financial indices remains at a high level due to the COVID-19 pandemic. This indicates that the impact of the COVID-19 outbreak on the volatility spillover effects of sustainability-related financial index markets is profound and persistent. Except for Green Bond, the dynamic skewness and kurtosis spillover from IDEMVT are transmitted to the other four sustainability-related financial indices in early 2020 because of the COVID-19 outbreak. However, the dynamic total skewness and kurtosis spillover delivered to Green Bond by IDEMVT not only fluctuates violently due to COVID-19, but also shows persistent fluctuations. This indicates that the skewness and kurtosis spillover effect of COVID-19 on the green bond market transmission is not transient but far-reaching and long-lasting.

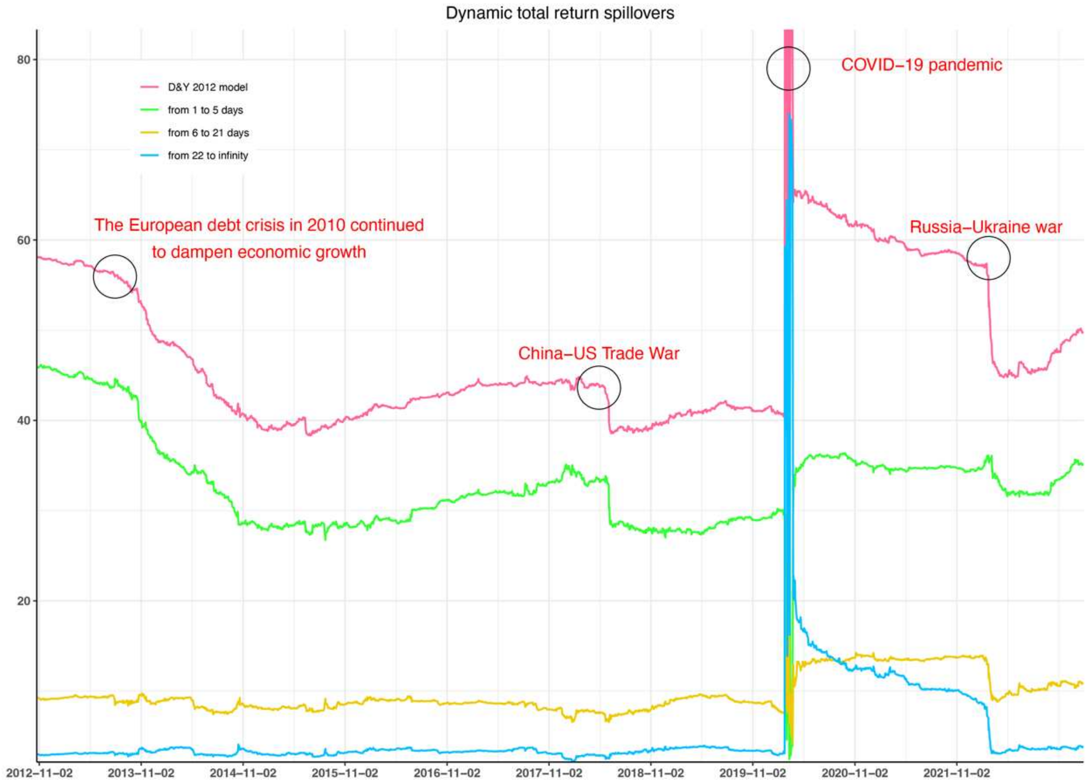

Figure 4.8. Dynamic total return spillover (window size=500 days).

Notes: The units of the values on the vertical coordinate are percentages; the pink line exhibits the dynamic total spillover results of the Diebold and Yilmaz method; the green line exhibits the dynamic total spillover results of "Frequency short-term" in the Barunik and Krehlik method; the yellow line exhibits the dynamic total spillover results of "Frequency medium-term" in the Barunik and Krehlik method; the blue line exhibits the dynamic total spillover results of "Frequency long-term" in the Barunik and Krehlik method.

Figure 4.9. Dynamic total volatility spillover (window size=500 days).

Notes: The units of the values on the vertical coordinate are percentages; the pink line exhibits the dynamic total spillover results of the Diebold and Yilmaz method; the green line exhibits the dynamic total spillover results of "Frequency short-term" in the Barunik and Krehlik method; the yellow line exhibits the dynamic total spillover results of "Frequency medium-term" in the Barunik and Krehlik method; the blue line exhibits the dynamic total spillover results of "Frequency long-term" in the Barunik and Krehlik method.

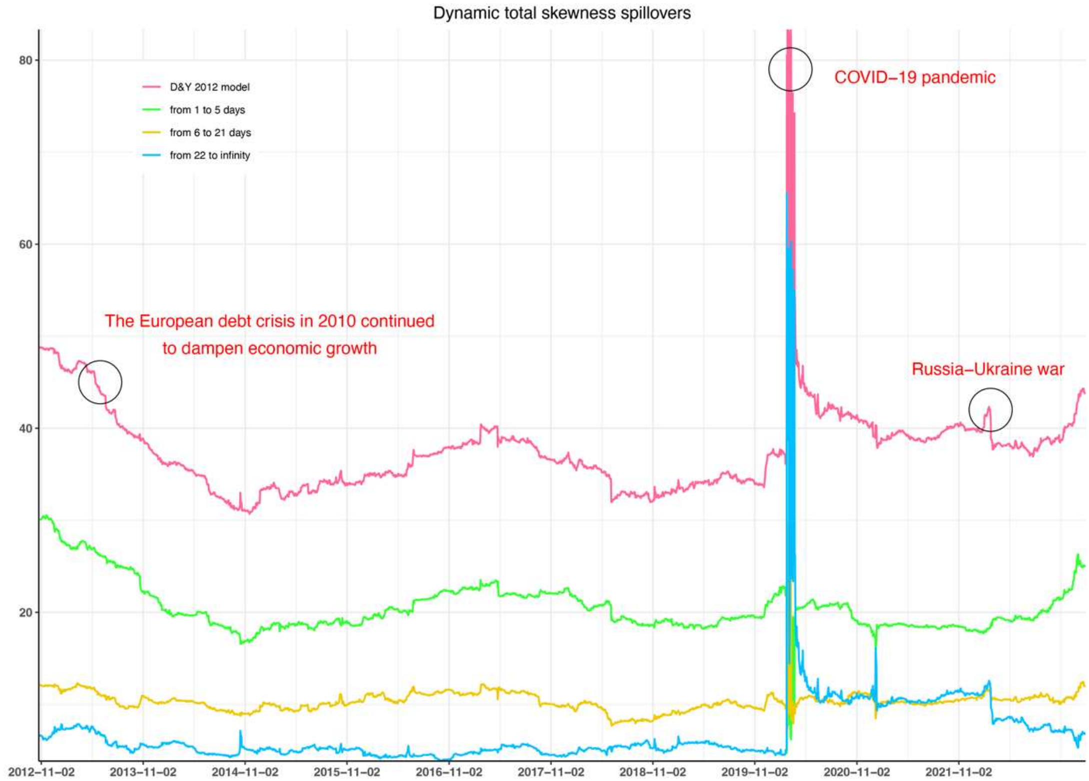

Figure 4.10. Dynamic total skewness spillover (window size=500 days).

Notes: The units of the values on the vertical coordinate are percentages; the pink line exhibits the dynamic total spillover results of the Diebold and Yilmaz method; the green line exhibits the dynamic total spillover results of "Frequency short-term" in the Barunik and Krehlik method; the yellow line exhibits the dynamic total spillover results of "Frequency medium-term" in the Barunik and Krehlik method; the blue line exhibits the dynamic total spillover results of "Frequency long-term" in the Barunik and Krehlik method.

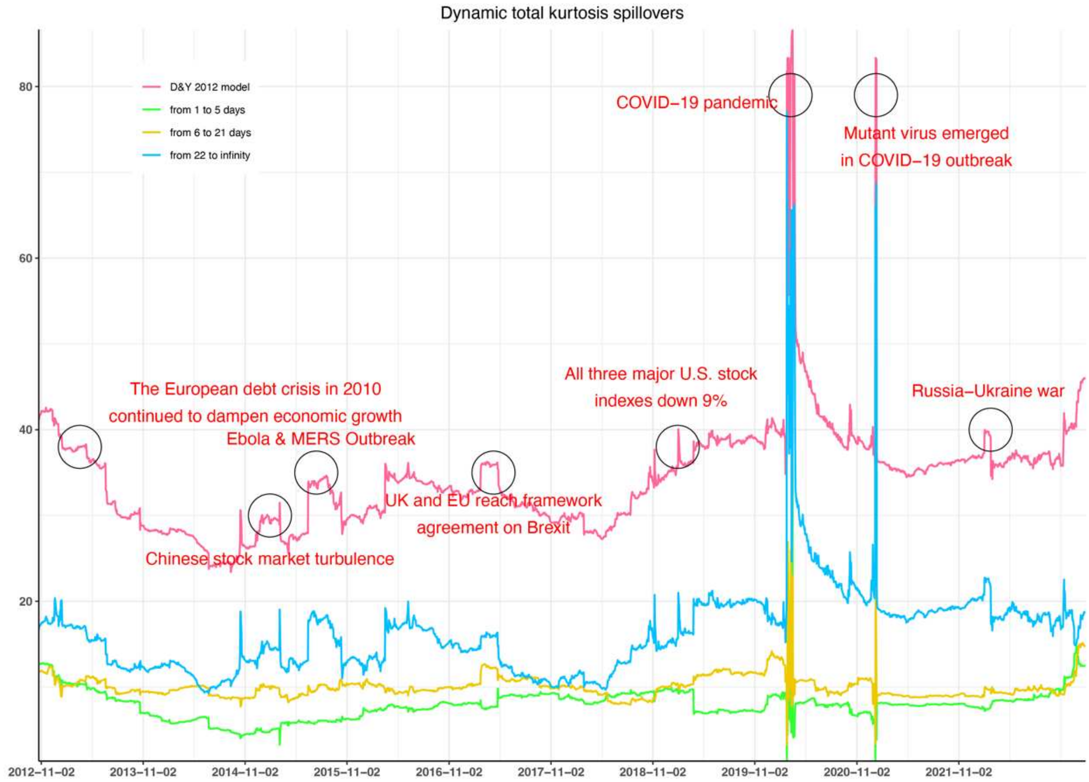

Figure 4.11. Dynamic total kurtosis spillover (window size=500 days).

Notes: The units of the values on the vertical coordinate are percentages; the pink line exhibits the dynamic total spillover results of the Diebold and Yilmaz method; the green line exhibits the dynamic total spillover results of "Frequency short-term" in the Barunik and Krehlik method; the yellow line exhibits the dynamic total spillover results of "Frequency medium-term" in the Barunik and Krehlik method; the blue line exhibits the dynamic total spillover results of "Frequency long-term" in the Barunik and Krehlik method.

Figure 4.12. Dynamic pairwise return spillover (window size=500 days).

Notes: The units of the values on the vertical coordinate are percentages; the pink line exhibits the dynamic total spillover results of the Diebold and Yilmaz method; the green line exhibits the dynamic total spillover results of "Frequency short-term" in the Barunik and Krehlik method; the yellow line exhibits the dynamic total spillover results of "Frequency medium-term" in the Barunik and Krehlik method; the blue line exhibits the dynamic total spillover results of "Frequency long-term" in the Barunik and Krehlik method.

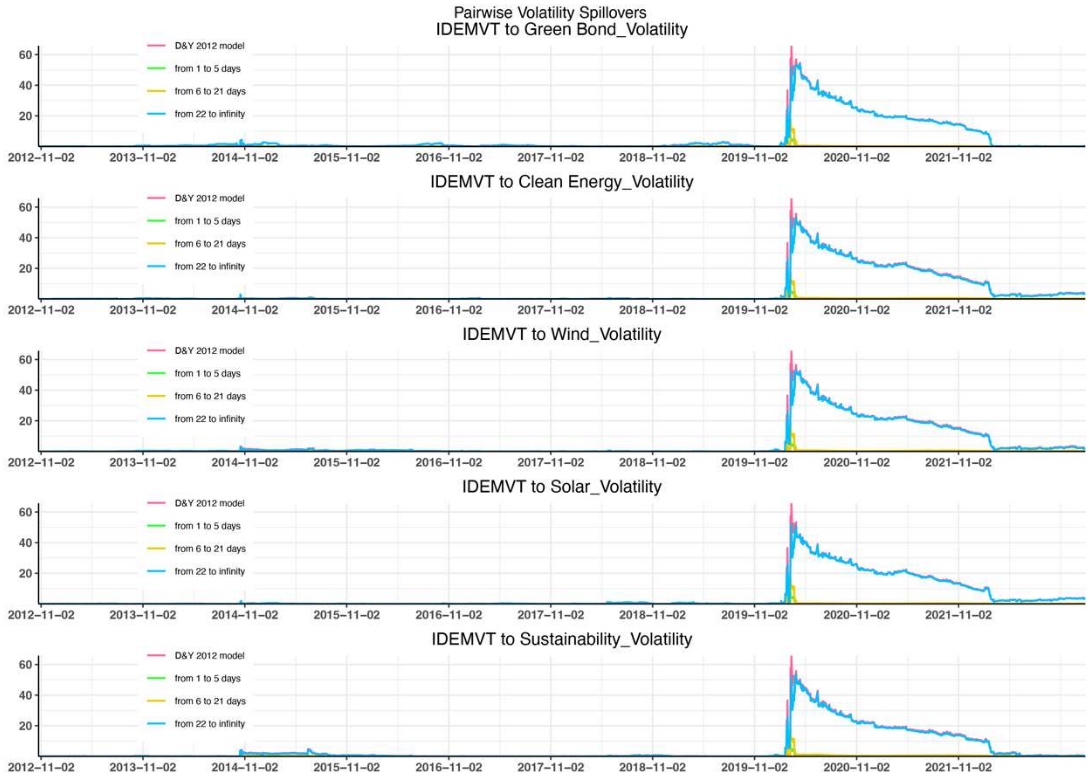

Figure 4.13. Dynamic pairwise volatility spillover (window size=500 days).

Notes: The units of the values on the vertical coordinate are percentages; the pink line exhibits the dynamic total spillover results of the Diebold and Yilmaz method; the green line exhibits the dynamic total spillover results of "Frequency short-term" in the Barunik and Krehlik method; the yellow line exhibits the dynamic total spillover results of "Frequency medium-term" in the Barunik and Krehlik method; the blue line exhibits the dynamic total spillover results of "Frequency long-term" in the Barunik and Krehlik method.

Figure 4.14. Dynamic pairwise skewness spillover (window size=500 days).

Notes: The units of the values on the vertical coordinate are percentages; the pink line exhibits the dynamic total spillover results of the Diebold and Yilmaz method; the green line exhibits the dynamic total spillover results of "Frequency short-term" in the Barunik and Krehlik method; the yellow line exhibits the dynamic total spillover results of "Frequency medium-term" in the Barunik and Krehlik method; the blue line exhibits the dynamic total spillover results of "Frequency long-term" in the Barunik and Krehlik method.

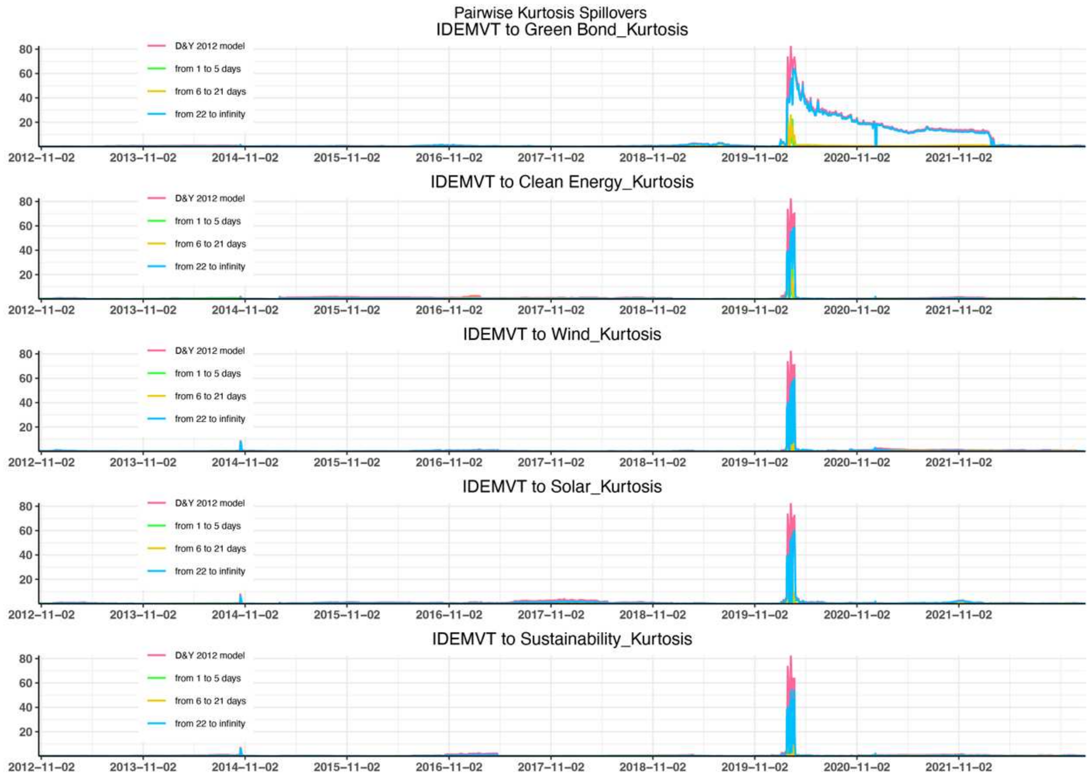

Figure 4.15. Dynamic pairwise kurtosis spillover (window size=500 days).

Notes: The units of the values on the vertical coordinate are percentages; the pink line exhibits the dynamic total spillover results of the Diebold and Yilmaz method; the green line exhibits the dynamic total spillover results of "Frequency short-term" in the Barunik and Krehlik method; the yellow line exhibits the dynamic total spillover results of "Frequency medium-term" in the Barunik and Krehlik method; the blue line exhibits the dynamic total spillover results of "Frequency long-term" in the Barunik and Krehlik method.

4.6. Conclusions

Since 2020, global oil and gas investments have plummeted due to the ongoing COVID-19 pandemic, global supply chain disruptions, and extreme weather events. As the global economy recovered in 2021, the global energy supply was insufficient, leading to a continuous increase in the price of chemical energy, such as oil. With the COVID-19 pandemic still ongoing and the outbreak of the Russia-Ukraine war, traditional energy prices have surged and sustained, affecting countries with moderate to high dependence on traditional energy imports in the industrial or power sector, as well as countries closely related to the EU energy market. In this context, renewable energy represented by green financial investments is in the spotlight.

On one hand, previous studies on stock market spillovers have only focused on the spillover effects of lower-order moments (returns and volatility). On the other hand, when considering the effect of risk asymmetry on the green finance market, it is particularly important to study the spillover effects of higher-order moments (skewness and kurtosis). Our study is the first to investigate the static and dynamic spillover effects of the COVID-19 pandemic and Russia-Ukraine war on lower-order moments (returns and volatility) and higher-order moments (skewness and kurtosis) of sustainability-related financial indices.

Previous studies that investigated spillovers in higher-order moments in financial markets tend to focus on skewness and neglect kurtosis spillovers (Greenwood-Nimmo et al., 2016; Hou and Li, 2020). However, our results demonstrate that kurtosis is more sensitive to extreme crisis events than skewness is. A large kurtosis indicates a high risk of investment because it indicates an extremely high probability and a very small return (Bouri et al., 2021). Therefore, focusing on kurtosis allows investors to track higher risks and achieve effective investment risk aversion.

To estimate volatility, skewness, and kurtosis, we employ the ACD model. Then, we use the Diebold and Yilmaz and Barunik and Krehlik methods to construct the static and dynamic spillover of the return, volatility, skewness, and kurtosis in the time and frequency domains.

The main conclusions can be summarized as follows:

First, in terms of the static spillover analysis in the time domain, our results confirm that there is a difference between the spillover effects of low- and high-order moments. Our results show that the total volatility spillover is the highest (60.617%), followed by the total return spillover (49.921%), total skewness spillover (36.636%), and total kurtosis spillover (29.496%). In other words, the spillover effect of higher-order moments is lower than that of lower-order moments. This result suggests that the contagion pathways of the spillover effects of lower-order moments are diverse, whereas the contagion pathways of the spillover effects of higher-order moments are singular. Our findings extend the results of Tiwari et al. (2022) from low to high-order moments. Furthermore, the pairwise spillover result between IDEMVT and other sustainability-related financial indexes indicates that, compared to other green financial markets, the COVID-19 pandemic has the largest impact on the return, skewness, and kurtosis spillover effects transmitted by the green bond market, and the largest impact on volatility spillover transmitted by clean energy. The return spillover in the wind market, volatility spillover in the green bond market, skewness spillover, and kurtosis spillover in the sustainability index market were relatively less affected by the COVID-19 outbreak.

Second, in terms of the static spillover analysis in the frequency domain, our results show that the total return spillover (first moment) and the total skewness spillover (third moment) mostly occur in the short term (35.398% and 20.152%, respectively). In contrast, the total volatility spillover (third moment) and total kurtosis spillover (fourth moment) are mainly concentrated in the long term (58.442% and 14.172%, respectively). He and Hamori (2021) also confirm that the total volatility spillover mostly occurs in the long term, and the total skewness spillover is mainly concentrated in the short term. Specifically, the return spillover from the IDEMVT to the wind energy market gradually decreases from the short to the long term and becomes 0% directly in the end. This indicates that the impact of the COVID-19 pandemic on the wind energy market did not last. Furthermore, the skewness and kurtosis spillover imparted by IDEMVT to the sustainability index market are the smallest in the short, medium, and long terms, which demonstrates that the COVID-19 outbreak did not have a significant impact on the higher-order spillover in the sustainability index market. Moreover, the skewness and kurtosis spillover from IDEMVT to Green Bond increases gradually from the short term to the long term, indicating the lasting influence of the COVID-19 pandemic on the higher-order spillover effect of the green bond market.

Third, we use network topology to depict static spillover tables to better understand the structure and monitor the strength and direction of spillover effects. In the time domain, the network figure indicates that the clean energy market transmits spillover at lower and higher moments. In contrast, IDEMVT receives spillover at lower and higher moments. In the frequency domain, the wind energy market delivers the largest volatility and kurtosis spillover, while the clean energy market is the largest return and skewness spillover transmitter in the short term. In the medium term, the wind energy market is also the largest volatility transmitter; however, the clean energy market is the largest return, skewness, and kurtosis spillover deliverer. In the long term, the clean energy market has the largest return spillover, volatility spillover, skewness spillover, and kurtosis spillover transmitters, consistent with the conclusion in the time domain. Our findings confirm the frequency-varying nature of the market-spreading impacts of lower and higher-order moments, which can also provide valuable insight for investors with different time horizons for making investments. However, IDEMVT receives the most spillover from sustainability-related financial markets in the short and medium term but is no longer a spillover receiver in the long term. This result suggests that the economic impact of COVID-19 on sustainability-related financial markets takes at least one month or more to become apparent. This conclusion is also supported by Zhang, He et al. (2022).

Fourth, to further compare the impacts of the COVID-19 outbreak, the Russia-Ukraine war, and other major global economic, political, and cultural crisis events on dynamic spillover, we use a rolling window approach to obtain results for dynamic total spillover and dynamic pairwise spillover. In the time domain, we observe that the total volatility spillover (second moment) and total kurtosis spillover (fourth moment) fluctuate more fiercely than the dynamic total return spillover (first moment) and total skewness spillover (third moment) because the total volatility spillover and total kurtosis spillover are more sensitive to extreme global economic, political, and other major crisis events. The outbreak of the Russia-Ukraine war causes only a small fluctuation in the spillover effect of the lower- and higher-order moments of the green finance market, which is consistent with Lorente et al. (2023). However, compared with the Russia-Ukraine war and other crisis events, the COVID-19 outbreak has had a huge and unprecedented impact on the spillover effects of lower- and higher-order moments in the green finance market, as confirmed by Tu et al. (2021) and Liu et al. (2022). The duration of the effects of the COVID-19 outbreak on the spillover effects of lower- and higher-order moments varies from long to short. The COVID-19 pandemic has a persistent effect on dynamic total returns and volatility spillover, while the effect on the dynamic total skewness spillover is transient. Only the dynamic total kurtosis experienced a sharp fluctuation in early 2021 due to the emergence of a new coronavirus mutant strain. In the frequency domain, we observe that the dynamic total return spillover and total skewness spillover are mostly concentrated in the short term, but the total volatility spillover is mostly concentrated in the long term. Prior to the COVID-19 outbreak, the dynamic total kurtosis spillover effect was haphazard, but after the outbreak, the dynamic total kurtosis spillover effect occurred mainly in the long term. This indicates that the COVID-19 pandemic has prolonged the contagion rate of the dynamic total kurtosis spillover effect in sustainable development-related financial markets for more than one month, which is complementary to the conclusions of Hou and Li (2020) and Bouri et al. (2021).

Finally, regarding the dynamic pairwise spillover results, prior to the COVID-19 outbreak, the spillover effect transmitted by IDEMVT to each sustainability financial index was almost 0%. This finding further confirms the unprecedented impact of COVID-19 on the sustainability financial index market. In contrast to the dynamic pairwise return spillover effect, the dynamic pairwise volatility spillover between IDEMVT and sustainability-related financial indices remains high over time, indicating a substantial and persistent impact of the COVID-19 outbreak on the volatility spillover effect of sustainability-related financial indices. Additionally, only the dynamic total skewness and kurtosis spillovers transmitted to the green bond by IDEMVT exhibit continuous fluctuations. This suggests that COVID-19 has far-reaching and persistent impacts on the skewness and kurtosis spillover effects of the green bond market.

Whenever spillover effects between financial markets are mentioned, most people are concerned about the spillover effects of returns and volatility between markets. The COVID-19 pandemic has severely impacted the world economy and has deeply affected the financial system, raising concerns about the possibility of another financial crisis. In the current complex financial market environment, it is essential to study the spillover effects of lower-order moments (mean and variance) as well as higher-order moments (skewness and kurtosis). While most studies have focused on low-order moment spillover effects, which are returns and volatilities, it is well-known that asset return distributions are usually non-normal, asymmetric, and fat-tailed. Therefore, it is suboptimal to limit the study of spillover effects to only the first and second moments (Zhang, Jin, et al., 2022). Higher-order moments such as skewness and kurtosis contain valuable information reflecting asymmetric risk or tail events (Amaya et al., 2015). Our extension from low-order moment dynamic spillovers to high-order moment dynamic spillovers in green financial markets could be beneficial to policymakers as it provides a new way of thinking about policymaking in times of economic and financial instability. Policymakers can develop and implement more fine-grained and targeted regulations and action plans while considering the hazards of tail information monitoring systems. In addition, risk contagion in green financial markets is inevitable due to the increasing level of internationalization of financial markets. Policymakers can capture the abnormal movements of fluctuations through dynamic spillover analysis of higher-order moments, such as the extreme value of skewness, and use stock indices that are prone to abnormal fluctuations as an early warning indicator of risk transmission. Thus, they can avoid butterfly effects when certain stocks are negatively affected by the market and transfer risk to the financial markets. Moreover, policymakers can identify relevant financial events such as COVID-19 while capturing abnormal fluctuations in higher-order moments, allowing policymakers and market regulators to improve risk warning mechanisms for different events and prevent further expansion of financial risks (Gao et al., 2022; Bouri et al., 2021).

The non-normal distribution of asset returns implies that studying skewness and kurtosis facilitates investors in deducing asymmetric or fat-tailed risks associated with extreme or downside (upside) risks. Jurczenko and Maillet (2006) found that investors prefer assets with positive skewness and low kurtosis performance. A positively skewed return distribution implies frequent small losses and some extreme gains, while a negatively skewed return distribution implies many small gains and some extreme losses. Therefore, the risk-return tradeoff is evaluated in terms of lower-order moments and higher-order moments, which benefit investors in terms of option valuation, value-at-risk, asset pricing, and portfolio gain more easily. Investors can construct a portfolio based on maximum skewness. More specifically, under this methodology, the optimal portfolio should consist of maximizing the mean and skewness while minimizing the variance (we call it a higher-moment portfolio strategy). This is a multi-objective optimization problem and a complex topic. Some researchers have already proposed solutions (e.g., Boudt et al., 2020). However, this goes beyond the scope of this work. Although our results suggest that the higher-order moment spillover effects of sustainability financial index markets are lower than the lower-order moment spillover effects, they cannot be ignored. As this result coincides with the risk asymmetry of the sustainability-linked financial index market, investigating risk asymmetry can help investors rebuild their diversified portfolios and hedging strategies. Furthermore, some researchers have proved that portfolio managers can use spillover information to design effective asset allocation and portfolio diversification strategies for the global minimum-variance portfolio (e.g., Kang et al., 2019). Examining the portfolio performance of higher moments portfolio strategies using skewness spillover information, especially during periods of financial crisis and turmoil, would be an interesting direction for future research.

In future research, it would be beneficial to further investigate the impact of economic policy uncertainty and geopolitical risks on green financial markets. Furthermore, it would be interesting to analyze the threshold effect using an ACD model. Additionally, it would be intriguing to explore the specific performance of risk hedging for higher-order moments based on our study. For example, we suggest examining the optimal hedging ratio (Kroner and Sultan, 1993), optimal portfolio weights (Kroner and Ng, 1998), minimum correlation portfolio (Christoffersen et al., 2014), and hedging effectiveness (Ederington, 1979).

Appendix

Figures A1, A2, A3, and A4 represent the dynamic total return, volatility, skewness, and kurtosis spillovers in the time domain for window sizes of 250, 370, and 500 days (the window size used in our study), respectively. The spillover performance of the 500-day window has a similar trend of fluctuation to the spillover performance of the 250-day and 370-day windows but is relatively more stable.

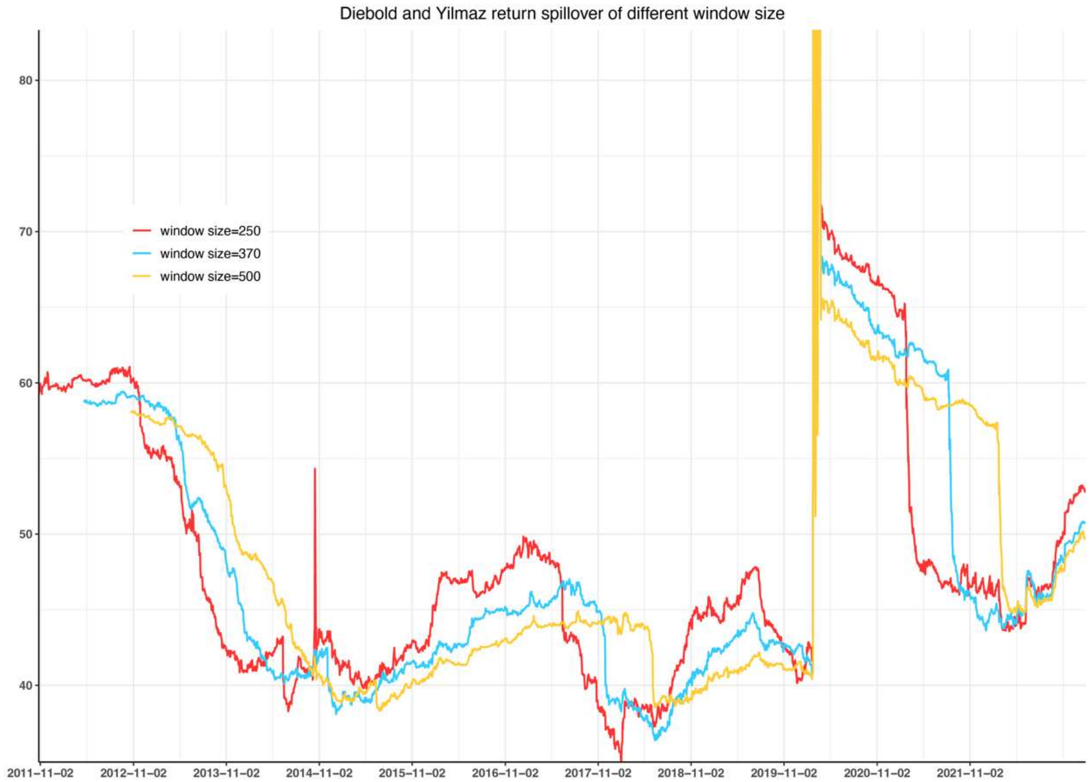

Figure A1. Dynamic total return spillover of window size 250, 300, and 500 days.

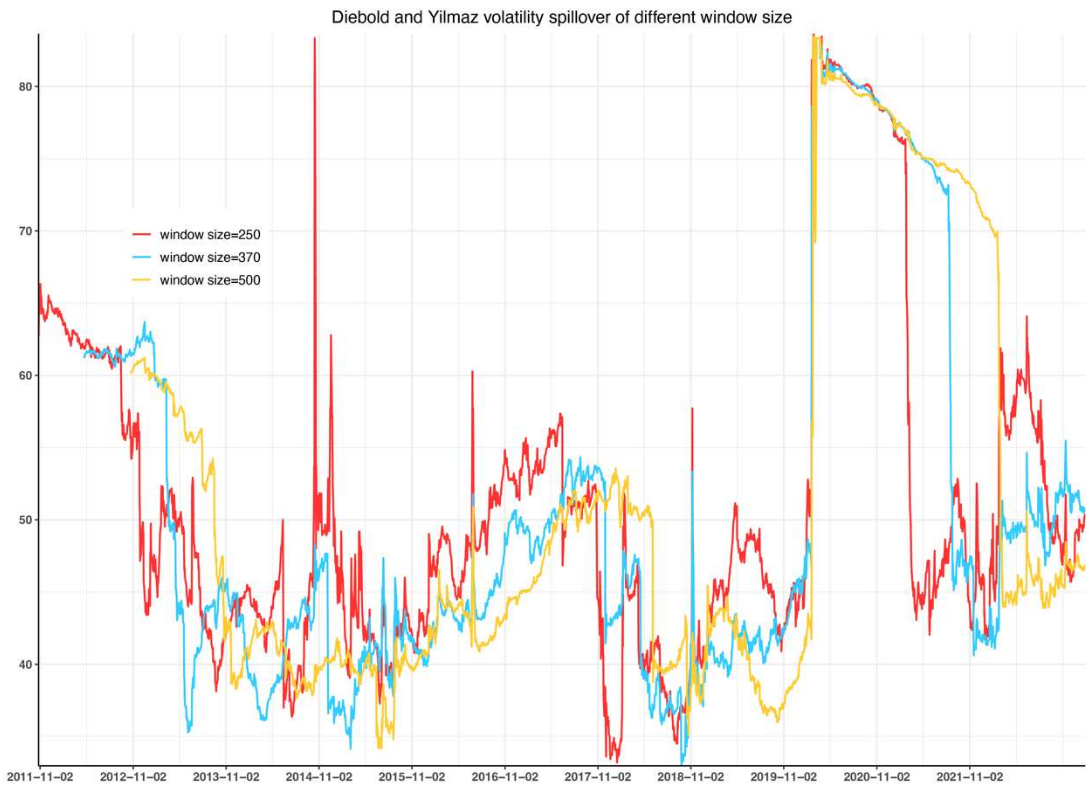

Figure A2. Dynamic total volatility spillover of window size 250, 300, and 500 days.

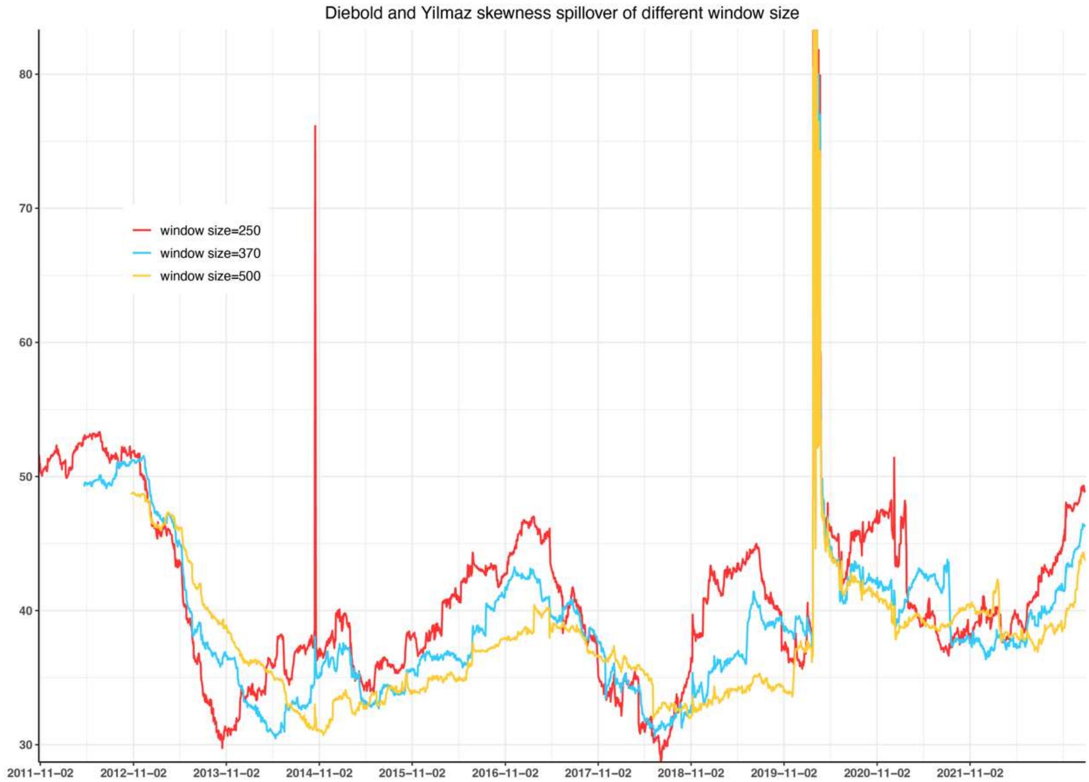

Figure A3. Dynamic total skewness spillover of window size 250, 300, and 500 days.

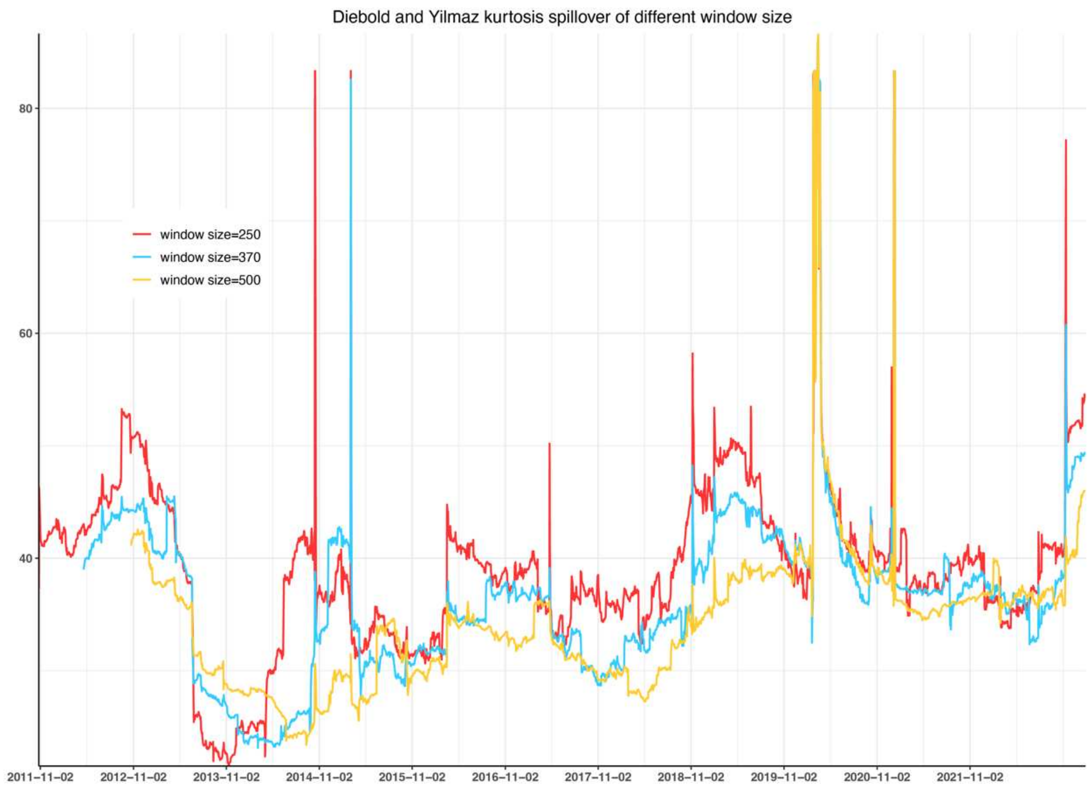

Figure A4. Dynamic total kurtosis spillover of window size 250, 300, and 500 days.

After calculating the low-order moment spillover and high-order moment spillover of growth rate using the Diebold and Yilmaz method, we present the results in Table A to compare them with those of logarithmic difference. The table shows that the spillover outcomes of growth rate are similar to those of the return series using logarithmic difference, indicating the robustness between the two approaches.

Table A. Diebold and Yilmaz spillover table based on growth rate.

Return spillover table of Diebold and Yilmaz (2012)

	Green Bond	Clean Energy	Wind	Solar	Sustainability	IDEMVT	FROM
Green Bond	63.887	6.642	12.738	3.498	13.127	0.108	6.019
Clean Energy	2.950	34.438	20.919	25.369	16.246	0.079	10.927
Wind	6.764	22.537	35.740	13.286	21.642	0.032	10.710
Solar	1.700	29.980	14.062	41.471	12.699	0.089	9.755
Sustainability	7.575	18.579	23.254	12.302	38.240	0.050	10.293
IDEMVT	0.007	2.737	2.365	1.164	2.547	91.180	1.470
TO	3.166	13.412	12.223	9.270	11.043	0.060	49.174

Volatility spillover table of Diebold and Yilmaz (2012)

	Green Bond	Clean Energy	Wind	Solar	Sustainability	IDEMVT	FROM
Green Bond	39.576	16.208	11.683	4.993	25.258	2.282	10.071
Clean Energy	4.587	33.180	13.214	17.802	18.583	12.633	11.137
Wind	7.956	23.383	21.791	11.555	26.511	8.804	13.035
Solar	4.889	28.341	10.120	32.600	15.895	8.155	11.233
Sustainability	9.685	18.745	15.346	7.886	42.274	6.063	9.621
IDEMVT	1.413	14.931	2.696	9.452	4.732	66.775	5.537
TO	4.755	16.935	8.843	8.615	15.163	6.323	60.634

Skewness spillover table of Diebold and Yilmaz (2012)

	Green Bond	Clean Energy	Wind	Solar	Sustainability	IDEMVT	FROM
Green Bond	72.102	4.846	8.936	5.518	5.299	3.300	4.650
Clean Energy	1.716	45.529	17.808	27.280	7.450	0.216	9.078
Wind	4.233	23.383	47.011	14.115	10.914	0.343	8.832
Solar	0.923	31.253	9.577	53.701	4.369	0.177	7.717
Sustainability	5.007	10.760	16.169	5.487	62.544	0.033	6.243
IDEMVT	0.150	0.151	0.230	0.183	0.066	99.220	0.130
TO	2.005	11.732	8.787	8.764	4.683	0.678	36.649

Kurtosis spillover table of Diebold and Yilmaz (2012)

	Green Bond	Clean Energy	Wind	Solar	Sustainability	IDEMVT	FROM
Green Bond	87.184	0.200	0.557	0.114	1.749	10.197	2.136
Clean Energy	0.149	51.700	15.623	29.658	2.476	0.394	8.050
Wind	0.219	19.442	58.894	12.689	7.979	0.776	6.851
Solar	0.288	29.443	8.165	59.414	2.439	0.252	6.764
Sustainability	1.137	5.120	15.803	3.371	74.548	0.021	4.242
IDEMVT	9.405	0.488	0.348	0.594	0.098	89.066	1.822
TO	1.866	9.116	6.749	7.738	2.457	1.940	29.866

Notes: Green Bond represents the return of the S&P Green Bond Index; Clean Energy represents the return of the S&P Global Clean Energy Index, Wind represents the return of the ISE Global Wind Energy Index, Solar represents the return of the MAC Global Solar Energy Index, Sustainability represents the return of the Dow Jones

Sustainability World Index, and IDEMVT represents the Infectious Disease Equity Market Volatility Tracker.

References

Adams, C.A., Abhayawansa, S., 2022. Connecting the COVID-19 pandemic, environmental, social and governance (ESG) investing and calls for “harmonisation” of sustainability reporting. Crit. Perspect. Acc. 82, 102309. https://doi.org/10.1016/j.cpa.2021.102309.

Albulescu, C.T., Demirer, R., Raheem, I.D., Tiwari, A.K., 2019. Does the U.S. economic policy uncertainty connect financial markets? Evidence from oil and commodity currencies. Energy Econ. 83, 375–388. https://doi.org/10.1016/j.eneco.2019.07.024.

Albuquerque, R., Koskinen, Y., Yang, S., Zhang, C., 2020. Resiliency of environmental and social stocks: An analysis of the exogenous COVID-19 market crash. Rev. Corp. Fin. Stud. 9(3), 593–621. https://doi.org/10.1093/rcfs/cfaa011.

Amaya, D., Christoffersen, P., Jacobs, K., Vasquez, A. 2015. Does realized skewness predict the cross-section of equity returns? J financ econ. 118(1), 135–167. https://doi.org/10.1016/j.jfineco.2015.02.009.

Baker, S.R., Bloom, N., Davis, S.J., Kost, K., 2019. Policy news and stock market volatility. SSRN Electron. J.. https://doi.org/10.2139/ssrn.3363862.

Baker, S.R., Bloom, N., Davis, S.J., Kost, K., Sammon, M., Viratyosin, T., 2020. The unprecedented stock market reaction to COVID-19. Rev. Asset Pricing Stud. 10(4), 742–758. https://doi.org/10.1093/rapstu/raaa008.

Barndorff-Nielsen, O.E., 1977. Exponentially decreasing distributions for the logarithm of particle size. Proc. R. Soc. Lond. A 353(1674), 401–419. https://doi.org/10.1098/rspa.1977.0041.

Barndorff-Nielsen, O.E., 1997. Normal inverse Gaussian distributions and stochastic volatility modelling. Scand. J. Stat. 24(1), 1–13. https://doi.org/10.1111/1467-9469.00045.

Barunik, J., Krehlik, T., 2016. Measuring the frequency dynamics of financial and macroeconomic connectedness. (Accessed Jun 6, 2022). Available online: http://www.econstor.eu. website. Available online: http://hdl.handle.net/10419/125824. SSRN Journal.

Baruník, J., Křehlík, T., 2018. Measuring the frequency dynamics of financial connectedness and systemic risk. J. Financ. Econ. 16(2), 271–296. https://doi.org/10.1093/jjfinec/nby001.

Bevilacqua, M., Tunaru, R., 2021. The SKEW index: Extracting what has been left. J. Financ. Stab. 53, 100816. https://doi.org/10.1016/j.jfs.2020.100816.

Bilgin, M., Yilmaz, K., 2018. Producer Price Inflation Connectedness and Input-Output Networks. SSRN Electron. J.. https://doi.org/10.2139/ssrn.3244645.

Bostanci, G., Yilmaz, K., 2020. How connected is the global sovereign credit risk network? J. Banking Fin. 113, 105761. https://doi.org/10.1016/j.jbankfin.2020.105761.

Boudt, K., Cornilly, D., Van Holle, F., & Willems, J. 2020. Algorithmic portfolio tilting to harvest higher moment gains. Heliyon, 6(3), e03516.

https://doi.org/10.1016/j.heliyon.2020.e03516.

Bouri, E., Lei, X., Jalkh, N., Xu, Y., Zhang, H., 2021. Spillovers in higher moments and jumps across US stock and strategic commodity markets. Resour. Policy 72, 102060. https://doi.org/10.1016/j.resourpol.2021.102060.

British Petroleum Company, 2021. BP statistical review of world energy. London: British Petroleum Co https://www.bp.com/content/dam/bp/business-sites/en/global/corporate/pdfs/energy-economics/statistical-review/bp-stats-review-2021-full-report.pdf.

Broadstock, D.C., Chan, K., Cheng, L.T.W., Wang, X., 2021. The role of ESG performance during times of financial crisis: Evidence from COVID-19 in China. Financ. Res. Lett. 38, 101716. https://doi.org/10.1016/j.frl.2020.101716.

Brzeszczyński, J., McIntosh, G., 2014. Performance of portfolios composed of British SRI stocks. J. Bus. Ethics 120(3), 335–362. https://doi.org/10.1007/s10551-012-1541-x.

Calvo, S.G., Reinhart, C.M., 1996. Capital Flows to Latin America: Is There Evidence of Contagion Effects?. *Papers.ssrn.com.* https://ssrn.com/abstract=636120.

Campiglio, E., 2016. Beyond carbon pricing: The role of banking and monetary policy in financing the transition to a low-carbon economy. Ecol. Econ. 121, 220–230. https://doi.org/10.1016/j.ecolecon.2015.03.020.

Chang, Y.-P., Hung, M.-C., Liu, H., Jan, J.-F., 2005. Testing symmetry of a NIG distribution. Commun. Stat. Simul. Comput. 34(4), 851–862.

https://doi.org/10.1080/03610910500307877.

Chowdhury, E.K., Dhar, B.K., Stasi, A., 2022. Volatility of the US stock market and business strategy during COVID-19. Bus. Strat. Dev.. https://doi.org/10.1002/bsd2.203.

Christoffersen, P., Errunza, V., Jacobs, K., Jin, X., 2014. Correlation dynamics and international diversification benefits. Int. J. Forecasting 30(3), 807–824. https://doi.org/10.1016/j.ijforecast.2014.01.001.

Corbet, S., Goodell, J.W., Günay, S., 2020. Co-movements and spillovers of oil and renewable firms under extreme conditions: New evidence from negative WTI prices during COVID-19. Energy Econ. 92, 104978. https://doi.org/10.1016/j.eneco.2020.104978.

De la Torre, O., Galeana, E., Aguilasocho, D., 2016. The use of the sustainable investment against the broad market one. A first test in the Mexican stock market. Eur. Res. Manag. Bus. Econ. 22(3), 117–123. https://doi.org/10.1016/j.iedee.2015.08.002.

de Oliveira, E.M., Cunha, F.A.FdS., Palazzi, R.B., Klotzle, M.C., Maçaira, P.M., 2020. On the effects of uncertainty measures on sustainability indices: An empirical investigation in a nonlinear framework. Int. Rev. Financ. Anal. 70, 101505. https://doi.org/10.1016/j.irfa.2020.101505.

Diebold, F.X., Yilmaz, K., 2009. Measuring financial asset return and volatility spillovers, with application to global equity markets. Econ. J. 119(534), 158–171. https://doi.org/10.1111/j.1468-0297.2008.02208.x.

Diebold, F.X., Yilmaz, K., 2012. Better to give than to receive: Predictive directional measurement of volatility spillovers. Int. J. Forecasting 28(1), 57–66. https://doi.org/10.1016/j.ijforecast.2011.02.006.

Diebold, F.X., Yılmaz, K., 2014. On the network topology of variance decompositions: Measuring the connectedness of financial firms. J. Econ. 182(1), 119–134. https://doi.org/10.1016/j.jeconom.2014.04.012.

Diebold, F.X., Yılmaz, K., 2015. Financial and Macroeconomic Connectedness: A Network Approach to Measurement and Monitoring. Oxford University Press, USA.

Diebold, F.X., Yilmaz, K., 2016. Trans-Atlantic equity volatility connectedness: U.S. and European Financial Institutions, 2004–2014. J. Financ. Econ. 14(1), 81–127. https://doi.org/10.1093/jjfinec/nbv021.

Dogan, E., Madaleno, M., Taskin, D., Tzeremes, P. 2022. Investigating the spillovers and connectedness between green finance and renewable energy sources. Renew. Energ., 197, 709–722. https://doi.org/10.1016/j.renene.2022.07.131.

Dornbusch, R., Park, Y.C., Claessens, S., 2000. Contagion: Understanding how it spreads. World Bank Res. Observer 15(2), 177–197.

Ederington, L.H., 1979. The hedging performance of the new futures markets. J. Fin. 34(1), 157–170. https://doi.org/10.1111/j.1540-6261.1979.tb02077.x.

Engle, R.F., 1982. Autoregressive conditional heteroscedasticity with estimates of the variance of United Kingdom inflation. Econometrica 50(4), 987.

https://doi.org/10.2307/1912773.

Ferriani, F., Natoli, F., 2021. ESG risks in times of Covid-19. Appl. Econ. Lett. 28(18), 1537–1541. https://doi.org/10.1080/13504851.2020.1830932.

Finta, M.A., Aboura, S., 2020. Risk premium spillovers among stock markets: Evidence from higher-order moments. J. Financ. Markets 49, 100533. https://doi.org/10.1016/j.finmar.2020.100533.

Gao, Y., Li, Y., Wang, Y., 2021. Risk spillover and network connectedness analysis of China's green bond and financial markets: Evidence from financial events of 2015–2020. North Am. J. Econ. Fin. 57, 101386.

Gao, Y., Li, Y., Zhao, C., Wang, Y. 2022. Risk spillover analysis across worldwide ESG stock markets: New evidence from the frequency-domain. North Am. J. Econ. Fin. 59, 101619. https://doi.org/10.1016/j.najef.2021.101619.

Garcia, A.S., Orsato, R.J., 2020. Testing the institutional difference hypothesis: A study about environmental, social, governance, and financial performance. Bus. Strat. Env. 29(8), 3261–3272. https://doi.org/10.1002/bse.2570.

Ghalanos, A., Rossi, E., Urga, G., 2015. Independent factor autoregressive conditional density model. Econ. Rev. 34(5), 594–616. https://doi.org/10.1080/07474938.2013.808561.

Greenwood-Nimmo, M., Nguyen, V.H., Rafferty, B., 2016. Risk and return spillovers among the G10 currencies. J. Financ. Markets 31, 43–62. https://doi.org/10.1016/j.finmar.2016.05.001.

Hansen, B.E., 1994. Autoregressive conditional density estimation. Int. Econ. Rev.

35(3), 705. https://doi.org/10.2307/2527081.

Hassan, M. K., Hasan, Md. B., Halim, Z. A., Maroney, N., & Rashid, Md. M. (2022). Exploring the dynamic spillover of cryptocurrency environmental attention across the commodities, green bonds, and environment-related stocks. North Am. J. Econ. Finance. 61, 101700. https://doi.org/10.1016/j.najef.2022.101700.

He, X., Hamori, S., 2021. Is volatility spillover enough for investor decisions? A new viewpoint from higher moments. J. Int. Money Fin. 116, 102412. https://doi.org/10.1016/j.jimonfin.2021.102412.

Hibbert, A.M., Daigler, R.T., Dupoyet, B., 2008. A behavioral explanation for the negative asymmetric return–volatility relation. J. Banking Fin. 32(10), 2254–2266. https://doi.org/10.1016/j.jbankfin.2007.12.046.

Hou, Y., Li, S., 2020 Volatility and skewness spillover between stock index and stock index futures markets during a crash period: New evidence from China. Int. Rev. Econ. Fin. 66, 166–188. https://doi.org/10.1016/j.iref.2019.11.003.

Iqbal, N., Abubakr Naeem, M., Tahir Suleman, M., 2022. Quantifying the asymmetric spillovers in sustainable investments. J. Int. Financ. Markets Inst. Money. 77, 101480. https://doi.org/10.1016/j.intfin.2021.101480.

Irena, S., 2020. IRENA-international renewable energy agency. *Dipetik June 30*, 2021. Available online: https://www.irena.org/Statistics/Statistical-Profiles.

Jain, M., Sharma, G.D., Srivastava, M., 2019. Can sustainable investment yield better financial returns: A comparative study of ESG indices and MSCI indices.

Risks 7(1), 15. https://doi.org/10.3390/risks7010015.

Jarque, C.M., Bera, A.K., 1987. A test for normality of observations and regression residuals. Int. Stat. Rev. Rev. Int. Stat. 55(2), 163. https://doi.org/10.2307/1403192.

Jensen, M.B., Lunde, A., 2001. The NIG-S&ARCH model: A fat-tailed, stochastic, and autoregressive conditional heteroskedastic volatility model. Econ. J. 4(2), 319–342. https://doi.org/10.1111/1368-423X.00070.

Jurczenko, E., Maillet, B., 2006. Multi-moment asset allocation and pricing models. Hoboken, NJ: John Wiley & Sons.

Kang, S. H., Maitra, D., Dash, S. R., Brooks, R. 2019. Dynamic spillovers and connectedness between stock, commodities, bonds, and VIX markets. Pacific Basin Finance J. 58, 101221. https://doi.org/10.1016/j.pacfin.2019.101221.

Koop, G., Pesaran, M.H., Potter, S.M., 1996Impulse response analysis in nonlinear multivariate models.. Hashem, & potter, S.M. J. Econ. 74(1), 119–147. https://doi.org/10.1016/0304-4076(95)01753-4.

Kroner, K.F., Ng, V.K., 1998. Modeling asymmetric comovements of asset returns. Rev. Financ. Stud. 11(4), 817–844. https://doi.org/10.1093/rfs/11.4.817.

Kroner, K.F., Sultan, J., 1993. Time-varying distributions and dynamic hedging with foreign currency futures. J. Financ. Quant. Anal. 28(4), 535. https://doi.org/10.2307/2331164.

Kumar, S., Managi, S., & Matsuda, A. (2012). Stock prices of clean energy firms, oil and carbon markets: A vector autoregressive analysis. *Energy Economics*, *34*(1), 215–226. https://doi.org/10.1016/j.eneco.2011.03.002

Le, T.L., Abakah, E.J.A., Tiwari, A.K., 2021. Time and frequency domain connectedness and spill-over among fintech, green bonds and cryptocurrencies in the age of the fourth Industrial Revolution. Technol. Forecast. Soc. Change 162, 120382. https://doi.org/10.1016/j.techfore.2020.120382.

Liu, L., Wang, E.-Z., Lee, C.-C., 2020. Impact of the COVID-19 pandemic on the crude oil and stock markets in the US: A time-varying analysis. Energy Res. Lett. 1(1). https://doi.org/10.46557/001c.13154.

Liu, N., Liu, C., Da, B., Zhang, T., Guan, F., 2021. Dependence and risk spillovers between green bonds and clean energy markets. J. Cleaner Prod. 279, 123595. https://doi.org/10.1016/j.jclepro.2020.123595.

Liu, T., Nakajima, T., Hamori, S., 2022. The impact of economic uncertainty caused by COVID-19 on renewable energy stocks. Empir. Econ. 62(4), 1495–1515. https://doi.org/10.1007/s00181-021-02087-3.

Li, Z., Kuo, T.-H., Siao-Yun, W., & The Vinh, L., 2022. Role of green finance, volatility and risk in promoting the investments in Renewable Energy Resources in the post-covid-19. Resources Policy, 76, 102563. https://doi.org/10.1016/j.resourpol.2022.102563

Lorente, D. B., Mohammed, K. S., Cifuentes-Faura, J., & Shahzad, U. (2023). Dynamic connectedness among climate change index, green financial assets and renewable energy markets: Novel evidence from sustainable development perspective. *Renewable Energy*, *204*, 94–105.

https://doi.org/10.1016/j.renene.2022.12.085

Mensi, W., Naeem, M.A., Vo, X.V., Kang, S.H., 2022. Dynamic and frequency spillovers between green bonds, oil and G7 stock markets: Implications for risk management. Econ. Anal. Policy 73, 331–344. https://doi.org/10.1016/j.eap.2021.11.015.

Morimoto, T., 2004. Estimating and forecasting instantaneous volatility through a duration model: An assessment based on VaR. Available online: https://core.ac.uk/download/pdf/7358454.pdf. Accessed 6. 30. 2022.

Mzoughi, H., Urom, C., Guesmi, K. 2022. Downside and upside risk spillovers between green finance and energy markets. Finance Res. Lett. 47, 102612. https://doi.org/10.1016/j.frl.2021.102612.

Naeem, M.A., Adekoya, O.B., Oliyide, J.A., 2021. Asymmetric spillovers between green bonds and commodities. J. Cleaner Prod. 314, 128100. https://doi.org/10.1016/j.jclepro.2021.128100.

Naeem, M. A., Karim, S., Uddin, G. S., & Junttila, J. (2022). Small fish in big ponds: Connections of green finance assets to commodity and sectoral stock markets. Int. Rev. Financial Anal. 83, 102283. https://doi.org/10.1016/j.irfa.2022.102283.

Naeem, M.A., Mbarki, I., Alharthi, M., Omri, A., Shahzad, S.J.H., 2021. Did COVID-19 impact the connectedness between green bonds and other financial markets? Evidence from time-frequency domain with portfolio implications. Front. Environ. Sci. 9. https://doi.org/10.3389/fenvs.2021.657533.

Nisticò, S., 2012. Monetary policy and stock-price dynamics in a DSGE framework. J. Macroecon. 34(1), 126–146. https://doi.org/10.1016/j.jmacro.2011.09.008.

Pesaran, H.H., Shin, Y., 1998 Generalized impulse response analysis in linear multivariate models. Econ. Lett. 58(1), 17–29. https://doi.org/10.1016/S0165-1765(97)00214-0.

Reboredo, J.C., Ugolini, A., 2020. Price connectedness between green bond and financial markets. Econ. Modell. 88, 25–38. https://doi.org/10.1016/j.econmod.2019.09.004.

Reboredo, J.C., Ugolini, A., Aiube, F.A.L., 2020. Network connectedness of green bonds and asset classes. Energy Econ. 86, 104629. https://doi.org/10.1016/j.eneco.2019.104629.

Sadorsky, P., 2012. Correlations and volatility spillovers between oil prices and the stock prices of clean energy and technology companies. Energy Econ. 34(1), 248–255. https://doi.org/10.1016/j.eneco.2011.03.006.

Said, S.E., Dickey, D.A., 1984. Testing for unit roots in autoregressive-moving average models of unknown order. Biometrika 71(3), 599–607. https://doi.org/10.1093/biomet/71.3.599.

Schaeffer, R., Borba, B.S.M.C., Rathmann, R., Szklo, A., Castelo Branco, D.A., 2012. Dow Jones sustainability index transmission to oil stock market returns: A GARCH approach. Energy 45(1), 933–943. https://doi.org/10.1016/j.energy.2012.06.066.

Scott, D.J., Würtz, D., Dong, C., Tran, T.T., 2011. Moments of the generalized hyperbolic distribution. Comput. Stat. 26(3), 459–476. https://doi.org/10.1007/s00180-010-0219-z.

Sharif, A., Aloui, C., Yarovaya, L., 2020. COVID-19 pandemic, oil prices, stock market, geopolitical risk and policy uncertainty nexus in the US economy: Fresh evidence from the wavelet-based approach. Int. Rev. Financ. Anal. 70, 101496. https://doi.org/10.1016/j.irfa.2020.101496.

Streimikiene, D., Kaftan, V. 2021. Green finance and the economic threats during COVID-19 pandemic. Terra Economicus, 19(2), 105–113. https://doi.org/10.18522/2073-6606-2021-19-2-105-113.

Szczygielski, J.J., Bwanya, P.R., Charteris, A., Brzeszczyński, J., 2021. The only certainty is uncertainty: An analysis of the impact of COVID-19 uncertainty on regional stock markets. Financ. Res. Lett. 43, 101945. https://doi.org/10.1016/j.frl.2021.101945.

Tiwari, A.K., Aikins Abakah, E.J., Gabauer, D., Dwumfour, R.A., 2022. Dynamic spillover effects among green bond, renewable energy stocks and carbon markets during COVID-19 pandemic: Implications for hedging and investments strategies. Glob. Fin. J. 51, 100692. https://doi.org/10.1016/j.gfj.2021.100692.

Toyoshima, Y., Hamori, S., 2018. Measuring the time-frequency dynamics of return and volatility connectedness in global crude oil markets. Energies 11(11), 2893. https://doi.org/10.3390/en11112893.

Tu, Q., Mo, J., Liu, Z., Gong, C., Fan, Y., 2021. Using green finance to counteract the adverse effects of COVID-19 pandemic on renewable energy investment-The case of offshore wind power in China. Energy Policy 158, 112542. https://doi.org/10.1016/j.enpol.2021.112542.

Wang, X., Wang, Y., 2019. Volatility spillovers between crude oil and Chinese sectoral equity markets: Evidence from a frequency dynamics perspective. Energy Econ. 80, 995–1009. https://doi.org/10.1016/j.eneco.2019.02.019.

Wen, F., Tao, M., He, Z., Chen, X., 2013. The Impact of Investors' Risk Attitudes on Skewness of return Distribution. Procedia Comput. Sci. 17, 664–670. https://doi.org/10.1016/j.procs.2013.05.086.

Wilhelmsson, A., 2009. Value at risk with time varying variance, skewness and kurtosis-the NIG-ACD model. Econ. J. 12(1), 82–104. https://doi.org/10.1111/j.1368-423X.2008.00277.x.

Yilmaz, K., 2010. Return and volatility spillovers among the East Asian equity markets. J. Asian Econ. 21(3), 304–313. https://doi.org/10.1016/j.asieco.2009.09.001.

Zhang, H., Jin, C., Bouri, E., Gao, W., Xu, Y. 2022. Realized higher-order moments spillovers between commodity and stock markets: Evidence from China. J. Commod. Mark. 100275. https://doi.org/10.1016/j.jcomm.2022.100275.

Zhang, W., Hamori, S., 2021. Crude oil market and stock markets during the COVID-19 pandemic: Evidence from the US, Japan, and Germany. Int. Rev. Financ. Anal. 74, 101702. https://doi.org/10.1016/j.irfa.2021.101702.

Zhang, W., He, X., Hamori, S., 2022. Volatility spillover and investment strategies among sustainability-related financial indexes: Evidence from the DCC-GARCH-based dynamic connectedness and DCC-GARCH t-copula approach. Int. Rev. Financ. Anal. 83, 102223. https://doi.org/10.1016/j.irfa.2022.102223.

Zhang, W., He, X., Nakajima, T., Hamori, S., 2020. How does the spillover among natural gas, crude oil, and electricity utility stocks change over time? Evidence from North America and Europe. Energies 13(3), 727. https://doi.org/10.3390/en13030727.

Zhang, X., Bouri, E., Xu, Y., Zhang, G., 2022. The asymmetric relationship between returns and implied higher moments: Evidence from the crude oil market. Energy Econ. 109, 105950. https://doi.org/10.1016/j.eneco.2022.105950.